DEPARTMENT OF CHEMISTRY

NOVA SCHOOL OF SCIENCE & TECHNOLOGY

AFONSO VICENTE PATRIARCA EVA

BSc in Biochemistry

# Evaluation and optimization of bioprocesses for $CO_2$ capture and biomass valorization into value-added products by green non-sulfur bacteria: *Chloroflexus aurantiacus*

Master's in Biotechnology

NOVA University Lisbon

September, 2023

DEPARTAMENT OF CHEMISTRY

# Evaluation and optimization of bioprocesses for $CO_2$ capture and biomass valorization into value-added products by green non-sulfur bacteria: *Chloroflexus aurantiacus*

**AFONSO VICENTE PATRIARCA EVA**

BSc in Biochemistry

**Adviser:** Dr. Joana Fradinho
*Researcher, NOVA University Lisbon*

**Co-advisers:** Dr. Roxana Ángeles Torres
Postdoctoral researcher, ISP-University of Valladolid

**Examination Committee:**

**Chair:** Name of the committee chairperson,
Full Professor, FCT-NOVA

**Rapporteurs:** Name of a rapporteur,
Associate Professor, Another University
Name of another rapporteur,
Assistant Professor, Another University

**Adviser:** Name of the adviser present in defense,
Associate Professor, University

**Members:** Yet another member of the committee,
Full Professor, Another University
Yet another member of the committee,
Assistant Professor, Another University

Master's in Biotechnology

NOVA University Lisbon
September, 2023

Evaluation and optimization of bioprocesses for $CO_2$ capture and biomass valorization into value-added products by green non-sulfur bacteria: *Chloroflexus aurantiacus*

Para a minha mãe, irmã e namorada, os meus 3 pilares nesta jornada.

# AGRADECIMENTOS

Esta tese não teria sido possível sem estas pessoas.

Um obrigado à Joana pelas grandes discussões científicas e todo o apoio que me deu durante o último ano.

Um obrigado à malta do laboratório 610 e 407, desde os mais jovens aos mais velhos, todos eles excelentes pessoas e cujo ânimo me aguentou nos dias de sampling mais longos.

Um obrigado à Roxana, pela sua grande paciência em ensinar, não só os protocolos, mas a maneira correta de trabalhar. Sinto que aprendi bastante num ano, não só sobre bactérias, mas sobre trabalho laboratorial, organização e responsabilidade.

Um obrigado aos meus amigos que tiveram a paciência de me ouvir falar de bactérias durante um ano sem parar.

Um especial obrigado à minha mãe e principal ídolo. Devo tudo a ti, obrigado. À minha irmã que a este ponto também deve estar farta de ouvir falar em ciência, mas que me apoia sempre. E por fim, à Mariana, que partilha a ciência no coração e partilha um espaço enorme no meu também. Obrigado por tudo, amo-te.

“I’m not arguing, I'm explaining why I'm right"
(Rick)

# ABSTRACT

In recent years, human activities have significantly impacted the environment through plastic pollution, $CO_2$ emissions that contribute to global warming, and the release of toxic compounds linked to the synthetic pigment industry. Consequently, there is a need to implement sustainable technologies to mitigate these problems. One promising solution lies in the utilization of photosynthetic microorganisms. This thesis focuses on developing a photosynthetic sustainable bioprocess to simultaneously capture $CO_2$, a crucial greenhouse gas, and remove sulfide while yielding value-added products like the biodegradable plastic polyhydroxyalkanoate (PHA) and natural pigments (carotenoids and bacteriochlorophylls *a* and *c*). This bioprocess explores the $CO_2$ fixation by the green non-sulfur bacteria *C. aurantiacus* which has the unique capability of assimilating $CO_2$ using routes alternative to the Calvin-Benson-Bassam cycle, increasing the potential PHA storage. Four different *C. aurantiacus* strains were tested under different pH (7, 8, 9), temperature (30ºC, 50ºC), and sulfide concentration (3, 5, 10, 20 mg S $L^{-1}$), either in autotrophic or heterotrophic conditions. The results obtained show that the best growth, PHA production, and pigment production occurred in heterotrophic conditions, at 50ºC, under 1.7 W $L^{-1}$ of continuous illumination. Nonetheless, biomass yield calculations show that there was $CO_2$ fixation in autotrophic conditions, despite a slower growth in comparison with heterotrophic conditions. Future tests involving higher sulfide concentration and yeast extract supplementation might allow for increased $CO_2$ fixation and autotrophic growth. PHA production was highest for strain *C. aurantiacus* 244-3 (DSM 638) at pH 8, amounting to a PHA content of 4.3 % gPHA/gVSS. Pigment production was highest for strain *C. aurantiacus* J-10-fl (DSM 635) at pH 7, amounting to a total carotenoid content of 0.94 % of the cell dry weight (cdw) and a bacteriochlorophyll content of 1.05 % of the cdw. Sulfide removal was high, amounting to more than 90 % in all conditions.

**Keywords**: Green non-sulfur bacteria, *Chloroflexus aurantiacus*, $CO_2$ Capture, Photosynthetic Pigments, Polyhydroxyalkanoates, sulfide removal

# RESUMO

Recentemente, as atividades humanas têm impactado negativamente o planeta através da poluição plástica, emissões de $CO_2$, contribuindo para o aquecimento global e a libertação de compostos tóxicos associados à produção de pigmentos sintéticos. Consequentemente, surge a necessidade de implementar tecnologias sustentáveis para mitigar estes problemas. Uma solução promissora é a utilização de microrganismos fotossintéticos. Esta tese foca-se no desenvolvimento de um bioprocesso fotossintético que simultaneamente captura $CO_2$, o principal gás com efeito de estufa e remove sulfureto, enquanto são produzidos produtos de valor acrescentado como plásticos biodegradáveis (polyhydroxyalkanoatos ou PHA) e pigmentos naturais (carotenoides e bacteriochlorofila). Este bioprocesso explora a fixação de $CO_2$ pela bactéria verde não sulfurosa *C. aurantiacus*, que possui a capacidade única de fixar $CO_2$ utilizando vias alternativas ao ciclo de Calvin-Benson-Bassam, aumentando o armazenamento de PHA. Quatro estirpes diferentes de *C. aurantiacus* foram testadas em diferentes pH (7, 8, 9), temperatura (30, 50 ºC) e concentração de sulfureto (3, 5, 10, 20 mg S $L^{-1}$), em condições autotróficas e heterotróficas. Os resultados obtidos mostram que o melhor crescimento, produção de PHA e pigmentos, ocorreu em condições heterotróficas. Contudo, os coeficientes de rendimento calculados mostram que existiu fixação de $CO_2$ em condições autotróficas ainda que com crescimento mais lento. Testes envolvendo maiores concentrações de sulfureto e extrato de levedura poderão permitir uma maior fixação de $CO_2$ e crescimento autotrófico. A maior produção de PHA foi para a estirpe *C. aurantiacus* 244-3 (DSM 638) a pH 8, com 4.3 % de PHA dos VSS. A maior produção de pigmentos foi para a estirpe *C. aurantiacus* J-10-fl (DSM 635) a pH 7, com 0.94 % de carotenoides totais por peso seco e 1.05 % de bacterioclorofila por peso seco. A remoção de sulfureto foi elevada, sendo maior que 90 % em todas as condições.

**Keywords**: Green non-sulfur bacteria, Chloroflexus *aurantiacus*, $CO_2$ Capture, Photosynthetic Pigments, Polyhydroxyalkanoates

# CONTENTS

# LIST OF FIGURES

# LIST OF TABLES

# ABBREVIATIONS

| | |
|---|---|
| 3-HPB | 3-hydroxypropionate bi-cycle |
| CBB | Calvin-Benson-Bassam cycle |
| GG | Glycylglycine |
| GHG | Greenhouse gas |
| IC | Inorganic carbon |
| mcl | Medium Chain Length |
| PDT | photodynamic therapy |
| PET | Polyethylene terephthalate |
| PHA | Polyhydroxyalkanoates |
| PHB | poly(3-hydroxybutyrate) |
| PHV | Poly(3-hydroxyvalerate) |
| ROS | reactive oxygen species |
| rTCA | reductive tricarboxylic acid |
| SS | Soluble sulfide |
| TC | Total Carbon |
| TOC | Total Organic Carbon |
| TSS | Total Suspended Solids |
| UV | Ultraviolet radiation |
| VSS | Volatile Suspended Solids |

# 1

# INTRODUCTION

## 1.1 Plastic pollution

Plastic is a synthetic or natural material, made from organic polymers, which may be shaped when soft and then hardened to retain the given shape[1]. Plastic was originally developed to have specific applications in industry such as tubing or even parachutes and ropes during World War II[2]. It was only in the 1950s, 89 years after its invention, that plastic, most specifically polyethylene terephthalate (PET), a clear, strong, and light 100 % recyclable plastic, started to be used as disposable packaging[3]. Current statistics indicate an annual production of approximately 390 million metric tons of plastic worldwide[4].

However, the dependency on plastics from the petrochemical industry has turned it into a significant problem associated with its disposal. Plastic pollution poses one of the biggest threats to wildlife, especially marine life[5]. A striking example highlighting the magnitude of this problem is the Great Pacific Garbage Patch (Figure 1.1), a huge accumulation of plastics and microplastics in the Pacific Ocean that kills many animals and threatens coastal ecosystems every year.

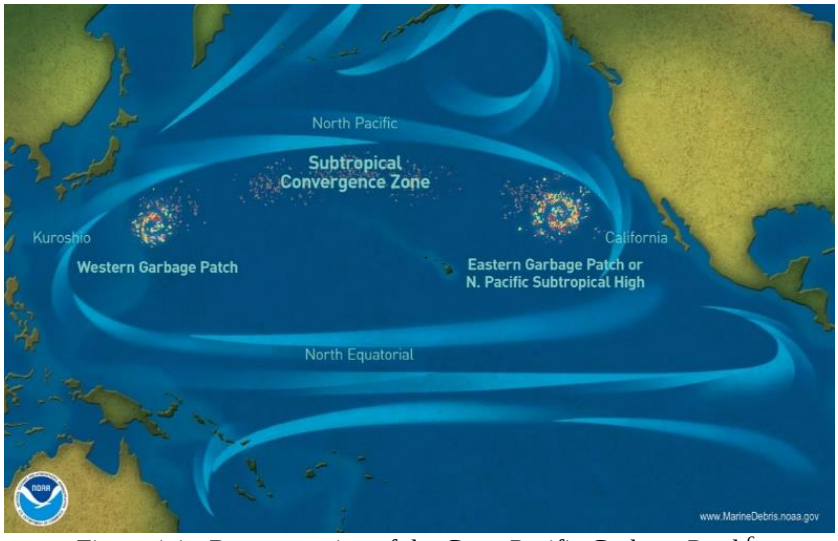


Figure 1.1 - Representation of the Great Pacific Garbage Patch[6].

Nowadays, there is a strong focus on addressing the plastic pollution problem, so several measures are being implemented, such as creating quality standards for secondary plastics, introducing mandatory rules on minimum recycled content in certain products and calls for a transition to bio-based, biodegradable, and compostable plastics[7].

### 1.1.1 Biodegradable bioplastics

Biodegradable plastics are plastics that degrade extensively in short periods, due to the attack of microorganisms such as bacteria and fungi via, for example, enzymatic action[8]. Bio-based plastics, on the other hand, are defined as plastics derived from biological material[9]. An example of a bio-based plastic could be bio-PET. Bio-PET is made from renewable raw materials, which makes it technically a bio-based plastic. However, despite being recyclable, it is not biodegradable[10].

On the other hand, polyhydroxyalkanoates (PHAs) are both biodegradable and bio-based plastics. These offer a promising solution to the plastic pollution problem, as they can be quickly decomposed by microorganisms naturally present in the environment[9,11], while at the same time posing as an alternative to fossil-based plastics. PHAs are biopolymers synthesized by several bacteria and some yeasts. It is decomposed in both anaerobic and aerobic environments, marine or terrestrial. If left alone in topsoil, it can take 60 to 140 days to naturally degrade[11], while PET takes 16 to 48 years[12].

At this time, the primary obstacle hindering the widespread adoption of biodegradable plastics like PHA is their cost and the competition from the huge market of compostable plastics[13], which are plastics that biodegrade under industrial composting conditions (e.g. Polylactic acid) or even under home composting (e.g. Mater-Bi) [9,14]. However, further advancements in PHA production could make it more readily available.

### 1.1.2 PHA synthesis

As previously mentioned, PHAs are being extensively studied as an alternative to non-degradable plastics. It is also a step closer to a sustainable economy[15].

The main PHA produced by bacteria is poly(3-hydroxybutyrate) (PHB)[16]. It is a fact that the commercial viability of a polymer relies heavily on key mechanical properties such as elongation at break, Young's modulus, and tensile strength. Regarding these properties, PHB is generally too brittle for many applications. However, technologies such as block copolymers, that is, molecules in which there is a linear arrangement in blocks, can be employed to enhance their elastomeric properties and overcome this limitation[15].

The biological synthesis of PHB begins with two molecules of acetoacetyl-CoA that, through the action of β-ketothiolase, form acetoacetyl-CoA. This is followed by an enzymatic reduction to form 3-Hydroxybutyryl-CoA. Finally, PHB is synthesized from this last precursor by PHA synthase. This is

described as pathway I in Figure 1.2. Pathways II and III both form other medium chain length (MCL) PHA and are more closely associated with fatty acid metabolism[17].

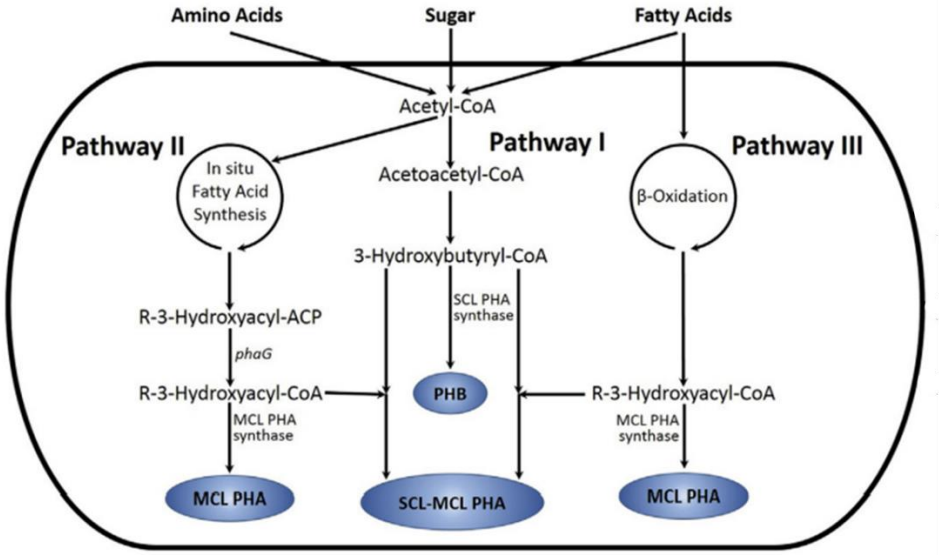


Figure 1.2 - Pathways for the biological synthesis of PHB and MCL PHA[17]. Adapted from: Chen et al. 2016

The price of PHA ranges between 2.4 and 5.5 US dollars per kilogram, significantly higher than that of synthetic plastics, which are typically sold at around 1.2 US dollars per kilogram[18]. The main reason for this difference is the cost of production. Nonetheless, better purification processes, access to cheaper electricity, and novel ways to produce PHA could decrease this price[18].

## 1.2 Global warming

Unfortunately, it is not just plastic pollution that affects our daily life on Earth. From rising temperatures that increase the occurrence of drought and wildfires to sea level rise that threatens coastal cities and marine life, global warming poses a significant threat to human, animal, and plant health[19]. It is an issue of utmost concern and as will be shown, several efforts have been, are being, and need to be made to prevent its consequences from being disastrous[20].

The primary greenhouse gas responsible for global warming is carbon dioxide ($CO_2$). Unfortunately, the concentration of $CO_2$ in the Earth's atmosphere has been steadily rising due to an increase in its emissions over the last century (Figure 1.3).

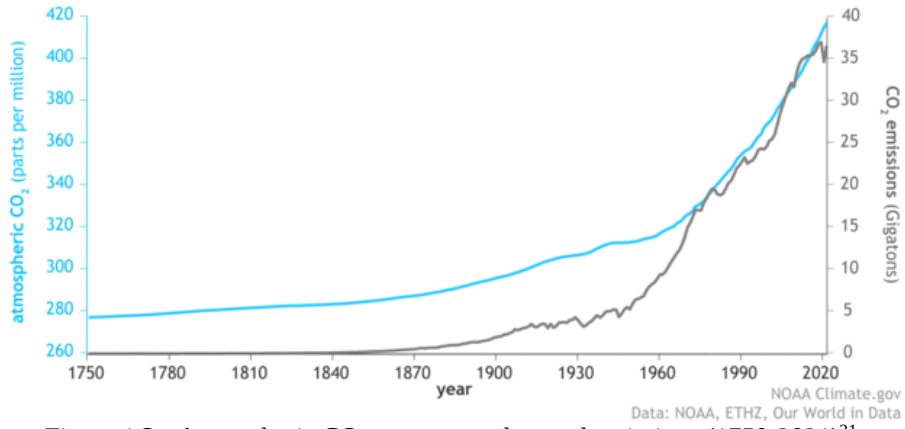


Figure 1.3 - Atmospheric $CO_2$ amounts and annual emissions (1750-2021)[21].

An even bigger cause for concern is the fact that the $CO_2$ levels in the past eight hundred thousand years have never been higher so we are seeing something unprecedented happening (Figure 1.4).

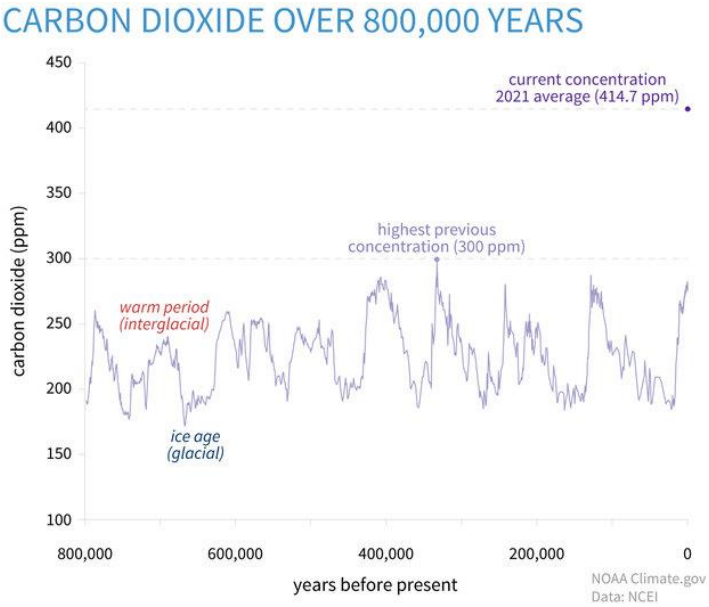


Figure 1.4 – Parts per million (ppm) of $CO_2$ in the atmosphere, over the last 800,000 years[21].

The high amount of $CO_2$ in the atmosphere can also have other consequences than "just" warming our planet. Following the reaction shown in equation 1, $CO_2$ can cause a decrease in water pH, leading to ocean acidification. Ocean acidification affects calcification, larval development, and the population equilibrium of ecosystems[22].

$$Equation\ (1):$$

$$CO_2 + H_2O \leftrightarrow H^+ + HCO_3^-$$

As a result of these concerns, numerous solutions have been proposed to mitigate the accumulation of $CO_2$ in the atmosphere. These solutions range from reducing emissions, by setting internationally agreed emission targets for example, to capturing $CO_2$ directly from the atmosphere. This last goal

can be achieved by promoting the growth of trees and protecting the existing forests since trees act as natural carbon sinks. Other novel technologies, such as the use of microorganisms which is the process addressed in this thesis, can also contribute to the capture of $CO_2$ and its transformation into value-added products, such as natural pigments and biodegradable plastics.

### 1.2.1 Biological technologies for $CO_2$ fixation

Converting $CO_2$ into valuable fuels, chemicals, and materials is a crucial strategy for capturing, sequestering, and utilizing $CO_2$ effectively. In nature, the conversion of $CO_2$ into organic substances is a fundamental process supporting life and serving as the foundation for biological evolution (Figure 1.5).

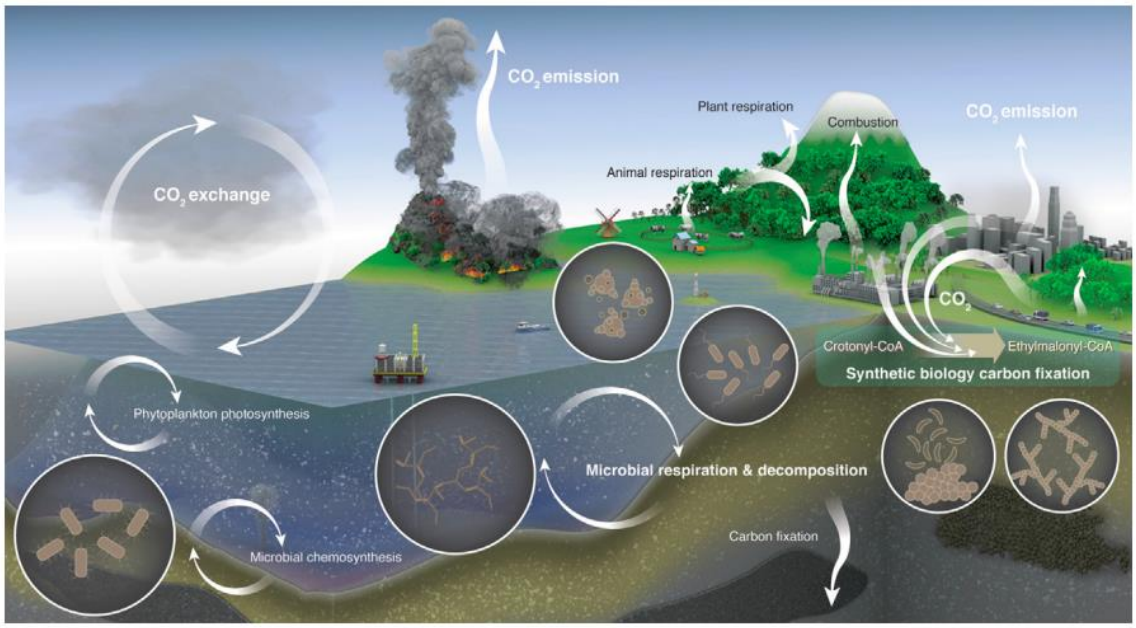


Figure 1.5 - The carbon cycle on Earth: human-caused natural carbon emissions and natural carbon sequestration pathways[23].

Several microorganisms are able to capture $CO_2$ from their surroundings, integrating it into their metabolic processes. They not only utilize $CO_2$ as a carbon source for growth but also employ it to regulate reductive power within their cells. This is because the reduction of $CO_2$ into organic compounds frequently necessitates the transfer of electrons and the involvement of reductive power carriers such as NADH or NADPH. The availability of these electron carriers and their redox state can influence the rate of $CO_2$ fixation and subsequent metabolic pathways. In this way, $CO_2$ utilization can be regulated to match the cellular redox requirements[24].

#### 1.2.1.1 Calvin-Benson-Bassam cycle

The Calvin-Benson-Bassam (CBB) cycle was discovered in 1950 and stands as one of the most well-known mechanisms of carbon assimilation. It is found in all types of plants, algae, microalgae,

cyanobacteria, and purple bacteria. It is also present in green non-sulfur bacteria like *C. aurantiacus*. This cycle constitutes the second phase of photosynthesis, succeeding the capture of solar energy in the light-dependent reactions. Its primary purpose lies in the conversion of $CO_2$ and energy-rich molecules (ATP and NADPH), produced during light-dependent reactions, into glucose and other essential organic compounds. A key enzyme, Ribulose-1,5-bisphosphate carboxylase/oxygenase (RuBisCO), which is the most abundant protein globally, catalyzes the reduction of $CO_2$ into carbohydrates in the CBB cycle[23]. Typically, purple bacteria and cyanobacteria can fix $CO_2$ via the CBB cycle, generating biomass with the potential to be further valorized in value compounds such as carbohydrates (e.g. glycogen) but resulting in a low PHB content[25] (Figure 1.6).

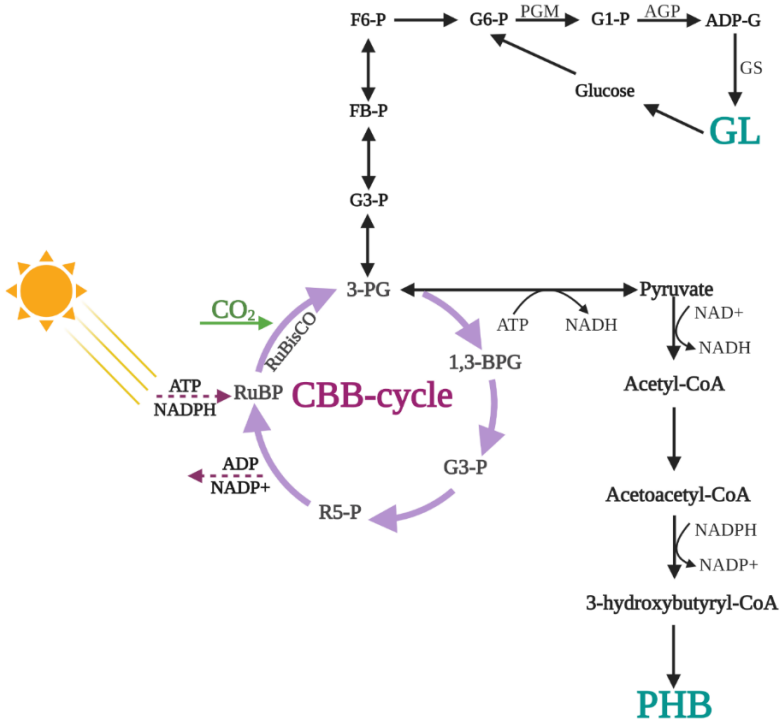


Figure 1.6 - Metabolic pathway for carbon assimilation and production of glycogen (GL) and PHB by cyanobacteria through the CBB cycle: ADP, adenosine–diphosphate; ADP–G, ADP–glucose pyrophosphorylase; AGP, adenosine diphosphate glucose pyrophosphorylase; ATP, adenosine-triphosphate; FB–P, fructose–1,6–bisphosphate; F6–P, fructose 6–phosphate; GS, glycogen synthase; G1–P, glucose–1–phosphate; G3–P, glyceraldehyde–3–phosphate; G6–P, glucose–6–phosphate; NADH, nicotinamide adenine dinucleotide (reduced); $NAD^+$, nicotinamide adenine dinucleotide (oxidized); NADPH, nicotinamide adenine dinucleotide phosphate (reduced); $NADP^+$, nicotinamide adenine dinucleotide phosphate (oxidized); PGM, phosphoglucomutase; RuBisCO, ribulose–1,5–biphosphate carboxylase/oxygenase; RuBP, ribulose–1,5–bisphosphate; R5–P, ribulose 5–phosphate; 3–PG, 3–phosphoglycerate[25].

Alongside the CBB cycle, there are five other natural $CO_2$ fixation pathways, reflecting the diverse array of organisms and ecological niches. One of these pathways is the reductive tricarboxylic acid (rTCA) cycle, prevalent among extremophile microorganisms. In this cycle, $CO_2$ is fixed to synthesize pyruvate and alpha-ketoglutarate. Another pathway is the reductive acetyl-CoA pathway, favored by anaerobic prokaryotes living close to the thermodynamic limit, such as acetogenic bacteria and methanogenic archaea. In this noncyclic route, one $CO_2$ molecule is reduced to CO, while another is

reduced to a methyl group, ultimately leading to the synthesis of acetyl-CoA. This pathway is the most favorable in terms of energy, but it requires many trace metals (Fe, Co, Ni, Mo, or W) as constituents of enzymes or coenzymes. Furthermore, the key enzyme, CO dehydrogenase/acetyl-CoA synthase, is among the most oxygen-sensitive enzymes known. Inorganic compounds such as CO and $H_2$ are used as energy sources[23].

Recently, two alternative carbon-fixation pathways, collectively known as the 4-hydroxybutyrate cycles, have been described: the Hydroxypropionate/4-hydroxybutyrate (HP/HB) cycle and the dicarboxylate/4-hydroxybutyrate (DC/HB) cycle. Both pathways yield acetyl-CoA as the final product but differ in their connection to carbon metabolism and oxygen sensitivity. Additionally, there is the 3-Hydroxypropionate bicycle, discovered in *Chloroflexus aurantiacus* (*C. aurantiacus*), which will be explored in detail in the following section. These diverse pathways illustrate the remarkable adaptability of organisms and their ability to harness and utilize carbon resources in several ways[26].

#### 1.2.1.2 3-Hydroxypropionate bi-cycle

A novel pathway for $CO_2$ fixation, the 3-hydroxypropionate bi-cycle (3-HPB), has been reported in both *C. aurantiacus* and several archaea[27]. In this pathway, two molecules of $HCO_3^-$ are used to synthesize one molecule of pyruvate through a route that is divided into two cycles, as represented in Figure 1.7.

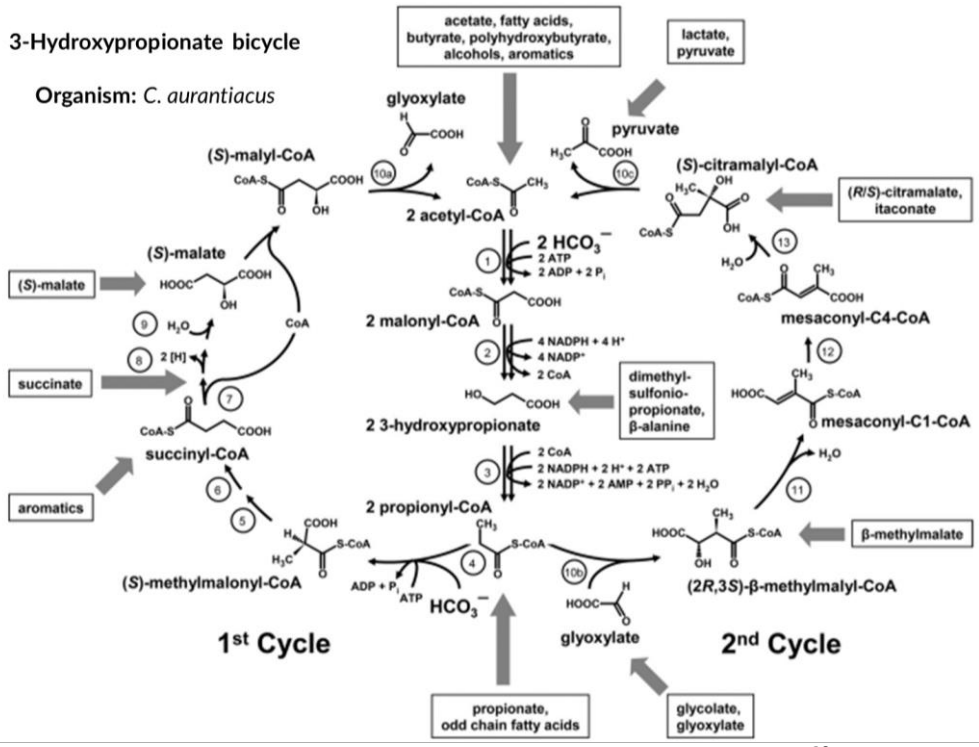


Figure 1.7 - Representation of the 3-hydroxypropionate bi-cycle, present in *C. aurantiacus*[28]. Adapted from: Hügler et al. 2005

It is called a bi-cycle since after the formation of propionyl-CoA, the reaction can move in the direction of assimilating another $HCO_3^-$ molecule (1st Cycle) or in the direction of formation of pyruvate (2nd Cycle).

Furthermore, the acetyl-CoA generated in the second stage, ensures the cycle's continuity, while the pyruvate produced from bicarbonate fixation serves as a precursor for biosynthesis[28,29].

*C. aurantiacus* is a facultative autotrophic species typically found in aquatic habitats. These microorganisms can co-assimilate trace amounts of organic compounds alongside $CO_2$. Under anoxic conditions, when more reduced organic substrates are assimilated, excess reducing equivalents are generated. The 3-HPB cycle is employed to fix $CO_2$, serving as a sink for these extra reducing equivalents. This unique capability of fixating $CO_2$ using routes alternative to the CBB cycle also increases its potential for the production and storage of PHA instead of glycogen. Given this, *C. aurantiacus'* utilization of this cycle makes it a very interesting species to explore[29].

## 1.3 Pigments

Colors have played a significant role in the social development of civilizations, from their use in cave paintings to their incorporation in various materials/formulations such as textiles, food, and cosmetics[30]. However, as the demand for more diverse, vibrant, and stable colors has grown, new synthetic pigments have emerged[31].

### 1.3.1 Synthetic pigments

Synthetic pigments are defined as pigments obtained by chemical synthesis, most often by introducing sulphonic or carboxyl groups into the natural dye molecule and, as the name suggests, they do not occur naturally in nature[32]. Some examples are alizarin, phthalocyanine, and azo pigments. However, these last ones, for example, have proven to be carcinogenic[33]. Others have been proven to cause DNA damage, in high concentrations, and in general, the untreated release of these pigments into the water by industries during the production process is a major public health concern[32]. Consequently, various methods have been explored to remove synthetic pigments from water, such as discoloration enzymatic treatment, using fungal laccases (EC 1.10.3.2)[30], or adsorption techniques[34].

Another approach to this problem is to diminish or stop the use of synthetic pigments, by providing a safer alternative.

### 1.3.2 Natural pigments

Natural pigments are colored substances derived from natural sources, such as minerals, plants, and insects[35]. Due to their genetic simplicity, when compared with plants, some microorganisms are also being engineered for the high-yield production of natural pigments[36].

As previously mentioned, the production of natural pigments can help reduce the number of synthetic pigments produced[37]. On top of that, their extraction from food waste and by-products in food industries also helps manage this waste[37]. They also offer a safer alternative to their synthetic counterparts. Carotenoids, such as carotenes, or even chlorophylls can be used as safe food coloring pigments[37]. Currently, due to their high fat-solubility, carotenoids can be seen in high-fat content products, such as meat products, soups, pickles, and snacks[37]

The food coloring market was valued at 3.71 billion USD in 2017 and has shown growth since then. Due to the human health concerns involving synthetic pigments, this market has always been dominated by natural pigments[37]. Carotenoids, as an example, hold significant commercial value, with market prices ranging from $350 to $7500 per kilogram[38].

Furthermore, bacteriochlorophyll (Bchl) has been shown to have skin anti-aging activities and antioxidant activities[39]. Another potential application of Bchl is related to the field of biomedicine, namely, in photodynamic therapy (PDT). PDT is a cancer treatment approach that relies on the administration of photothermal sensitizers into tumor tissue. These sensitizers are then activated by external light sources, generating local reactive oxygen species (ROS) in the presence of $O_2$, which are toxic to eukaryotic cells, killing the cancer cells. Some studies have been exploiting the use of Bchl as natural photosensitizers in this type of antitumoral strategy, due to both their very high extinction coefficients at long wavelengths, where light penetration into tissues is maximal, and to the presence of a central metal that contributes to the generation of ROS[40].

However, several challenges persist, particularly regarding the color stability, brightness, and intensity achieved with these natural pigments[37]. Nevertheless, developing a sustainable and effective method for producing natural pigments could present a solution to the environmental issues associated with synthetic pigment production and pave the way forward for the coloring industry.

## 1.4 Green Non-Sulfur Bacteria: *Chloroflexus aurantiacus*

*C. aurantiacus* is a filamentous green non-sulfur anoxygenic bacterium that belongs to the Chloroflexota phylum. It is classified as a thermophile and thrives within the optimal temperature range of 52 to 60ºC[41]. First discovered and studied in the late 1960s[42], *C. aurantiacus* exhibits a filamentous morphology, with filament lengths ranging from 0.6 to 0.7 µm, as illustrated in Figure 1.8.

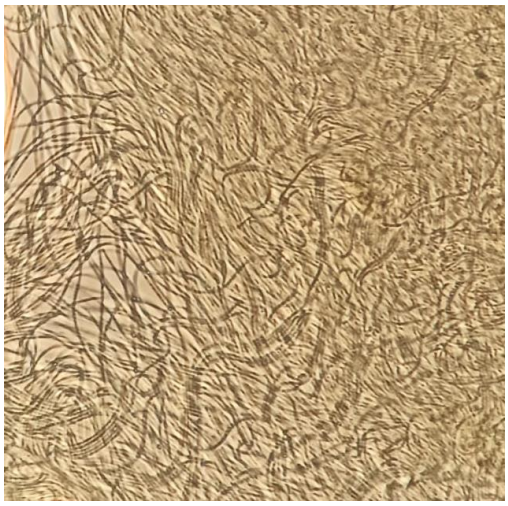

Figure 1.8 - *C. aurantiacus* Y-400-fl (DSM 637) as seen in the microscope, amplified 1000x. Anoxygenic growth conditions, under high light intensity, 4.8 W $L^{-1}$. The medium used was M1 (see section 2.3 Medium preparation2.3), supplied with sulfide for a final concentration of 10 mg S $L^{-1}$.

This remarkable bacterium is capable of growth under anaerobic or aerobic conditions. Under aerobic, dark conditions, it can grow chemoheterotrophically. Under anaerobic, illuminated conditions, it can grow photoheterotrophically or photoautotrophically, depending on whether the carbon source is organic or inorganic, respectively[43–45]. The best growth is achieved under anaerobic, highly illuminated conditions, with organic carbon as the carbon source, where production of PHB has been observed[41]. In photoautotrophic growth, *C. aurantiacus* utilizes the 3-hydroxypropionate bicycle to capture $CO_2$. Sulfide is used as an electron donor[41]. This metabolic versatility makes *C. aurantiacus* an interesting bacterium to explore.

Furthermore, *C. aurantiacus* demonstrates the ability to synthesize both bacteriochlorophyll *a* and *c*, along with carotenoids. Under low light intensity, the culture has a green color. Under high light intensity, the culture color is orange[41]. This happens because under low light intensity, the culture produces more Bchl to capture more light, which is scarce, resulting in a green color due to Bchl abundance. Under high light intensity however, this is not needed, and thus carotenoids are present in higher concentrations, producing the orange color[46].

The main carotenoids produced by *C. aurantiacus* are β-carotene and Ɣ-carotene[47]. As mentioned before, these hold significant value in the food coloring industry, but also beverage, nutraceuticals, and pharmaceuticals industry[48]. Consequently, exploring the production of these valuable byproducts in microorganisms like *C. aurantiacus* is of great interest.

Previous results show that *C. aurantiacus* is a very fast-adapting species, which can grow under different light intensities and adapt to different sulfide concentrations. These results also hint at the capacity of *C. aurantiacus* strain DSM 637, to utilize bicarbonate (from $Na_2CO_3$) as carbon source[49].

*C. aurantiacus* also showed the capacity for PHA production, being able to produce it in almost every condition where there was growth. Sulfide addition assured anaerobic and reductive conditions,

while reducing contaminations, since many organisms are not able to tolerate it at the concentration levels that *C. aurantiacus* does. Previous work also hints that there are still challenges to be overcome when it comes to improving $CO_2$ fixation and utilization for growth[50].

## 1.5 Thesis objectives and outline

This thesis focused on the development of a photosynthetic sustainable bioprocess aimed at capturing $CO_2$, which is the most important GHG, and the simultaneous removal of sulfide while producing value-added products, such as PHA and natural pigments, in a single-stage process. This biotechnology is based on the fixation of $CO_2$ by anoxygenic photosynthetic bacteria, more specifically, green non-sulfur bacteria like *C. aurantiacus*. Green non-sulfur bacteria have the unique capability of assimilating $CO_2$ using routes alternative to the CBB cycle, thus increasing the potential to store PHAs. In this context, the benefits of using $CO_2$ as a substrate for PHAs production are twofold: the production of cost-competitive bio-based and biodegradable polymers, which will reduce current dependency on plastic from the petrochemical industry, their associated pollution, and the concomitant mitigation of one of the most detrimental GHG. Thus, the main objective of this thesis was to explore the potential to produce value-added products (i.e. PHAS and photosynthetic pigments) by four different strains of *C. aurantiacus*: J-10-fl (DSM 635), OK-70-fl (DSM 636), Y-400-fl (DSM 637), and 244-3 (DSM 638) using $CO_2$ as carbon source and sulfide as electron donor.

Firstly, three tests with strain DSM 637 were conducted, to establish the relationship between biomass concentration as TSS and VSS with $OD_{610}$ and understand its capability of $CO_2$ fixation. Changes in parameters like medium composition, vitamin supplementation and sulfide adjustments were studied. Two abiotic controls were also performed.

Next, strains DSM 635, DMS 636 and DSM 638 were used for kinetic assays either in heterotrophic or autotrophic conditions.

Lastly, strain DSM 635 was subject to further tests involving sulfide adjustments, changes in pH and temperature.

# 2

# MATERIALS AND METHODS

## 2.1 Reactivation of dried cultures

Four different strains of *C. aurantiacus* were used, *C. aurantiacus* J-10-fl (DSM 635), *C. aurantiacus* OK-70-fl (DSM 636), *C. aurantiacus* Y-400-fl (DSM 637), and *C. aurantiacus* 244-3 (DSM 638), which were obtained from the culture collection of Leibniz Institute DSMZ – German Collection of Microorganisms and Cell Cultures GmbH (Braunschweig, Germany). These strains came as a lyophilized powder, inside a double-vial glass ampoule that was heat-sealed and under vacuum (Figure 2.1).

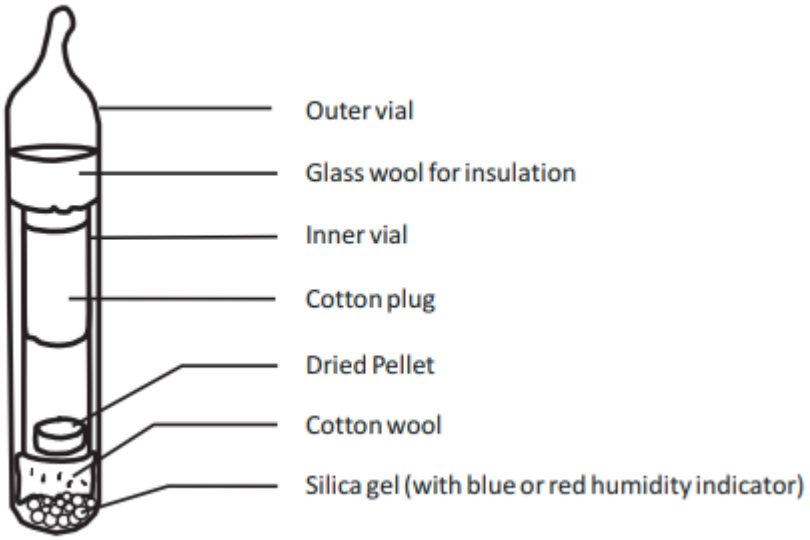


Figure 2.1 - Scheme of the double-vial glass ampoule as received from DSMZ.

All the work to reactivate the cultures was carried out under sterilized conditions, inside a flow chamber and next to a flame, while using previously sterilized material. The growth flasks were sterilized before and after being filled with the growth medium (M1, see section 2.3 Medium preparation). Sterilization was performed by autoclave at 120°C for 20 min. Ultraviolet radiation (UV) was used to sterilize the flow chamber. Next, a second UV cycle was done to sterilize the entirety of the material.

Firstly, the outer vial was heated with a flame for about 10-15 sec. Then, a few drops of medium were dropped onto the heated part, using a syringe, which cracked the glass. Then, using metal tongs, previously sterilized in the flame, the broken glass and insulating glass wool were removed. This made it possible to access the inner vial, which was removed in the same way. The dried pellet inside the inner vial was protected with a cotton plug. With a stream of sterile nitrogen ($N_2$), from a $N_2$ gas bottle fitted with a tube and a 0.2 µm sterile filter, directed to the vial, this cotton plug was removed. A needle was used at the tip of the filter to better direct the flow. After this step, 0.5 mL of sterile M1 was added to the vial using a sterile syringe. The mixture showed many black and white clusters. After 25 min, there were a few clumps, but they did not seem to be dissolving any further. Thus, the mixture was moved using a sterile syringe into a serum flask containing 30 mL of M1, supplemented with sulfide to a final concentration of ≈ 10 mg S $L^{-1}$. The flask was incubated at 50°C, 175 rpm, in a IKA incubator KS 3000i control (Germany) with an average light intensity of 73.49 W $m^2$ (4.78 W $L^{-1}$).

After the cultures reached the exponential phase, identified by the change in color and density of the culture, cryovials were prepared and used for inoculum preparation (see section 2.2 Cryovial preparation and section 2.4.1 Inoculum preparation, respectively). Strain DSM 637 was already available in the laboratory, preserved in cryovials.

## 2.2 Cryovial preparation

Reactivation of the cultures followed by their preservation as cryovials was conducted for strains DSM 635, DSM 636, and DSM 638.

For this, a solution of 20 % *v/v* glycerol was prepared inside a 50 mL serum flask, in deionized water, and closed using a butyl rubber stopper and aluminum caps. Sterile $N_2$ was used to flush the liquid phase to remove any oxygen. This was done using syringes and a 0.2 µm membrane filter, taking about 10 minutes. This serum flask was sterilized by autoclave at 120ºC for 20 min.

The empty cryovials were first autoclaved at 120°C for 20 min. After this step, inside a sterile flow chamber, 0.2 mL of the previously prepared 20 % *v/v* glycerol sterile solution was added using sterile syringes and needles. Then, 0.8 mL of cell culture, in the exponential phase, was added using sterile syringes and needles. The cryovials were closed and put in a freezer at -80ºC.

## 2.3 Medium preparation

The medium used throughout the experiments was M1 medium (M1, Table 2.1) from Leibniz Institute and M1-IC medium (M1-IC, Table 2.3), adapted from M1. Nevertheless, the medium composition changed through the batch test series, as will be explained in more detail in this section.

Table 2.1 - M1 composition for 1L.

| M1 (1L) | |
|---|---|
| Yeast extract | 0.947 g |
| Glycyl-glycine | 0.947 g |
| $Na_2HPO_4 \cdot 2H_2O$ | 0.095 g |
| $MgSO_4 \cdot 7H_2O$ | 0.095 g |
| $KNO_3$ | 0.095 g |
| $NaNO_3$ | 0.473 g |
| NaCl | 0.095 g |
| $CaCl_2 \cdot 2H_2O$ | 0.047 g |
| Fe(III) citrate solution (0.1 g 100 $mL^{-1}$) | 4.7 mL |
| Trace element solution SL-6 | 0.947 mL |

To prepare M1, a trace element solution (SL-6) was previously prepared, as shown in Table 2.2, and stored in the fridge at -4ºC.

Table 2.2- Trace element solution SL-6 composition for 1L.

| Trace element solution SL-6 (1L) | |
|---|---|
| $ZnSO_4 \cdot 7H_2O$ | 0.10 g |
| $MnCl_2 \cdot 4H_2O$ | 0.03 g |
| $H_3BO_3$ | 0.30 g |
| $CoCl_2 \cdot 6H_2O$ | 0.20 g |
| $CuCl_2 \cdot 2H_2O$ | 0.01 g |
| $NiCl_2 \cdot 6H_2O$ | 0.02 g |
| $Na_2MoO_4 \cdot 2H_2O$ | 0.03 g |

Calcium chloride ($CaCl_2$) was always added last during M1 preparation since it acts as a precipitating agent to any solid components added afterward. After all the components had been added, the volume was adjusted to 1L with distilled water, using a volumetric balloon, and the pH was adjusted to 8.2 using 6M sodium hydroxide (NaOH) and a 5012T Crison pH sensor (Switzerland).

The medium was transferred either to 90 mL serum flasks (illuminated area of 58.9 $cm^2$) or 500 mL Erlenmeyer flasks (illuminated area of 122 $cm^2$), depending on the test. The 90 mL serum flasks were closed using a butyl rubber stopper and aluminum caps. Sterile $N_2$ was used to flush the liquid phase to remove any oxygen. This was done using syringes and a 0.2 µm membrane filter, taking about 10 minutes. These flasks were then autoclaved for 20 min at 120ºC. The 500 mL Erlenmeyer flasks were autoclaved for 20 min at 120ºC using a regular Schott cap and then, inside a sterile flow chamber, the regular Schott cap was replaced by a sterile open cap fitted with a sterile rubber stopper. This procedure overcomes the rubber displacement that occurs in the autoclave due to pressure buildup in the flasks. The flasks were then flushed, inside the sterile flow chamber, with sterile $N_2$ using the same procedure

as the 90 mL flasks but for 15 min this time. After the flasks had been prepared with M1, sulfide was added from a neutralized sulfide solution (see section 2.3.2 Neutralized sulfide solution).

M1-IC medium was also used (tests 3, 4, 5, 7, 8). Its composition is shown in Table 2.3.

Table 2.3 - M1-IC composition for 1L.

| M1-IC (1L) | |
|---|---|
| $NH_4Cl$ | 0.36 g |
| $Na_2HPO_4 \cdot 2H_2O$ | 0.095 g |
| $MgSO_4 \cdot 7H_2O$ | 0.095 g |
| $KNO_3$ | 0.095 g |
| $NaNO_3$ | 0.473 g |
| NaCl | 0.095 g |
| $CaCl_2 \cdot 2H_2O$ | 0.047 g |
| Fe(III) citrate solution (0.1 g 100 $mL^{-1}$) | 4.7 mL |
| Trace element solution SL-6 | 0.947 mL |

As shown in Table 2.3, this medium contained 0,36 g $L^{-1}$ of ammonium chloride ($NH_4Cl$), to make sure the cultures had a nitrogen source for growth. The medium was prepared the same way as M1, but the pH was not adjusted (adjusted after $Na_2CO_3$ supplementation, see 2.3.3 Sodium carbonate solution). After the flasks had been prepared with M1-IC, YE and $Na_2CO_3$ were supplemented from a YE solution and $Na_2CO_3$ solution, respectively (see sections 2.3.4 Yeast extract solution and 2.3.3 Sodium carbonate solution, sulfide was added last). The final concentrations in the flasks were 0.0947 g YE $L^{-1}$ (10% of the amount in M1) and 12.96 g $Na_2CO_3$ $L^{-1}$. The amount of IC supplemented in this way was enough to compensate for the lack of GG and YE in this medium, corresponding to a final concentration of 1.47 g IC $L^{-1}$. The addition of YE was necessary to provide vitamins and nutrients, as the lack of YE could pose different limitations to the growth of *C. aurantiacus*.

### 2.3.1 Resazurin solution

To monitor the anaerobiosis of the flasks during the tests, a resazurin solution was used. For the preparation of this solution, 13 mg of resazurin sodium salt was mixed with 50 mL of distilled water in a 50 mL serum flask (for a final concentration of 260 mg $L^{-1}$).

From this solution, 0.9 mL was added to 90 mL test flasks, and 1.2 mL to 500 mL test flasks, for a final concentration of 0.6 mg $L^{-1}$.

Resazurin undergoes a series of reactions, depicted in Figure 2.2. First, the resazurin solution prepared is blue but after being added to the flasks, it undergoes a reduction reaction to resorufin, and the medium becomes pink. After this, depending on the reduction potential of the medium, resorufin can be further reduced to dihydroresorufin, which makes the medium colorless. This happens in redox potential of -110 mV or lower, thus, providing a good indicator for the test flask's anaerobiosis.


Figure 2.2 – Redox reactions undergone by resazurin. Resazurin shows a blue color, resorufin a pink color, and dihydroresorufin is colorless. The reaction from resazurin to resorufin is irreversible, while the reaction from resorufin to dihydroresorufin is reversible and only happens at -110 mV (reduction reaction).

### 2.3.2 Neutralized sulfide solution

In all the tests, the sulfide addition was done from a neutralized sulfide solution. This solution was prepared by adding 3 g of $Na_2S \cdot 9H_2O$, weighed using a scale inside a fume hood, to 100 mL of deionized water (previously flushed with sterile $N_2$ in the liquid phase to remove any oxygen), in a serum flask (for a final concentration of 4 g S $L^{-1}$). The flask was closed using a butyl rubber stopper and an aluminum cap, with a magnetic stirrer inside to mix the solution after the flask had been closed. This was done using needles and a 0.2 µm membrane filter, taking about 10 minutes. It was then autoclaved for 20 min at 120ºC. After that, the flask was left to cool down to room temperature, and the pH was adjusted using 2M $H_2SO_4$. The acid was added slowly, drop by drop, using sterile syringes and needles while mixing, to prevent the precipitation of elemental sulfur. This was done until the solution turned yellow and clear, meaning the pH was close to 8. A sample of the solution was taken with a sterile syringe and needle to verify the pH was equal to 8 (the desired pH since most of the tests were carried out at pH 8) with pH strips. Lastly, the exact concentration of the neutralized sulfide solution was measured according to section 2.5.2.1 Sulfide concentration.

This solution was added to the cultivation flasks in the batch tests. This was done inside a flow chamber, using sterile syringes and needles. A 2 L Tedlar® gas sampling bag (Sigma-Aldrich®, USA) filled with $N_2$ and connected to a 0.2 µm membrane filter and a needle was used each time to replace with $N_2$ the volume of sulfide solution taken from the flask, avoiding the entry of air into the flask.

### 2.3.3 Sodium carbonate solution

The $Na_2CO_3$ solution was prepared in a 500 mL volumetric balloon by thoroughly mixing 90g of $Na_2CO_3$ with distilled water (for a final concentration of 180 g $Na_2CO_3$ $L^{-1}$). The solution was then stored in a 500 mL Schott bottle closed using an open cap fitted with a rubber stopper. Sterile $N_2$ was used to flush the liquid phase to remove any oxygen. This was done using syringes and a 0.2 µm membrane filter, taking about 15 minutes. $Na_2CO_3$ dissociates in aqueous solution resulting in $CO_3^{2-}$, increases the solution pH. Thus, the pH of this solution is very high, meaning there is little $CO_2$ to escape during this process.

A volume of 36 mL of $Na_2CO_3$ was supplemented to 500 mL flasks as the source of IC in batch tests 4, 5, 7, and 8 and 7 mL of $Na_2CO_3$ was supplemented to 90 mL flasks in batch test 3, for a final concentration in the flasks of 12.96 g $Na_2CO_3$ $L^{-1}$ (1.47 g IC $L^{-1}$). This step was done inside a flow chamber, using sterile syringes and needles. Since the $Na_2CO_3$ solution was not autoclaved, a 0.2 µm membrane filter was used between the syringe and the needle to filter the solution while adding it to the flasks. A gas sampling bag connected to a 0.2 µm membrane filter and a needle were used each time to replace the volume taken with $N_2$.

After adding $Na_2CO_3$, the pH of the flasks increased and was adjusted with 6M HCL. This was done using sterile syringes and needles, to take samples from the flasks, and to measure the pH with MQuant® pH strips (Burlington, USA). These strips measure the pH in a range from pH 0 to pH 14 in a 1 pH degree of change.

### 2.3.4 Yeast extract solution

The YE solution (100 g $L^{-1}$) was prepared in a 50 mL volumetric balloon by mixing 5 g of YE with deionized water. The solution was then stored in a 50 mL serum flask closed using a butyl rubber stopper and an aluminum cap. Sterile $N_2$ was used to flush the liquid phase to remove any oxygen. This was done using needles and a 0.2 µm membrane filter, taking about 10 minutes. Then, the solution was autoclaved for 20 min at 120ºC.

YE was supplemented to the flasks in batch tests 4, 5, 7, and 8. This step was done in sterile conditions with the assistance of a gas sampling bag filled with $N_2$.

### 2.3.5 Vitamins stock solution

A vitamins stock solution was prepared for batch test 5, according to Table 2.4. From this stock solution, 1 mL was transferred to the 500 mL batch test flasks. This was done before inoculation, in sterile conditions, with the assistance of a gas sampling bag filled with $N_2$. The final quantity of each vitamin in the test flasks is also shown in Table 2.4.

Table 2.4 – Vitamin stock solution composition for 50 mL and final quantity in the batch test 5 flasks.

| Vitamin | Stock solution (50 mL) | M1-IC (500 mL) |
|---|---|---|
| Cobalamin (B12) | 10000 µg | 100 µg |
| Calcium D-panthothenate (B5) | 5000 µg | 50 µg |
| Biotin (B7) | 10000 µg | 100 µg |
| 4-aminobenzoic acid (B10) | 50 µg | 0,5 µg |
| Thiamine (B1) | 3000 µg | 30 µg |

## 2.4 Experimental procedures

### 2.4.1 Inoculum preparation

Figure 2.3 shows the timeline representation of inoculum preparation and the batch tests carried out. To begin with, from cryovials of *C. aurantiacus*, the culture was revived by growing it in anaerobic conditions in 100 mL of serum flasks containing 90 mL of M1 (see section 2.3 Medium preparation) and incubated at 175 rpm, 50ºC with continuous illumination of 4.6 W $L^{-1}$ (70 W $m^{-2}$). Once the culture reached the exponential growth phase, which took about 5 days in most cases, the inocula for the batch tests were prepared, in detail: 5 mL of the revived culture was added into 90 mL serum flasks containing M1 (tests 1, 6, 9, and 10), 250 mL shake Erlenmeyer flask (test 1), 500 mL Erlenmeyer flasks containing M1 (tests 6, 9, and 10), 90 mL serum flasks containing M1-IC and 100 % *w/v* of YE (tests 4, 5, 7 and 8), 500 mL Erlenmeyer flasks containing M1-IC and 100 % *w/v* of YE (tests 4, 5, 7 and 8), and incubated at 175 rpm, 50ºC with continuous illumination. After ≈3 days, the inocula reached the exponential growth phase, and the cultivation broth was harvested and resuspended in the batch tests flasks targeting an initial optical density (OD) of 0.05 (0.062 ± 0.034 is the average value obtained for all the batch tests performed) at 610 nm in the corresponding medium (M1, and M1-IC and 10 % *w/v* of YE depending on the batch test). Batch Tests with M1-IC were carried out for up to 11 days, while tests with M1 were carried out for only 7 days due to the faster culture growth under M1 medium.

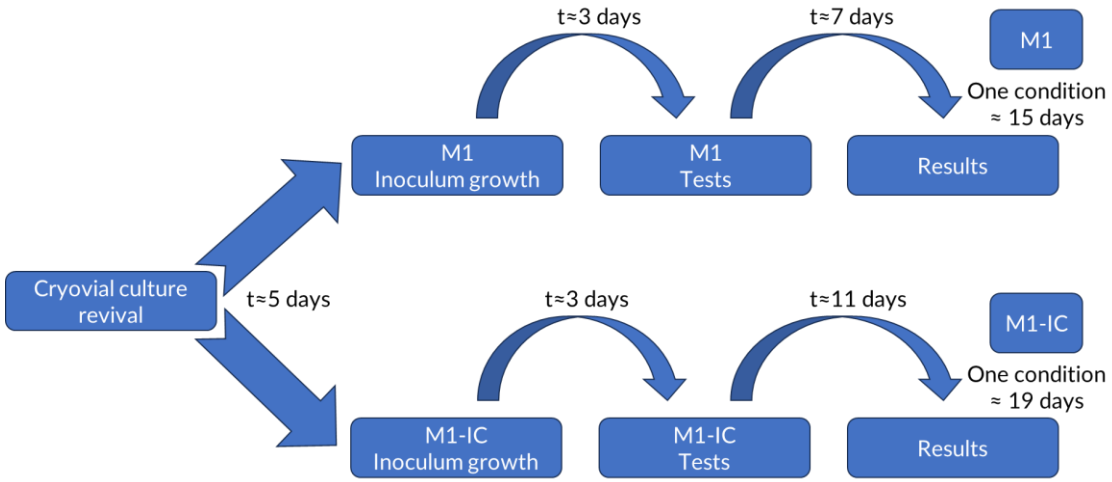


Figure 2.3 - Schematic of the full process and length of *C. aurantiacus* growth in M1, from the revival of the culture to the results of the test.

### 2.4.2 Methodology of the batch tests performed

Several batch test series were performed to evaluate the feasibility of $CO_2$ capture by *C. aurantiacus* coupled with the accumulation of PHA and photosynthetic pigments production through the impact of different initial sulfide concentrations, vitamin supplementation, ammonia supplementation,

sulfide adjustments, temperature, and pH of the cultivation broth. Figure 2.4 shows the experimental conditions of the different test series carried out.

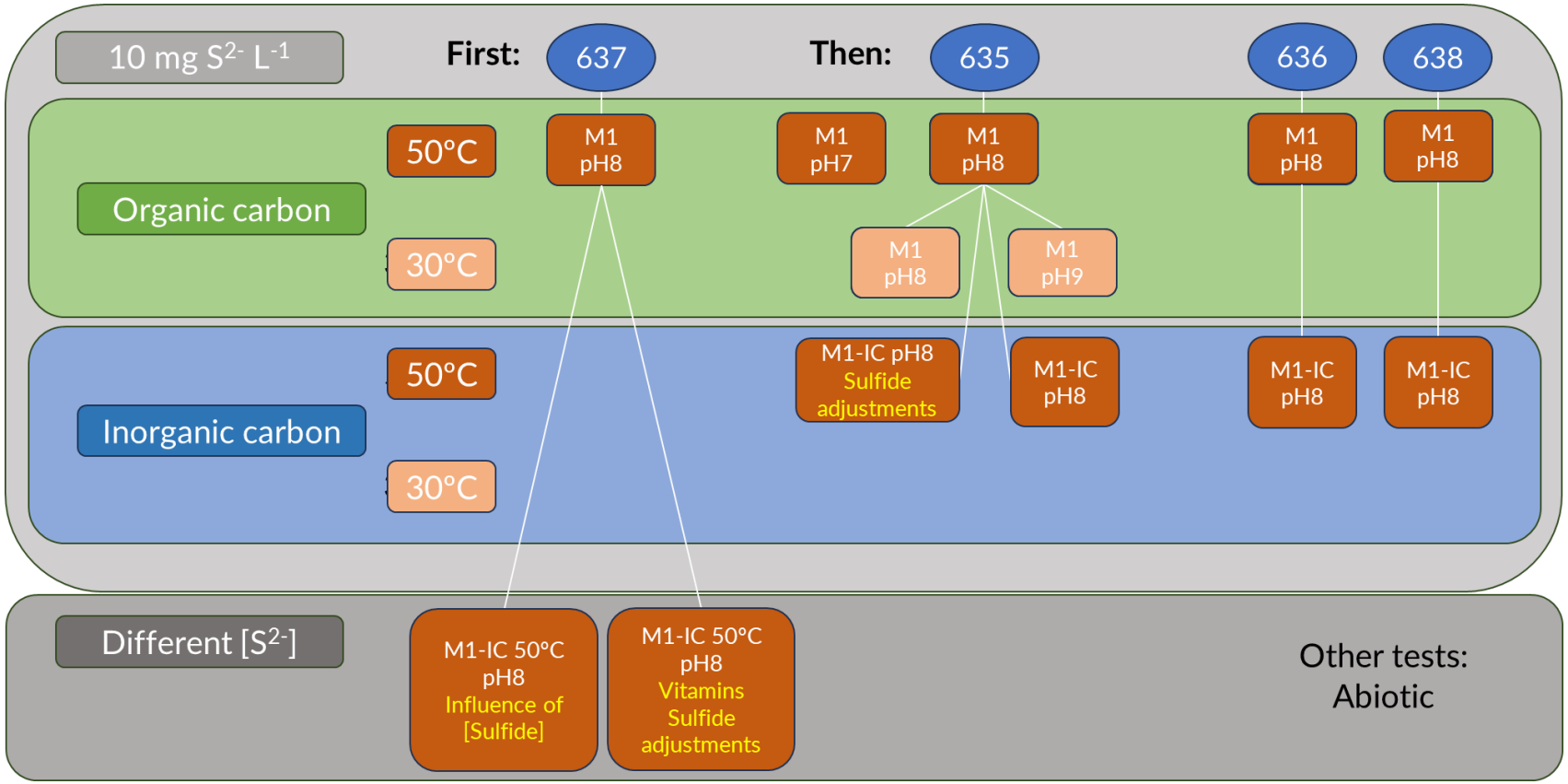


Figure 2.4 - Experimental conditions of the batch tests performed. Firstly, a series of tests were performed with *C. aurantiacus* strain DSM 637. Then, strains DSM 635, DSM 636 and DSM 638 were used.

#### 2.4.2.1 Test 1: Correlating biomass concentration as TSS and VSS with $OD_{610}$

The relationship between $OD_{610}$ and TSS and VSS of *C. aurantiacus* strain DSM 637 was evaluated in a single 250 mL Erlenmeyer flask containing M1 (illuminated area of 78.5 $cm^2$). The flask was supplemented with sulfide at 10 mg S $L^{-1}$. *C. aurantiacus* DSM 637 was used as the inoculum, for an initial $OD_{610}$ of 0.096. The culture was grown under continuous illumination of 75.3 W $m^{-2}$, corresponding to 4.77 W $L^{-1}$ for 96 hours. Samples for $OD_{610}$, pH, and sulfide analysis were taken every day. TSS and VSS measurements were done every day except for day 0. $OD_{610}$ was measured using a Camspec M509T single-beam spectrophotometer, always at a wavelength of 610 nm. The pH was measured using pH-measuring paper strips.

#### 2.4.2.2 Test 2: Influence of the environmental parameters on sulfide removal in abiotic control using M1

To rule out any potential S removal due to environmental conditions, such as sampling or temperature changes, an abiotic test was performed. This test was carried out with M1, in duplicates, in 90 mL serum flasks. The flasks were supplemented with sulfide at 15 mg S $L^{-1}$. The test was carried out for 96 hours. Samples for sulfide analysis and TOC analysis were taken at the beginning and the end of the test.

#### 2.4.2.3 Test 3: Influence of the environmental parameters on sulfide and IC removal in abiotic control

To rule out any potential sulfide removal due to adsorption or photolysis, another abiotic test was performed, where the influence of environmental parameters such as light was evaluated. This test was carried out with M1-IC, in duplicates (90 mL serum flasks). Two conditions were tested, where two replicates were covered in aluminum foil, in a way that no light could get in the flask, and two other replicates were not covered. All flasks were supplemented with sulfide at 20 mg S $L^{-1}$. The test was carried out for 96 hours. Samples for sulfide analysis and TOC analysis were taken at the beginning and the end of the test.

#### 2.4.2.4 Test 4: Influence of the sulfide concentration on the autotrophic growth and $CO_2$ fixation capability of *C. aurantiacus* strain DSM 637

The influence of sulfide concentration, together with a low concentration of YE and high concentration of IC, on *C. aurantiacus* DSM 637 growth and $CO_2$ fixation was evaluated. Four 500 mL Erlenmeyer flasks containing M1-IC were supplemented with four different sulfide amounts, at 20.6, 10.7, 5.8, and 3.3 mg S $L^{-1}$, respectively. *C. aurantiacus* DSM 637 was used as the inoculum, for an initial $OD_{610}$ of 0.052 ± 0.003 (average of all flasks). The cultures were grown under continuous illumination (see Table 2.5 for more details) for 93 hours. Samples for $OD_{610}$, pH, sulfide analysis, ammonium,

and phosphate analysis, VFA analysis, TOC analysis, PHA analysis and pigment analysis were taken every 24 hours from every flask. At the start and end of the exponential phase, TSS/VSS measurements were made. Inoculum characterization was done previously from inoculation of the batch tests

#### 2.4.2.5 Test 5: Exploring the capability of *C. aurantiacus* strain DSM 637 to grow autotrophically and utilize $CO_2$ with the support of vitamins

Four 500 mL Erlenmeyer flasks containing M1-IC were supplemented with a vitamin solution (1 mL was added in each flask from the Vitamins stock solution), and its influence on *C. aurantiacus* DSM 637 growth and $CO_2$ fixation was evaluated, in duplicates. The four 500 mL Erlenmeyer flasks were supplemented with different sulfide amounts, at 20.6 (2 flasks) and 10.7 (2 flasks) mg S $L^{-1}$. *C. aurantiacus* DSM 637 was used as the inoculum, for an initial $OD_{610}$ of 0.062 ± 0.005, and 0.105 ± 0.011, respectively. The cultures were grown under continuous illumination (see Table 2.5 for more details) for 95 hours. The replicates with 10.7 mg $L^{-1}$ of starting sulfide concentration were pulsed every 24 hours (except on day 0), with 1.2 mL of sulfide (10 mg $L^{-1}$) from the neutralized sulfide solution. Samples for OD, pH, sulfide analysis, ammonium, and phosphate analysis, VFA analysis, and TOC analysis, PHA analysis and pigment analysis were taken every 24 hours from every replicate. At the start and end of the exponential phase, TSS/VSS measurements were made. Inoculum characterization was done previously from inoculation of the batch tests

#### 2.4.2.6 Test 6: Exploring the capability of *C. aurantiacus* strains DSM 635, DSM 636, and DSM 638 to grow under heterotrophic conditions and synthesize value-added products

The ability of *C. aurantiacus* DSM 635, DSM 636, and DSM 638 to grow under heterotrophic conditions was evaluated, in duplicates. Six 500 mL Erlenmeyer flasks containing M1 were supplemented with sulfide at 10 mg S $L^{-1}$. Cultures of *C. aurantiacus* DSM 635, DSM 636, and DSM 638 were used as the inoculum, for an initial $OD_{610}$ of 0.026 ± 0.001 (2 flasks), 0.034 ± 0.016 (2 flasks), and 0.016 ± 0.001 (2 flasks), respectively. The cultures were grown under continuous illumination (see Table 2.5 for more details) for up to 216 hours. Samples for $OD_{610}$, pH, sulfide analysis, ammonium, and phosphate analysis, VFA analysis, and TOC analysis, PHA analysis and pigment analysis were taken every 24 hours from every replicate. At the start and end of the exponential phase, TSS/VSS measurements were made. Inoculum characterization was done previously from inoculation of the batch tests

#### 2.4.2.7 Test 7: Exploring the ability of *C. aurantiacus* strains DSM 635, DSM 636, and DSM 638 to grow autotrophically and utilize $CO_2$

The ability of *C. aurantiacus* DSM 635, DSM 636, and DSM 638 to grow under autotrophic conditions was evaluated, in duplicates. Six 500 mL Erlenmeyer flasks containing M1-IC were supplemented with sulfide at 10 mg S $L^{-1}$. Cultures of *C. aurantiacus* DSM 635, DSM 636, and DSM 638 were used as the inoculum, for an initial $OD_{610}$ of 0.070 ± 0.030 (2 flasks), 0.13 ± 0.016 (2 flasks), and 0.009 ± 0.004 (2 flasks), respectively. The cultures were grown under continuous illumination (see Table 2.5 for more details) for up to 216 hours. Samples for $OD_{610}$, pH, sulfide analysis, ammonium, and phosphate analysis, VFA analysis, and TOC analysis, PHA analysis and pigment analysis were taken every day from every replicate. At the start and end of the exponential phase, TSS/VSS measurements were made. Inoculum characterization was done previously from inoculation of the batch tests

#### 2.4.2.8 Test 8: Influence of sulfide adjustments on the autotrophic growth and $CO_2$ fixation capability of *C. aurantiacus* strain DSM 635

The influence of sulfide adjustments on *C. aurantiacus* DSM 635 growth and $CO_2$ fixation was evaluated. The test was carried out in duplicates. Two 500 mL Erlenmeyer flasks containing M1-IC were supplemented with sulfide at 10 mg S $L^{-1}$. *C. aurantiacus* DSM 635 was used as the inoculum, for an initial $OD_{610}$ of 0.101 ± 0.030. The cultures were grown under continuous illumination (see Table 2.5 for more details) for 168 hours. Sulfide pulses were given at 48h and 96h, where sulfide concentration was low (determined as described in 2.5.2.1.1 Quantitative determination of sulfide concentration). Samples for $OD_{610}$, pH, sulfide analysis, ammonium, and phosphate analysis, VFA analysis, and TOC analysis, PHA analysis and pigment analysis were taken every day from both replicates. At the start and end of the exponential phase, TSS/VSS measurements were made. Inoculum characterization was done previously from inoculation of the batch tests

#### 2.4.2.9 Test 9: Influence of pH on the heterotrophic growth and production of value-added products by *C. aurantiacus* strain DSM 635

The influence of pH on *C. aurantiacus* DSM 635 growth and production of value-added products was evaluated. The test was carried out in duplicates. Four 500 mL Erlenmeyer flasks containing M1 were supplemented with sulfide at 10 S mg $L^{-1}$. Two of the flasks were adjusted to pH 7 and two were adjusted to pH 9. *C. aurantiacus* DSM 635 was used as the inoculum, for an initial $OD_{610}$ of 0.69 ± 0.08 and 0.067 ± 0.014, respectively. The cultures were grown under continuous illumination (see Table 2.5 for more details) for up to 194 hours. Samples for $OD_{610}$, pH, sulfide analysis, ammonium, and phosphate analysis, VFA analysis, and TOC analysis, PHA analysis and pigment analysis were taken every day from both replicates. At the start and end of the exponential phase, TSS/VSS measurements were made. Inoculum characterization was done previously from inoculation of the batch tests

#### 2.4.2.10 Test 10: Influence of temperature on the heterotrophic growth of *C. aurantiacus* strain DSM 635

The influence of temperature on *C. aurantiacus* DSM 635 growth was evaluated. The test was carried out in duplicates. Four 500 mL Erlenmeyer flasks containing M1 were supplemented with sulfide at 10 mg S $L^{-1}$. Two of the flasks remained at the regular pH 8 and two were adjusted to pH 9. All flasks, however, were grown at 30ºC instead of the regular 50ºC. *C. aurantiacus* DSM 635 was used as the inoculum, for an initial $OD_{610}$ of 0.060 ± 0.03 and 0.055 ± 0.02, respectively. The cultures were grown under continuous illumination (see Table 2.5 for more details) for up to 170 hours. Samples for $OD_{610}$, pH, sulfide analysis, ammonium, and phosphate analysis, VFA analysis, and TOC analysis were taken every day from both replicates. Inoculum characterization was done previously from inoculation of the batch tests

Table 2.5 – Batch tests conditions.

| Batch Test Series | *C. aurantiacus* Strain | Medium | Temperature (ºC) | pH | Volumetric light intensity (W $L^{-1}$) | Sulfide Concentration (mg $L^{-1}$) |
|---|---|---|---|---|---|---|
| 1 | DSM 637 | M1 | 50 | 8 | 4.77 | 10 |
| 2 | Abiotic | M1 | 50 | 8 | 6.08 | 15 |
| 3 | Abiotic | M1-IC without $NH_4Cl$ | 50 | 8 | 0 | 20 |
| | | | | | 4.5 | |
| 4 | DSM 637 | M1-IC without $NH_4Cl$ | 50 | 8 | 2.54 W $L^{-1}$ | 20.6 |
| | | | | | 2.26 W $L^{-1}$ | 10.7 |
| | | | | | 2.60 W $L^{-1}$ | 5.8 |
| | | | | | 2.15 W $L^{-1}$ | 3.3 |
| 5 | DSM 637 | M1-IC | 50 | 8 | 2.40 ± 0.20 | 10.7 + Pulses |
| | | | | | 2.38 ± 0.32 | 20.6 |
| 6 | DSM 635 | M1 | 50 | 8 | 1.86 ± 0.10 | 20 |
| | DSM 636 | | | | 2.05 ± 0.14 | 20 |
| | DSM 638 | | | | 1.70 ± 0.11 | 20 |
| 7 | DSM 635 | M1-IC | 50 | 8 | 1.70 ± 0.07 | 10 |
| | DSM 636 | | | | 1.73 ± 0.05 | 10 |
| | DSM 638 | | | | 1.71 ± 0.03 | 10 |
| 8 | DSM 635 | M1-IC | 50 | 8 | 1.71 ± 0.03 | 10 + Pulses |
| 9 | DSM 635 | M1 | 50 | 7 | 1.72 ± 0.08 | 10 |
| | | | | 9 | 1.66 ± 0.15 | 10 |
| 10 | DSM 635 | M1 | 30 | 8 | 1.67 ± 0.12 | 10 |
| | | | | 9 | 1.36 ± 0.32 | 10 |

## 2.5 Analytical methods

### 2.5.1 Biomass valorization

#### 2.5.1.1 Photosynthetic pigments

Quantitative determination of BChl *a*, BChl *c*, and total carotenoids from wet biomass was carried out by adapting an organic solvent method[51]. 1.5 mL of the cultivation broth was centrifuged (10500 g, 3 min) and the supernatant was discarded using a syringe and needle, carefully so as not to lose any biomass. Then, 1.5 mL of acetone:methanol (7:2 *v/v*) solution was added to the pellet and incubated overnight at room temperature in the dark. After completion of extraction, the solution was centrifuged (10500 g, 3 min) and the supernatant was pipetted onto a quartz cuvette (Hellma Analytics, QS-10mm). A scan from 190 nm to 900 nm was performed by a UV-Vis M509T spectrophotometer (United Kingdom). Acetone:methanol (7:2 *v/v*) solution was used as blank.

For the conversion between absorbance and pigment concentration in grams of pigment per gram of cdw (g $g_{cdw}^{-1}$), the Lamber-Beer law was used (equation 2) where $c$ is the pigment concentration, $\varepsilon$ is the molar absorption coefficient in $g^{-1}$ $cm^{-1}$, $l$ is the optical path length in cm, and $Abs$ is the absorbance. Equations 3, 4, and 5 were used for Bchl *a*, Bchl *c*, and total carotenoids (TC), respectively[52,53]. In this case, an approximation of cdw ≈ TSS was used.

$$Equation\ (2):$$
$$Abs = \varepsilon * l * c$$

$$Equation\ (3):$$
$$Bchl\ a\ (\mathrm{g\ g_{cdw}}^{-1}) = \frac{Abs_{771\ nm}}{71.6\ g^{-1}\ cm^{-1} * 1\ cm} * \frac{1}{dcw\ (g)}$$

$$Equation\ (4):$$
$$Bchl\ c\ (\mathrm{g\ g_{cdw}}^{-1}) = \frac{Abs_{666\ nm}}{86\ g^{-1}\ cm^{-1} * 1\ cm} * \frac{1}{dcw\ (g)}$$

$$Equation\ (5),:$$
$$TC\ (\mathrm{g\ g_{cdw}}^{-1}) = \frac{Abs_{450\ nm}}{163.9\ g^{-1}\ cm^{-1} * 1\ cm} * \frac{1}{dcw\ (g)}$$

#### 2.5.1.2 PHA analysis

The PHA content in the batch test series was analyzed by gas chromatography (GC). For this, 1.5 mL of the cultivation broth was centrifuged (10500 g, 3 min) and the supernatant was discarded. Then, these pellets were lyophilized for 24h. A minimum of 2 mg from these pellets was weighed for each analysis and added to a Pyrez® tube. Afterward, 1 mL of acidic methanol 5% (v/v) $H_2SO_4$ was added to this tube, followed by 1 mL of chloroform (0.5 g $L^{-1}$ benzoic acid methyl ester as internal standard). The tubes were closed and digested in a SBH130D Stuart thermoblock (Biocote) for 2h at 100ºC. After this step, the tubes were left to cool down inside a fume hood. 1 mL of deionized water was added to each tube and a vortex was used for 45 seconds to mix efficiently the water and organic phase. The tubes were left to rest inside a fume hood for 1h until both phases were fully separated. A glass Pasteur pipette was used to remove the water phase (carefully not to remove organic phase). This process of adding and removing deionized water was repeated one more time. The organic phase was removed using glass Pasteur pipettes and added to a GC vial with molecular sieves. Finally, using a different pipette, the organic phase was removed from this vial and filtered with 0.22 µm PTFE filters to another GC vial. This vial was covered with aluminum caps and sealed.

The GC analysis was done using a Claurus 590 GC with a flame ionization detector from PerkinElmer, equipped with a Restek column (specifications: 60m, 0.53mmID, 1uM df). 1.5 µL of sample was injected and a run was performed at 14.50 psi for 32 min.

Standards were prepared by weighing ≈33 mg of a co-polymer of PHB-PHV (1 pellet) in 25 mL of chloroform (0.5 g $L^{-1}$ benzoic acid methyl ester). Then, seven standards with concentrations ranging from 0.73 (Standard 1) to zero (Standard 7) mg PHB $mL^{-1}$ and 0.12 (Standard 1) to zero (Standard 7) mg PHV $mL^{-1}$ were prepared and treated the same way as the samples.

### 2.5.2 Cultivation broth characterization

#### 2.5.2.1 TSS/VSS measurements

The total suspended solids (TSS) and volatile suspended solids (VSS) concentration (mg L-1) were measured using Whatman® glass microfiber filters, Grade GF/F (0.7 µm pore size and a 0.42 mm thickness), according to a standard method[54].

First, the filters were placed into a 550ºC Mufla for 45 min followed by 30 min in a 105ºC oven. Then, the filters were placed in the desiccator for 30 min and weighed.

1.5 mL of the cultivation broth was filtered and left in a 105ºC oven overnight. Before weighing the filters, these were left in a desiccator full of silica, for 30 min. The filters were weighed. Next, the filters went into a 550ºC Mufla for 45 min[54]. Then, the filters were placed in the 105ºC oven for 30 min and in the desiccator for 30 min. The filters were weighed. The values for TSS and VSS were calculated in the following way:

$$Equation\ (6):$$

$$TSS(mg\ l^{-1}) = \frac{Filter\ weight\ 105\ °C\ (mg) - Filter\ weight\ (mg)}{Volume\ Filtered\ (l)}$$

$$Equation\ (7):$$

$$VSS\ (mg\ l^{-1}) = \frac{Filter\ weight\ 105\ °C\ (mg) - Filter\ weight\ 550\ °C\ (mg)}{Volume\ Filtered\ (l)}$$

#### 2.5.2.1 Sulfide concentration

The sulfide concentration (mg S $L^{-1}$) of the reactors was measured throughout the experiments. Samples were taken for both soluble sulfide (SS) and total sulfide (TS) using the methylene blue method[54,55]. This method consists of a colorimetric reaction between the sulfide, ferric chloride ($FeCl_3$), and N,N-diethyl-p-phenylenediamine, resulting in the formation of methylene blue.

For the SS, 1.5 mL of culture was filtered using a 0.45 µm filter, into an empty Eppendorf. From this Eppendorf, 1 mL of the filtered sample was transferred using a pipette into another Eppendorf containing 100 µL of 0.5 M zinc acetate and 400 µL of 6M NaOH. The addition of zinc acetate effectively traps the sulfide present in the sample, preventing its evaporation in the form of hydrogen sulfide ($H_2S$), while the NaOH increases the pH, which must be around 9 for effective sulfide precipitation with zinc.

For the TS, 2 mL of cultivation broth was mixed with 2 mL of 6M HCL directly in the syringe used for the sampling. The HCl lowers the pH, making it possible for the acid-volatile metallic sulfides that may be present to solubilize. After this, 1.5 mL of this solution was filtered using a 0.45 µm filter into an Eppendorf containing a drop of zinc acetate at the bottom, added previously. From this Eppendorf, precisely 900 µL were pipetted onto another Eppendorf, containing 100 µL of 0.5 M zinc acetate and 500 µL of 6M NaOH. As mentioned previously, the pH must be around 9, so the addition of 500 µL of 6M NaOH instead of 400 µL serves to maintain this pH.

##### 2.5.2.1.1 Quantitative determination of sulfide concentration

First, 200 µL of the coloring reagent (0.4 g of N,N-dimethyl-p-phenylenediamine sulfate, and 0.6 g of $FeCl_3$ in 100 mL of 6 M HCl) was transferred into glass tubes using a micropipette. After this step, 200 µL of SS and ST samples were added. The mixture was left reacting for 15 min, then, 5 mL of 0.1 M HCL was added to each tube. The absorbance was then measured at 666 nm in a DR2800 Hach® spectrophotometer (Germany). A solution of 0.6 g of $FeCl_3$ in 100 mL of 6 M HCl was used as the blank.

#### 2.5.2.1.1 Sulfide calibration curve

To establish a correlation between the absorbance and sulfide concentration, a calibration curve was generated using a Hach® sulfide testing kit LCK 653 (Germany). 0.5 mL of the neutralized sulfide solution (4 g S $L^{-1}$, see section 2.3.2 Neutralized sulfide solution) was used to prepare solution A (50 mg S $L^{-1}$) in 40 mL of deionized water. Solution A was utilized to prepare six sulfide standards following the specified dilutions in Table 2.6.

All the standards and solution A were prepared inside serum flasks. Deionized water was added using regular glass pipettes. The serum flasks were then closed using a rubber stopper and a metal cap and flushed with $N_2$ for about 5 minutes. Both the neutralized sulfide solution and solution A were added to these serum flasks using Pressure Lok® precision analytical syringes (VICI Precision Sampling, Baton Rouge, Louisiana, USA). A cleaning step was done with deionized water between every transfer to remove residual sulfide inside the syringes. To use the sulfide testing kit, the tested solution must have a sulfide concentration between 0.1 to 2 mg $L^{-1}$, so standard 6 was used for this purpose. Since the dilution factor is known, the real concentration of sulfide in the neutralized sulfide solution was determined. A correlation between the concentration of the standards and their absorbance at 666 nm was used to plot a calibration curve (see Figure 7.1 in Supplementary materials).

Table 2.6 - Sulfide standards preparation, corresponding dilutions, and theoretical sulfide concentration.

| Standard | Solution A (mL) | Deionized water (mL) | Final Volume (mL) | Theoretical concentration (mg S $L^{-1}$) |
|---|---|---|---|---|
| 1 | 2 | 2 | 4 | 25 |
| 2 | 1.5 | 2.5 | 4 | 19 |
| 3 | 1 | 3 | 4 | 13 |
| 4 | 0.5 | 3.5 | 4 | 6.3 |
| 5 | 0.2 | 3.8 | 4 | 2.5 |
| 6 | 3 | 100 | 103 | 1.5 |

### 2.5.2.1 Total Organic Carbon and Inorganic Carbon

1.5 mL of cultivation broth and one drop of 6M NaOH were centrifuged at 10500 g for 3 minutes. The supernatant was removed using a syringe and needle and filtered with a 0.2 µm filter to a sampling tube of 5 ml. This tube was stored in a 4ºC fridge until further analysis of the total organic carbon (TOC) and inorganic carbon concentration (mg TOC $L^{-1}$ and mg IC $L^{-1}$, respectively).

The samples were diluted at 1:15 with deionized water. These were then analyzed in a Shimadzu TOC-VCSH analyzer (Jiangsu, China). Total carbon (TC) concentration in the cultivation broth was measured by catalytic oxidation. By heating the sample to 680ºC in the presence of a platinum catalyst, all the carbon present is vaporized and then quantified by a Nondispersive Infrared Sensor (NDIR). The

IC was measured by acidifying the sample. This makes IC concentration present to be released as $CO_2$ and quantified using the same sensor. TOC concentration was then calculated as an indirect measurement, by subtracting the IC from the TC.

#### 2.5.2.2 Ammonium and Phosphate quantification

Dissolved ammonium and phosphate were determined in the cultivation broth. 1.5 mL of the cultivation broth was centrifuged (10500 g, 3min), the supernatant was removed using a syringe and needle and filtered with a 0.2 µm filter to a sampling tube of 5 ml. This tube was stored in a 4ºC fridge until further analysis.

0.5 mL of the sample was diluted in 2 mL of deionized water, and ammonium and phosphate were determined using a Skalar Sann++ Segmented Flow Analyzer. This equipment allows for the quantification of both these species by performing colorimetric reactions.

The ammonium quantification was done by a modified Berthelot reaction. In this reaction, ammonia is buffered, dialyzed, and chlorinated to monochloramine which reacts with salicylate to 5-aminosalicylate. After oxidation and oxidative coupling, a green-colored complex is formed. The resulting absorbance of this complex is measured at 660 nm.

The phosphate quantification was done following the reaction of ammonium heptamolybdate with potassium antimony (III) oxide tartrate, in an acidic medium with diluted solutions of phosphate. This reaction forms an antimony-phosphomolybdate complex. This complex is reduced to an intensely blue-colored complex by L(+)ascorbic acid. The resulting absorbance of this last complex was measured at 880 nm.

Since the detection range of this analysis ranges from 0.2 to 20 mg P $L^{-1}$ and 0.2 to 20 N $L^{-1}$ (ppm), the necessary dilutions to the sample were performed using deionized water.

#### 2.5.2.1 Volatile Fatty Acids

VFAs concentrations (mg $L^{-1}$) of acetic acid, propionic acid, isobutyric acid, butyric acid, isovaleric acid, and valeric acid were determined in the cultivation broth. 1.5 mL of the cultivation broth was centrifuged (10500 g, 3min), the supernatant was removed using a syringe and needle and filtered with a 0.2 µm filter to a sampling tube of 5 ml. This tube was stored in a 4ºC fridge until further analysis.

Samples of 1.5 mL were acidified with one drop of $H_2SO_4$ (0.01N) for the determination of VFA concentration. The analysis was performed in a VWR Hitachi Chromaster HPLC (China), equipped with a pump 5160, autosampler 5260, column Oven 5310, diode array detector 5430, RI detector 5450, and the column used was the Aminex HPX-87H 300x7.8MM from Biorad with 0.01 N $H_2SO_4$ as eluent. The run was done at 30ºC, with a flow rate of 0.5 mL $min^{-1}$ and an injection volume of 99 uL.

#### 2.5.2.1.1 Volatile Fatty Acids calibration curve

To prepare the VFAs standards, a mother solution was first prepared. For this, 25 mg of each VFA were weighed, inside a fume hood, and added to a 25 mL volumetric balloon. The volume was adjusted using 0.01N $H_2SO_4$ filtered (0.20 µm). The final concentration in the mother solution was ~1 g $L^{-1}$ of each VFA. Next, standard 1 was prepared by adding, in small volumetric balloons, 1.4 mL of this mother solution to 8.6 mL of 0.01N $H_2SO_4$, for a total volume of 10 mL and a final concentration of 140 mg $L^{-1}$. The other standards were prepared from standard 1 according to Table 2.7. Finally, 1.5 mL of each standard was added to HPLC autosampler vials and analyzed in the same conditions as the samples. A correlation between the concentration of the standards and their area was used to plot a calibration curve.

Table 2.7 – VFA standards preparation, corresponding dilutions, and theoretical VFA concentration.

| Standard | Mother solution (mL) | Standard 1 (mL) | 0.01N $H_2SO_4$ (mL) | VFA concentration (mg $L^{-1}$) |
|---|---|---|---|---|
| 1 | 1.4 | - | 8.6 | 140 |
| 2 | - | 2.8 | 1.2 | 98 |
| 3 | - | 1.6 | 2.4 | 84 |
| 4 | - | 0.80 | 3.2 | 28 |
| 5 | - | 0.20 | 3.8 | 7.0 |

### 2.5.3 Light intensity measurements

The light intensity was measured using a LI-COR LI-250A Light Meter, connected to a LI-200SA Pyranometer. The batch tests were carried out inside an incubator, set to the temperature of 50ºC and 175 rpm. Each position in the incubator was measured as shown in Figure 2.5 and when necessary, an average was calculated. The surface area considered was half the one calculated by the shape formula since only one side of each flask was illuminated by the light source. This corresponds to the illuminated area (Table 2.8). A 28 W halogen light bulb was fitted in a desktop lamp holder. The illumination was directed to the flasks to attain the same light intensity in all the flasks.

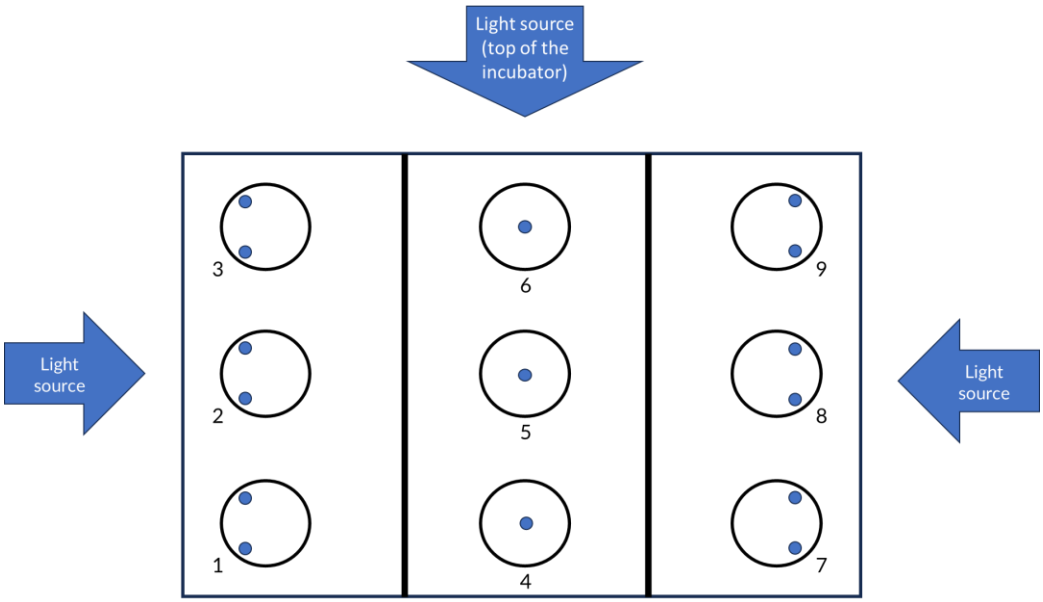


Figure 2.5 – Schematic representation of the light measurements done in the incubator used for the batch tests. The blue dots represent the positions where light intensity was measured. The numbers represent the position in the incubator, Position 1, Position 2, etc. The blue arrows show the position and the direction of the light sources. Positions 4, 5, and 6 were illuminated from lamps placed directly above the incubator.

For the conversion between W $m^2$ and W $L^{-1.}$ the flask dimensions were necessary. These are shown in Table 2.8.

Table 2.8 - Flask dimensions, corresponding shape, and illuminated area.

| Working Volume (mL) | Radius (cm) | Height (cm) | Slant height (cm) | Shape | Illuminated area ($cm^2$) |
|---|---|---|---|---|---|
| 500 | 5 | 15 | 15.5 | Cone | 122 |
| 250 | 4 | 12 | 12.5 | Cone | 78.5 |
| 90 | 2.5 | 7.5 | - | Cylinder | 58.9 |

## 2.6 Calculation of kinetic and stoichiometric parameters

To better understand the results, the maximum specific growth rate ($\mu_{max}$), biomass productivity and doubling time were calculated (equations 8, 9 and 10, respectively).

$$Equation\ (8):$$

$$Maximum\ specific\ growth\ rate\ (\ d^{-1}) = \left(\frac{\ln VSS_n - \ln VSS_0}{t_n - t_0}\right) * 24$$

$$Equation\ (9):$$

$$Biomass\ productivity\ (mg\ L^{-1}d^{-1}) = \left(\frac{VSS_n - VSS_0}{t_n - t_0}\right) * 24$$

$$Equation\ (10):$$

$$Doubling\ time\ (d) = \frac{\ln 2}{\mu_{max}}$$

The removal efficiency was also calculated to better analyze sulfide, IC, and organic carbon removal (equation 11).

$$Equation\ (11):$$

$$Removal\ efficiency\ (\%) = \frac{Concentration_0 - Concentration_n}{Concentration_0} * 100$$

Finally, the biomass yield was calculated to showcase the $CO_2$ fixation capabilities of *C. aurantiacus* (equation 12). For this, VSS was assumed to be a measure of the active biomass since the amount of PHA and glycogen is low. Furthermore, 50 % of this biomass was assumed to be carbon[56].

$$Equation\ (12):$$

$$Biomass\ Yield = \frac{g\ C_{active\ biomass}}{g\ C_{Substrate}} = \frac{(VSS_n - VSS_0) * 0.5}{g\ C_{medium}}$$

.

# 3

# RESULTS AND DISCUSSION

## 3.1 Test 1: Correlating biomass concentration as TSS and VSS with $OD_{610}$

Test series 1 had the goal of making possible an indirect calculation of TSS and VSS from an $OD_{610}$ value. This is useful since the $OD_{610}$ is a quick and cheap measurement, while the conventional way of measuring TSS and VSS requires more time and material. This test was carried out in a 250 mL flask with M1 at 50ºC, pH 8, with a light intensity of 4.77 W $L^{-1}$.

Figure 3.1A shows the growth profile of *C. aurantiacus* DSM 637. As shown, growth was observed until the $OD_{610}$ was close to 1, reached at 72h. Sulfide removal was 57 % at the end of the test (96h). The error bars are small because a technical replica was used, meaning there were two measurements of $OD_{610}$ from the same flask.

The maximum specific growth rate was achieved at 24h, with a value of 0.660 $d^{-1}$. Biomass productivity and time of duplication were also calculated at 24h with values of 166 mg $L^{-1}$ $d^{-1}$ and 1.05 d, respectively. These results are also shown in Table 3.3 where they are compared with the other *C. aurantiacus* strains.

Figure 3.1B shows the linear adjustment made to establish the relationship between TSS and $OD_{610}$. The same was done for VSS, as shown in Figure 3.1C. Both show a good fit with $R^2$ higher than 0.98.

Figure 3.1D represents the relationship between VSS and TSS. A linear adjustment was done and an ash content of 9.3 % was calculated based on this adjustment, which showed an $R^2 = 0.99$.

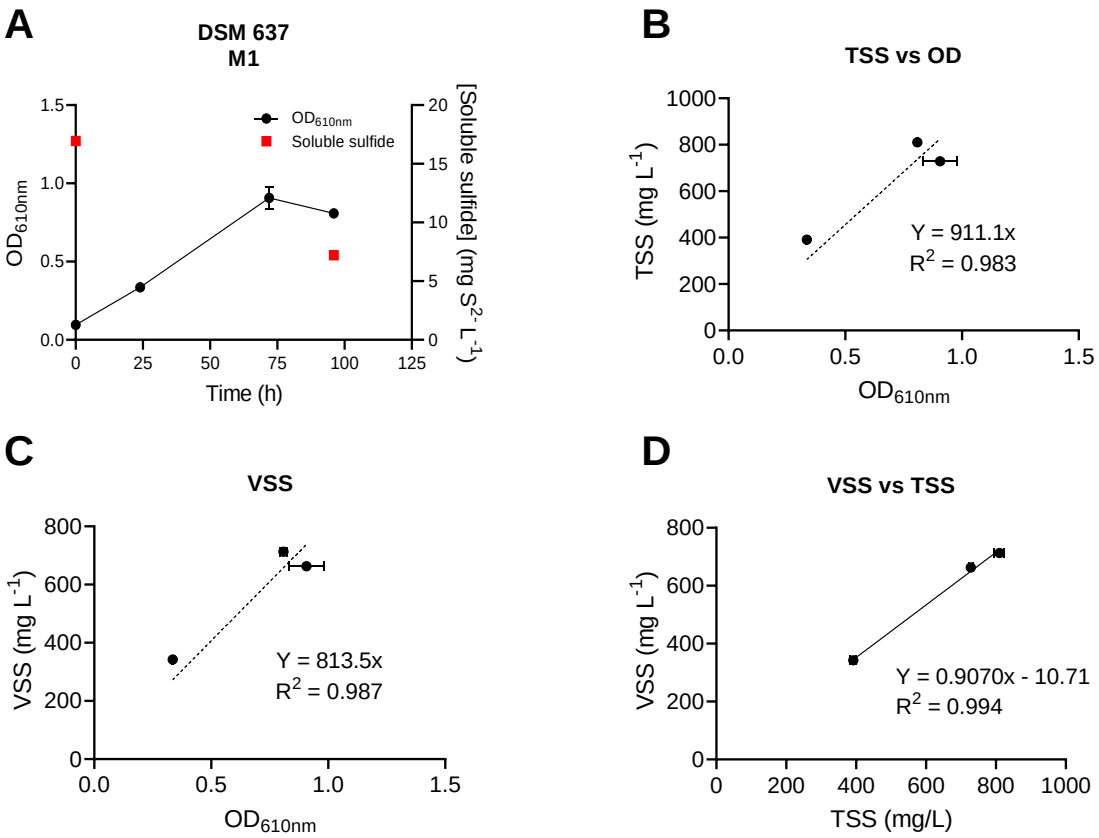


Figure 3.1 – *C. aurantiacus* DSM 637 growth profile in M1 (50ºC, 4.77 W $L^{-1}$, pH 8) (A) and linearization of the TSS/$OD_{610}$ (B), VSS/$OD_{610}$ (C), and VSS/TSS (D) relationship. (A) – Optical density (left axis, black dots) and Soluble sulfide concentration (right axis, red squares) plotted against time. (B) TSS and (C) VSS, plotted against time. Linear adjustments were made, and both the equations and the fit are shown. The linear adjustments intercept y/x = 0. (D) – VSS plotted against TSS. A linear adjustment was made, and both the equation and the fit are shown.

Another linear adjustment was made for TSS and VSS, using all data available. This was only possible after analyzing all the filter measurements of TSS and VSS. Figure 3.2 represents these linear adjustments, for TSS (A) and VSS (B). A color separation was done to distinguish tests with different pH values since, while analyzing the data, this seemed to be the most differentiating variable between the tests, producing the most dissimilar values of both TSS and VSS. Furthermore, only tests with M1 were considered, since tests with M1-IC presented high values for TSS, due to the sodium bicarbonate salt present, and mostly low values for VSS, due to the lack of growth in these tests.

As it is possible to see by the equations displayed in Figure 3.2, these linear adjustments were not as good as in Figure 3.1. This was to be expected as there are several more data points. Nonetheless, the slope for TSS plotted against OD was similar in both cases. The slope for VSS plotted against OD, however, was much lower. VSS is not usually this low, compared to the TSS, accounting usually to 90 % of TSS[49,50]. In this case it accounted for 56 % of the TSS. Utilizing the values from Figure 3.1, a percentage of 89 % of the TSS was obtained, which are much closer to the 90 %.

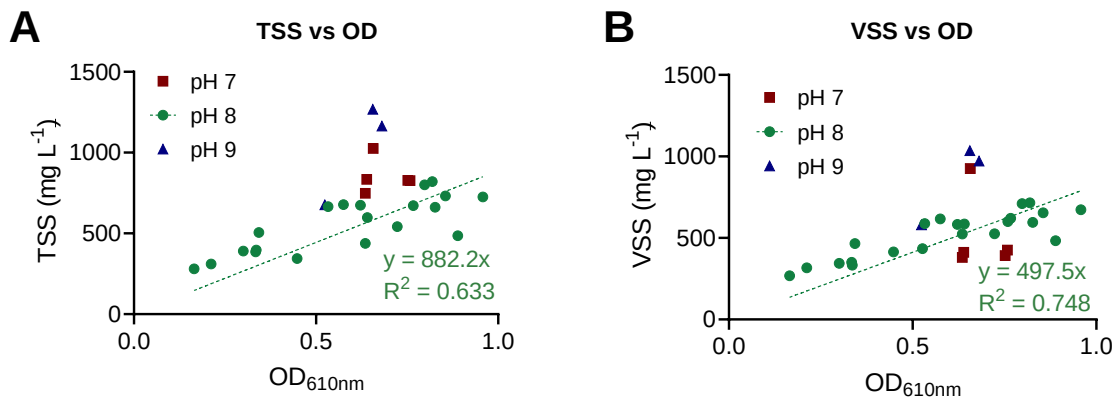


Figure 3.2 – TSS and VSS as calculated from filter weight, for every test in M1, with every strain. Different colors highlight tests with different pH since this factor seemed to produce the most disparate results. (A) TSS and (B) VSS plotted against time. Linear adjustments were made, and both the equation and the fit are shown. The linear adjustments intercept y/x = 0.

The biomass yield was also calculated (based on 2.6 Calculation of kinetic and stoichiometric parameters). A value of 0.32 g $C_{active\ biomass}$ per g $C_{Medium}$ was obtained. This means that 32 % of the organic carbon present in the medium was assimilated for growth.

## 3.2 Tests 2 and 3: Abiotic control: influence of environmental conditions

Teste series 2 and 3 had the goal of ruling out any potential sulfide removal due to environmental conditions, such as sampling, temperature changes or illumination. It was carried out in 2x90 mL flasks with M1 at 50ºC, pH 8, with a light intensity of 6.8 W $L^{-1}$, as well as 4x90 mL flasks (2 covered with aluminum foil) with M1-IC at 50ºC, pH 8, with a light intensity of 4.5 W $L^{-1}$.

Table 3.1 shows the results in M1. Sulfide removal was 47 % ± 13 % (average of both flasks), after 96 hours of continuous illumination.

Table 3.1 - Concentration and removal efficiency (RE) of sulfide and TOC in abiotic test with M1.

| M1 | | | | |
|---|---|---|---|---|
| Time (h) | [Sulfide] (mg $L^{-1}$) | Sulfide RE (%) | [TOC] (mg $L^{-1}$) | TOC RE (%) |
| 0 | 15 ± 1.6 | - | 326 ± 3.0 | - |
| 96 | 7.8 ± 1.3 | 47 ± 13 % | 313 ± 7.0 | 4.0 ± 1.7 % |

Similar results were found in M1-IC (Table 3.2). After 96 hours, sulfide removal was 47 % (value for only one flask since oxygen was present in the other one) in light conditions and 41 % ± 32 % in dark conditions (average of both flasks).

Table 3.2 - Concentration and removal efficiency (RE) of sulfide and IC in abiotic test with M1-IC.

| M1-IC | | | | |
|---|---|---|---|---|
| Time (h) | Light Conditions | | | |
| | [Sulfide] (mg $L^{-1}$) | Sulfide RE (%) | [IC] (mg $L^{-1}$) | IC RE (%) |
| 0 | 21 | - | 622 | - |
| 96 | 11 | 47 % | 584 | 6.2 % |
| Time (h) | Dark Conditions | | | |
| | [Sulfide] (mg $L^{-1}$) | Sulfide RE (%) | [IC] (mg $L^{-1}$) | IC RE (%) |
| 0 | 19 ± 1.2 | - | 476 ± 44 | - |
| 96 | 11 ± 6.3 | 41 ± 32 | 639 ± 43 | -34 ± 4.7 |

The increase in temperature alone, from the first sampling to the next ones (first sampling was done at room temperature and the next ones at a higher temperature since the flasks were incubated at 50ºC) is not enough to explain the loss of sulfide observed, since the change in solubility of the sulfide in the liquid phase within the temperature range of 25ºC and 35ºC is not significant[57]. Another hypothesis for the concentration decrease in soluble sulfide is the entrance of oxygen while sampling. $H_2S$ reacts with oxygen to form elemental sulfur[58]. The entrance of oxygen was confirmed by the change to a pink color, due to the resazurin present in the medium. This would happen often, while sampling the flasks. An important aspect to consider is that the pH did not change during the test, so sulfide solubility due to pH changes was not a factor in the concentration decrease in sulfide observed.

The removal of sulfide content was close to being the same in both dark and light conditions (Table 3.1), so it can be inferred that light does not play a significant role in the abiotic removal of sulfide in M1-IC and most likely in M1. These results showcase the importance of an abiotic test as a removal of up to 47 % of soluble sulfide is significant and must be kept in mind when analyzing future biotic results.

Furthermore, 4 % of the TOC was removed after 96h in M1. However, this fluctuation may be due to the analysis sensitivity. In M1-IC, after 96h, the IC shows an increase of 34 % in dark conditions. This might have happened because of an operator mistake, where the two samples (0h and 96h) might have been switched. If this happened, it would be in fact a decrease in the IC concentration which could have happened due to losses while sampling. The same could be said for the increase of 6 % seen in the light conditions, in M1-IC.

## 3.3 Exploring the ability of *C. aurantiacus* Y-400-fl (DSM 637) to grow and utilize $CO_2$ under autotrophic conditions

*C. aurantiacus* DSM 637 has been previously reported to have the potential to grow under heterotrophic conditions[43–45,49]. In this section, *C. aurantiacus* DSM 637's natural capability of growing under autotrophic conditions using $CO_2$ as carbon source under anaerobic conditions and accumulating it as PHA and photosynthetic pigments was evaluated.

### 3.3.1 Test 4: Influence of the sulfide concentration on the autotrophic growth and $CO_2$ fixation capability of *C. aurantiacus* strain DSM 637

Test series 4, evaluated the influence of the sulfide concentration on *C. aurantiacus* DSM 637 growth under four different sulfide concentrations supplemented in M1-IC media (the inoculum was grown in M1-IC with 100 % YE and with 10 mg S $L^{-1}$). The test was carried out in 4x500 mL flasks containing M1-IC, at 50ºC, pH 8, under 2.4 W $L^{-1}$. Figure 3.3 shows the growth in the four different starting conditions. A pattern of growth emerges across all concentrations with cultures reaching around 0.17 $OD_{610}$. The culture with 10.7 mg S $L^{-1}$ grew slightly past 0.2 $OD_{610}$.

Phosphate and ammonium were present during the test in all conditions (see Table 7.1 in Supplementary materials).

Sulfide was depleted in the first 24h, as seen in Figure 3.3A, D, 48h as seen in Figure 3.3B, or 72h as seen in Figure 3.3C. Nonetheless, much different from the past abiotic tests, all sulfide was removed at the end of the test, with the removal efficiency surrounding 95 %. The exception was the culture depicted in Figure 3.3D, which only showed a 22 % removal of sulfide. The starting sulfide concentration in this case was very low, 3.3 mg S $L^{-1}$ so the values measured were more prone to fluctuations due to the analysis sensitivity. This might explain why the value is not as low as expected.

Another interesting aspect that this test reveals is the sulfide tolerance shown by this strain, as concentrations as high as 17 mg S $L^{-1}$ were tolerated, not visibly negatively affecting the growth.

The maximum specific growth rate was achieved at 23h for all conditions. The highest value belonged to the culture depicted in Figure 3.3A, with a value of 0.25 $d^{-1}$. Biomass productivity and time of duplication were also calculated at 23h with the best values, also for the culture depicted in Figure 3.3A, of 40 mg $L^{-1}$ d-1 and 2.8 d, respectively. These values were much lower than the previous test in M1 (Figure 3.1A) which, with values three times higher, clearly shows strain 637 preference for heterotrophic growth conditions.

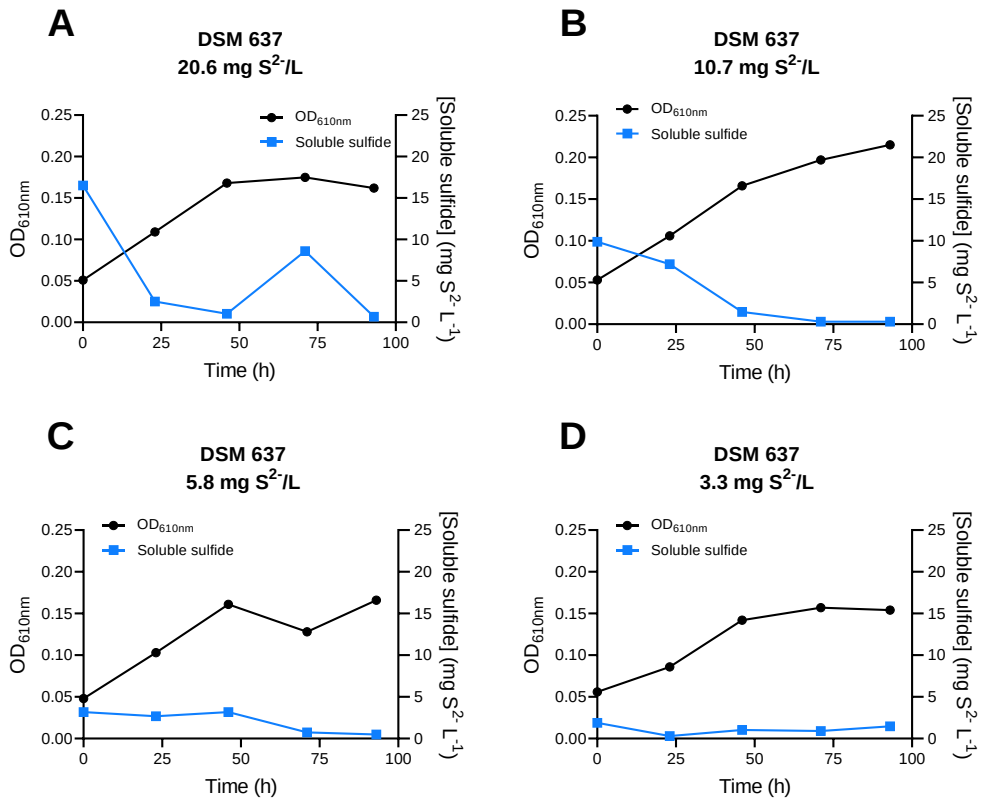


Figure 3.3 – *C. aurantiacus* DSM 637 growth profile with different starting sulfide concentrations in M1-IC (50ºC, 2.4 W $L^{-1}$, pH 8). Optical density (left axis, black dots) and Soluble sulfide concentration (right axis, blue squares) plotted against time.

Even though the culture that started with 20.7 mg S $L^{-1}$ showed the best values for the maximum specific growth rate, biomass productivity, and time of duplication, the culture that started with 10.7 mg S $L^{-1}$ did not differ from these by more than 9 %. Given this, and the fact that this culture grew slightly past 0.2 $OD_{610}$, 10.7 mg S $L^{-1}$ seems like the best condition, but more replicates would be necessary to confirm this.

To evaluate if IC was consumed during the test, the IC content was analyzed. Figure 3.4 shows the IC removal efficiency during the test. Since it is the removal efficiency that is represented, the negative values mean the IC content increased. It is possible to observe that, overall, there was an increase in IC since the values are always negative. This could be attributed to organic carbon consumption, which was present in the form of YE. This consumption produces $CO_2$ thus increasing the IC value[59]. The exception was the flask with 3.3 mg S $L^{-1}$ which showed an increase in IC concentration at 71h, but this was probably a mistake in the measurement since there should not be any YE present in the medium at this time These results hint at the possibility that there was no significant IC consumption.

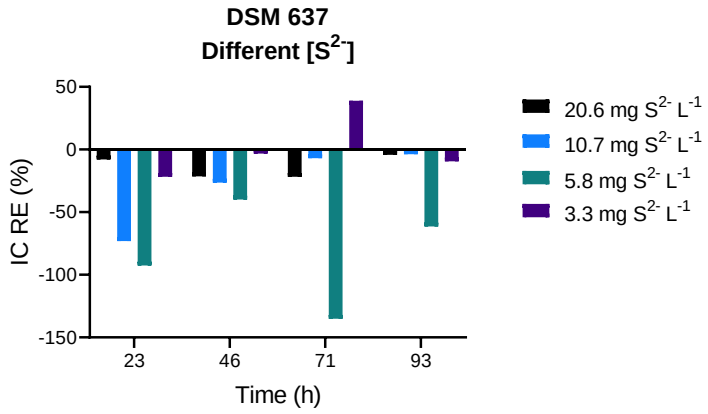


Figure 3.4 - IC removal efficiency (RE %) of *C. aurantiacus* DSM 637 cultures with different starting sulfide concentrations, in M1-IC, plotted against time

Nonetheless, these results alone do not make it possible to conclude for sure if strain DSM 637 was consuming the IC present in the medium. Most likely, due to the little growth observed, the cultures might have grown on the 10% (in relation to M1) of YE present, since it is known from M1 tests (Figure 3.1) that this strain grows very well with YE as the carbon source. Also, the fact that strain DSM 637 seemed to be unaffected by the starting sulfide concentration hints at the hypothesis that it was not growing photoautotrophically, but photoheterotrophically, where sulfide does not play an essential role. To understand if this was the case, the amount of organic and inorganic carbon present in both M1 and M1-IC were compared to the carbon assimilated for growth. This is represented in Figure 3.5. For these calculations, VSS was assumed to be a measure of the active biomass since the amount of PHA and glycogen is low. Furthermore, 50 % of this biomass was assumed to be carbon[56].

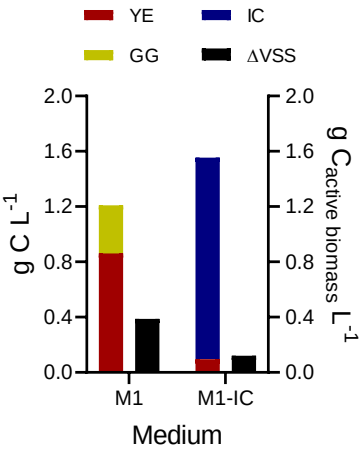


Figure 3.5 – Organic (YE, red bars and GG, yellow bar) and inorganic (IC) carbon source in M1 and M1-IC compared to the carbon assimilated for growth (black bars), according to the results from "Test 1: Correlating biomass concentration as TSS and VSS with OD610" and "Test 4: Influence of the sulfide concentration on the autotrophic growth and CO2 fixation capability of *C. aurantiacus* strain DSM 637".

As depicted in Figure 3.5, the ratio between the carbon used for growth and the amount of carbon present is different in M1 and M1-IC. Assuming GG is not providing carbon for growth, in M1 a ratio of 0.45 g $C_{active\ biomass}$ $L^{-1}$ to g $C_{YE}$ $L^{-1}$ was obtained. In M1-IC, this ratio was 1.27 g $C_{active\ biomass}$ $L^{-}$

[1] to g $C_{YE}$ $L^{-1}$. These values are, in fact, the biomass yield for the respective M1 and M1-IC tests. According to this ratio, which was about 3 times higher in M1-IC, some IC must have been consumed for growth. Nonetheless, the limiting factor in the "Test 4: Influence of the sulfide concentration on the autotrophic growth and CO2 fixation capability of *C. aurantiacus* strain DSM 637" test was not the IC present in the medium, but the culture was not able to grow further. The lack of sulfide may have been the cause, since, if the culture was consuming IC, sulfide is required to act as the electron donor. Sulfide concentration was close to zero at 48h, in the case of the tests with 20.6 and 10.7 mg S $L^{-1}$ of starting sulfide, so it might not have been available once the YE consumption finished, and the IC consumption started. Furthermore, it could also be the case that DSM 637 requires some vitamins supplement to effectively capture and fix $CO_2$. So, it was important to test vitamin supplementation to the culture and assure the presence of sulfide during the whole test.

### 3.3.2 Test 5: Exploring the capability of C. aurantiacus strain DSM 637 to grow autotrophically and utilize $CO_2$ with the support of vitamins and ammonium

According to the results obtained in test series 4, test series 5 explored the $CO_2$ fixation capacity of *C. aurantiacus* DSM 637 under autotrophic conditions with the support of vitamins supplied in the medium at the beginning of the test in IC media. Also, from this test forward, the M1-IC medium already contained the ammonia supplement shown in Table 2.3, in the methods. Moreover, with the key objective of stimulating the $CO_2$ fixation two different sulfide concentrations were evaluated along with the vitamins presence: 1) 10 mg S $L^{-1}$ at the beginning of the test plus daily sulfide addition, referred to as pulses; 2) concentration of 20 mg S $L^{-1}$at the beginning of the test. The inoculum was grown in M1-IC (with 100 % YE) with 10 mg S $L^{-1}$, without the vitamins supplement. The test was carried out in 4x500 mL flasks containing M1-IC, at 50ºC, pH 8, under 2.4 W $L^{-1}$. Figure 3.6 shows the growth obtained in both conditions. $OD_{610}$ reached a maximum value of 0.2 (VSS = 241 mg $L^{-1}$), similarly to the results found in test 4 without vitamins addition.

Phosphate and ammonium were present during the test in both conditions (see Table 7.2 in Supplementary materials).

Sulfide was only depleted at 95h in the case of the culture that did not receive the sulfide pulses (Figure 3.6B). The sulfide removal was 90 %. In the case of the culture that received the sulfide pulses, sulfide never decreased much below 10 mg $L^{-1}$ (Figure 3.6A). For this culture, soluble sulfide values, got as high as 40 mg $L^{-1}$, without any visible effect on the culture. This, again, shows the remarkable sulfide tolerance of this strain.

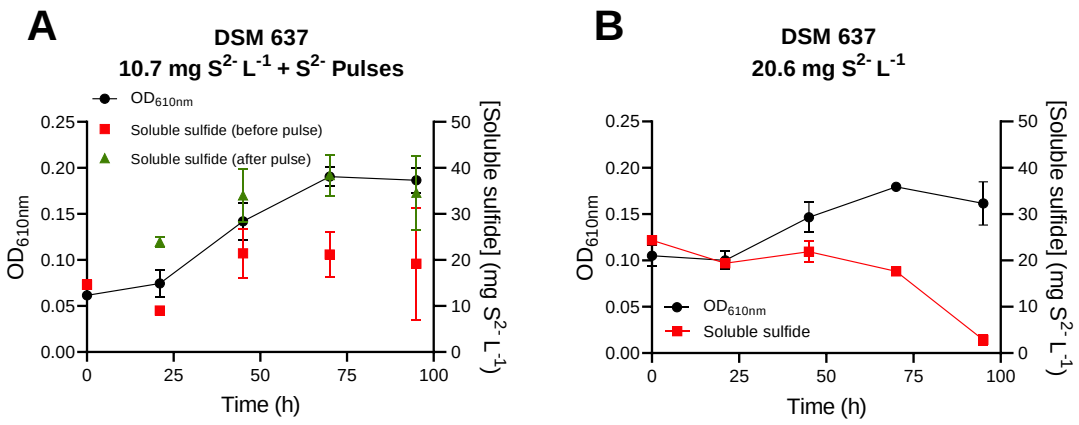


Figure 3.6 – *C. aurantiacus* DSM 637 growth profile with vitamins supplementation and different starting sulfide concentrations in M1-IC (50ºC, 2.4 W $L^{-1}$, pH 8),10.7 mg S $L^{-1}$ (A) and 20.6 mg S $L^{-1}$(B). (A) – Pulses of sulfide were given every day except on day 0. Optical density (left axis, black dots) and Soluble sulfide concentration before the addition of sulfide (right axis, red squares) and after the addition of sulfide (right axis, green triangles) plotted against time. (B) - Optical density (left axis, black dots) and Soluble sulfide concentration (right axis, red squares) plotted against time.

Nevertheless, in the culture that received sulfide pulses, the maximum specific growth rate was achieved at 45h with a value of 0.16 $d^{-1}$. Biomass productivity and time of duplication were also calculated at 45h with values of 29 mg $L^{-1}$ $d^{-1}$ and 4.2 d, respectively. For the culture that didn't receive sulfide pulses, the maximum specific growth rate was achieved at 70h with a value of 0.085 $d^{-1}$. Biomass productivity and time of duplication were also calculated at 45h with values of 17 mg $L^{-1}$ $d^{-1}$ and 8.2 d, respectively. Thus, vitamins supplementation did not seem to help growth. All these values were still far from the ones obtained with M1, which were more than three times higher.

The VFA content (Figure 3.7) was also analyzed to understand if the culture was consuming VFAs for growth. It is noticeable that the values are all very low, below the standards used in the calibration curve (7 mg VFA $L^{-1}$) so these are residual values. Propionic acid may have come from the inoculum since it was measured there as well, or naturally, from YE consumption. Since the culture had a small concentration of YE, by-products of its consumption, like VFAs, would have been immediately consumed by the culture. These low concentrations of VFAs prove that the culture did not have organic carbon available to grow.

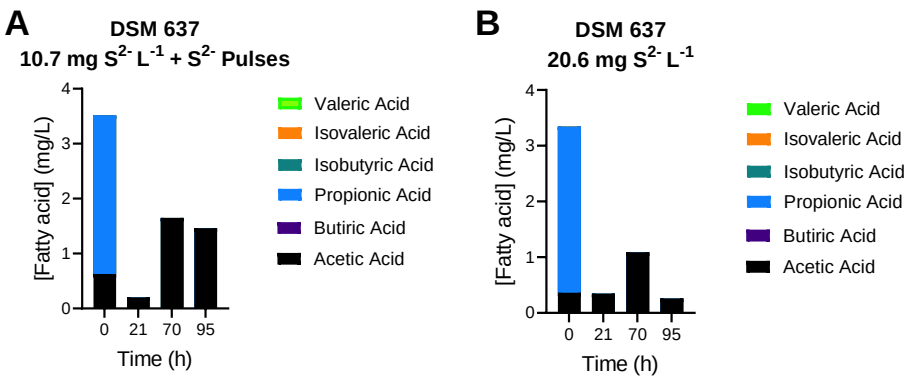


Figure 3.7 - Volatile fatty acids (VFA) residual content of *C. aurantiacus* cultures with different starting sulfide concentrations in M1-IC,10.7 mg S $L^{-1}$ (A) and 20.6 mg S $L^{-1}$ (B). The lowest standard from the calibration curve was 7 mg VFA $L^{-1}$. (A) - Pulses of sulfide were given every day except on day 0.

Looking at the IC removal efficiency data (Figure 3.8), a decrease in IC content can be observed in the first 21h by both cultures, even though it was higher in the case of the culture that received the sulfide pulses. This decrease, however, is not proportional to the growth observed in either condition, as in the first 21h, little or no growth was observed. Furthermore, this decrease in concentration was not sustained, and the IC content increased in the next day (negative values mean an increase in IC concentration). Since the $OD_{610}$ only increased after 24h and only to 0.2, it leads to the conclusion that the first decrease in IC concentration was most likely due to losses while sampling. The subsequent increase in IC might have been a result of heterotrophic growth, meaning the culture was using the organic carbon from the YE present in the medium and/or from the inoculum and producing $CO_2$ as a result[49].

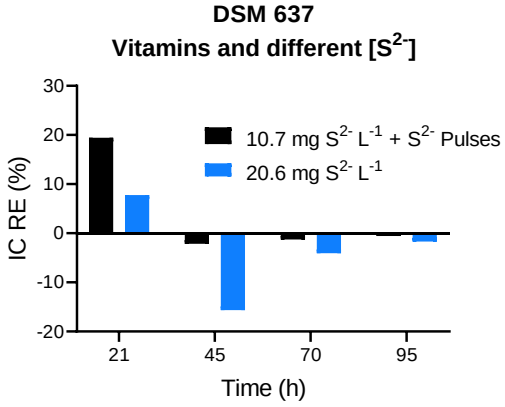


Figure 3.8 - IC removal efficiency of *C. aurantiacus* DSM 637 cultures growing with different starting sulfide concentrations in M1-IC, plotted against time. The culture represented by the black bars was given pulses of sulfide every day except on day 0.

Again, similarly to the last test in M1-IC (Figure 3.3), strain DSM 637 reached only a maximum of 0.2 $OD_{610}$. This means that the biomass yield calculated before also stands here as validation that the culture must have consumed some IC. Ultimately, the results from this test show that it was not the lack

of vitamins that was limiting the growth of strain DSM 637 in M1-IC, nor was the lack of sulfide, since, as intended, it was always present, reaching values as high as 40 mg S $L^{-1}$.

## 3.4 Test 6: Exploring the capability of *C. aurantiacus* strains DSM 635, DSM 636, and DSM 638 to grow under heterotrophic conditions and synthesize value-added products

Due to the small capability observed in *C. aurantiacus* DSM 637 to utilize $CO_2$ as the carbon source for growth, three other strains were tested. First, kinetic assays were performed with each of these strains in M1, at 50ºC, pH 8, under 1.9 W $L^{-1}$. The results obtained in test series 6 are shown in Figure 3.9. It is noticeable that the initial concentration of sulfide is 20 mg S $L^{-1}$, despite the attempt to control it to be 10 mg S $L^{-1}$. This might have happened because of a miscalculation of the concentration of the neutralized sulfide solution (section 2.3.2).

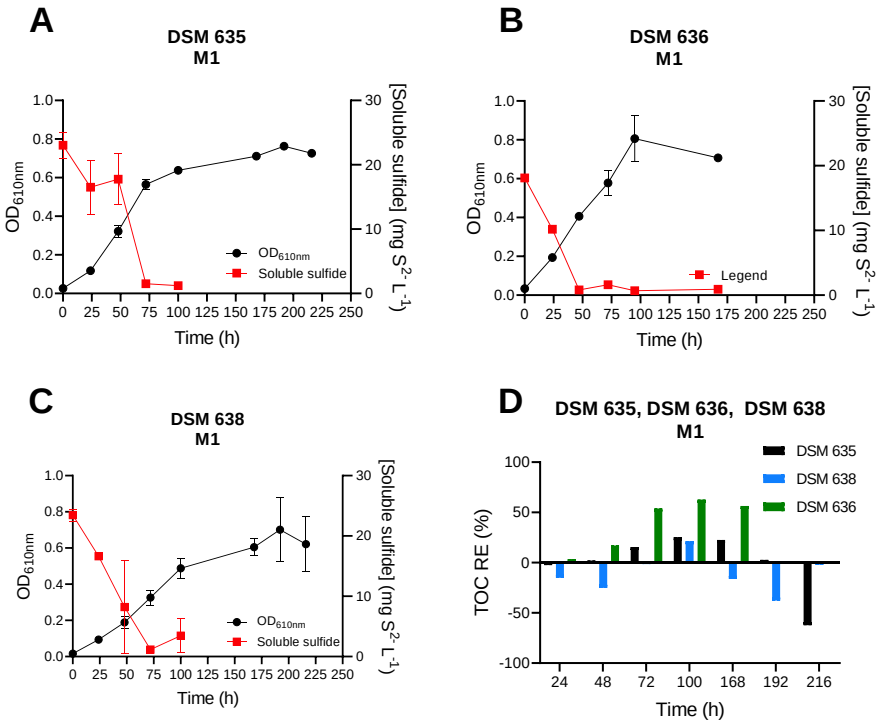


Figure 3.9 - *C. aurantiacus* DSM 635 (A), *C. aurantiacus* DSM 636 (B), and *C. aurantiacus* DSM 637 (C) growth profiles in M1 (50ºC, 1.9 W $L^{-1}$, pH 8), and TOC removal efficiency (RE) data (D). (A), (B), (C) – Optical density (left axis, black dots) and Soluble sulfide concentration (right axis, red squares) plotted against time. (D) – TOC RE (%) data for all three strains.

Contrary to DSM 637, the new strains reached the stationary phase much later. DSM 637 reached the stationary phase at around 72h while DSM 635 and DSM 638 reached the stationary phase at 168h and DSM 636 at 95h. DSM 635 and DSM 636 reached about 0.8 $OD_{610}$ while DSM 638 reached about 0.6. These values were slightly lower than the 1.0 $OD_{610}$ reached by DSM 637. Thus, the new strains grow slower and slightly less compared to DSM 637.

Phosphate and ammonium were present during the test in all conditions (see Table 7.3 in Supplementary materials).

Sulfide was depleted at 72h in the case of DSM 635 and DSM 638, while at 47h there was no more sulfide in the case of DSM 636. Sulfide removal was higher than 90 % in this test, for all strains.

The highest values obtained in these conditions, for all strains, for maximum specific growth rate, biomass productivity and doubling time are represented in Table 3.3, as well as the time of the test they were achieved. Compared to DSM 637, these values are slightly lower, the closest being strain DSM 636. Nonetheless, the test in M1 with the strain DSM 637 had the highest volumetric light intensity, since it was carried out in a 250 mL flask, which could explain the slightly faster growth.

Table 3.3 - Representation of the highest values achieved for maximum specific growth rate, biomass productivity and doubling time for all four *C. aurantiacus* strains, DSM 635, DSM 363, DSM 637 and DSM 638, as well as the time they were achieved. Conditions were growth in M1, 50ºC with pH 8. The volumetric light intensity is also shown.

| | M1, 50ºC, pH 8 | | | |
|---|---|---|---|---|
| | 1.86 ± 0.10 W $L^{-1}$ | 2.05 ± 0.14 W $L^{-1}$ | 4.77 W $L^{-1}$ | 1.70 ± 0.11 W $L^{-1}$ |
| | DSM 635 @ 48h | DSM 636 @ 24h | DSM 637 @ 24h | DSM 638 @ 24h |
| Maximum specific growth rate ($d^{-1}$) | 0.47 | 0.60 | 0.66 | 0.37 |
| Biomass productivity (mg $L^{-1}$ $d^{-1}$) | 99 | 107 | 166 | 52 |
| Doubling time (d) | 1.5 | 1.2 | 1.1 | 1.9 |

Looking at the TOC removal efficiency data (Figure 3.9D), it is observed that DSM 636 showed a removal of up to 50 %. Meanwhile, DSM 635 and DSM 638 appeared to remove TOC, but after 168h the TOC values started to increase again. This increase was probably due to the biomass degradation, since the culture had reached the death phase at this point, which can release organic compounds to the medium, which are detected in this analysis.

Figure 3.10 shows the VFAs concentration in the cultivation broth of the three strains during the experiment. It shows high concentrations of butyric acid and propionic acid, as well as low concentrations of isobutyric acid, valeric acid, isovaleric acid and acetic acid. These most likely resulted from

the consumption of the high amounts of YE present in M1. The reason why butyric acid was present in higher concentrations is likely because it requires $CO_2$ to be consumed. Since this test was done in M1, there was no $CO_2$ addition, and butyric acid, unlike the other VFAs, was not being consumed. This raises the possibility of complementing M1 tests with $CO_2$ addition, to further metabolize butyric acid and improve growth while assimilating $CO_2$.

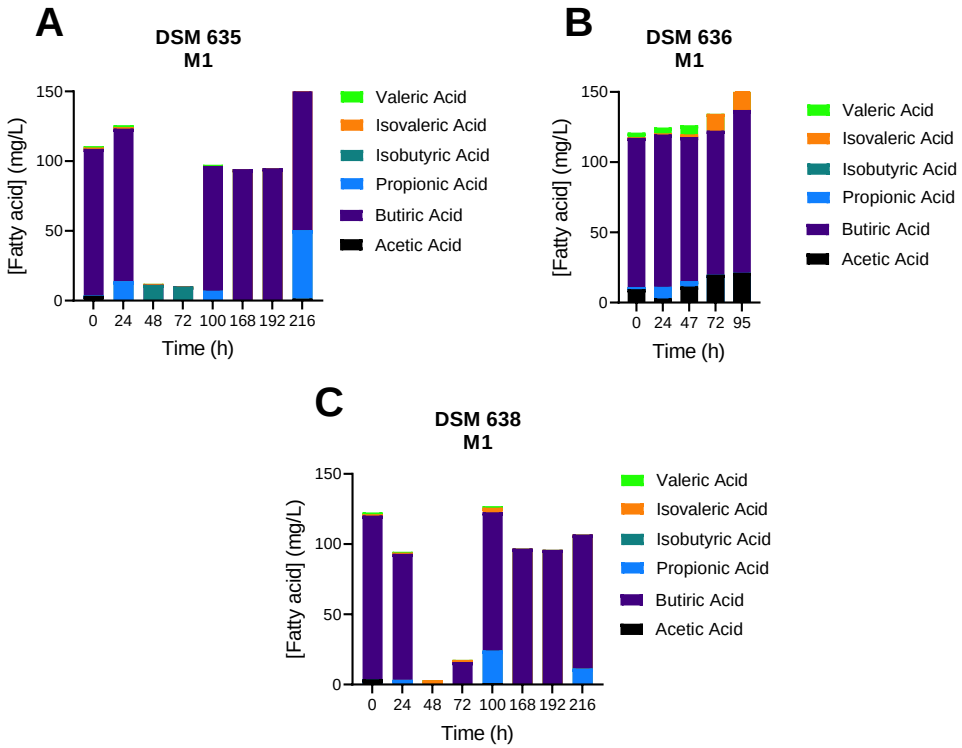


Figure 3.10 - Volatile fatty acids (VFA) content (mg $L^{-1}$) of *C. aurantiacus* DSM 635 (A), DSM 636 (B), and DSM 638 (C) cultures growing in M1.

## 3.5 Test 7: Exploring the ability of *C. aurantiacus* strains DSM 635, DSM 636, and DSM 638 to grow autotrophically and utilize $CO_2$

Teste series 7 had the goal of understanding if these strains were able to utilize IC to grow. The growth of each strain and sulfide concentration is represented in Figure 3.11. This test was carried out in M1-IC, at 50ºC, pH 8, under 1.7 W $L^{-1}$. The inocula was grown in M1-IC (with 100 % YE) with 10 mg S $L^{-1}$. Despite the attempt to control sulfide concentration to 10 mg S $L^{-1}$, this was in fact closer to 20 mg S $L^{-1}$ in the case of strain DSM 635 and 15 mg S $L^{-1}$ in the case of strain DSM 636. In the case of strain DSM 638, only one of the replicates is showing since in the other replicate the OD reached zero after 96h.

Out of the three strains, DSM 638 performed the worst, reaching only 0.05 $OD_{610}$. Given this $OD_{610}$ value, it is possible to conclude that this strain did not grow under these conditions. DSM 636, like DSM 637, reached about 0.2 $OD_{610}$. DSM 635 did not grow as much, reaching about 0.12 OD.

Contrary to previous results, phosphate did not show positive values during the whole test in the case of strain DSM 635 (see Table 7.4 in Supplementary materials). In the case of the other strains, this was not observed. Ammonium was present in all cultures. Still, in the case of strain DSM 635, some points in time show the presence of phosphate, which hints at the possibility that the negative values are due to low concentrations that go outside the range of detection of the equipment. Also, the other strains showed phosphate throughout the test and the $OD_{610}$ was not significantly higher.

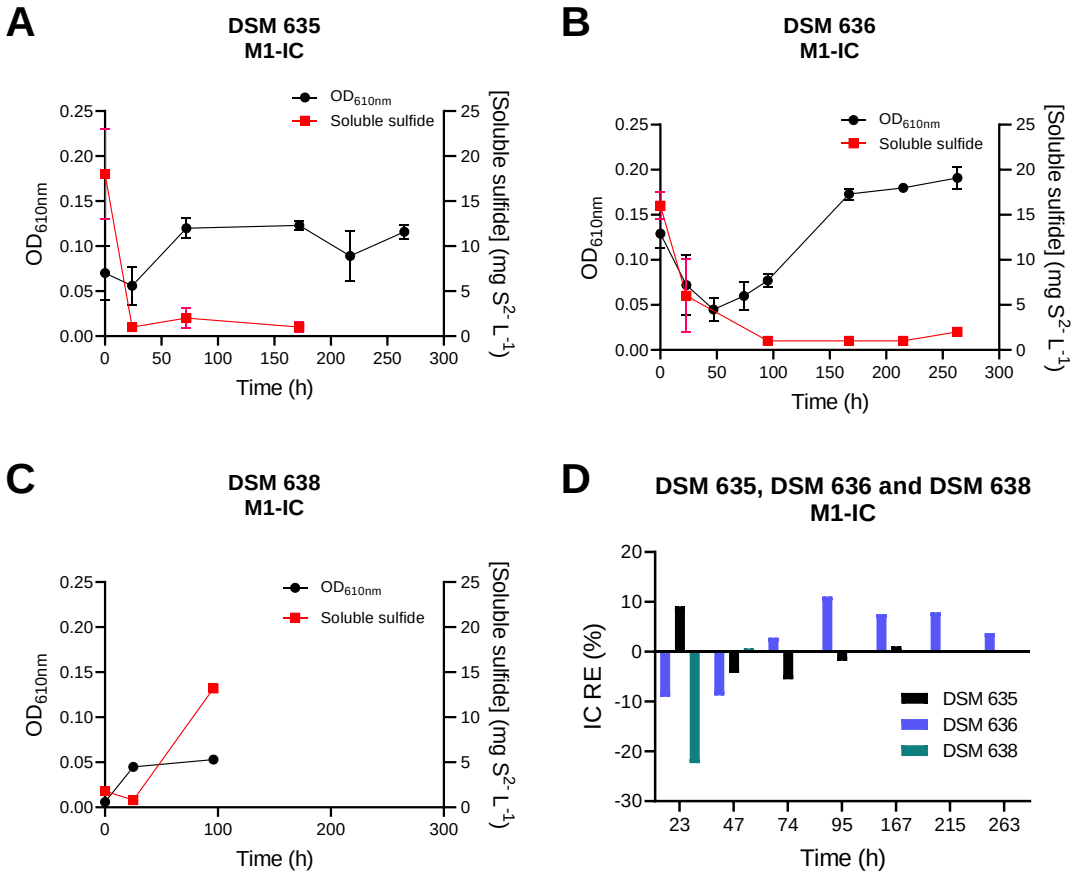


Figure 3.11 - *C. aurantiacus* DSM 635 (A), *C. aurantiacus* DSM 636 (B), and *C. aurantiacus* DSM 637 (C) growth profiles in M1-IC (50ºC, 1.7 W $L^{-1}$, pH 8), and IC removal efficiency (RE) data (D). (A), (B), (C) – Optical density (left axis, black dots) and Soluble sulfide concentration (right axis, red squares) plotted against time. (D) – IC RE( %) data for DSM 635 and DSM 636.

Figure 3.11 shows soluble sulfide concentration, which was depleted at 24h in the case of strain DSM 635. In the case of DSM 638, the sulfide concentration looks to have been low in the beginning but then looks to be high at 96h. This might be due to an operator mistake in the measurements, wherein

maybe the first and last samples were switched. In the case of DSM 636, the sulfide content steadily decreased until 95h, at which point it was close to zero.

The highest values obtained in these conditions, for all strains, for maximum specific growth rate, biomass productivity and doubling time are represented in Table 3.4, as well as the time of the test they were achieved. For the calculation of these parameters, it was assumed that growth started after 24h in the case of DSM 635, and 47h in the case of DSM 636. This first period where there was no growth might have happened due to the adaptation of the cultures to a new medium (M1-IC is chemically different from the medium of the inoculum, which had 10 times more YE).

Table 3.4 - Representation of the highest values achieved for maximum specific growth rate, biomass productivity and doubling time for all four *C. aurantiacus* strains, DSM 635, DSM 363, DSM 637 and DSM 638, as well as the time they were achieved. Conditions were growth in M1-IC, 50ºC with pH 8. The volumetric light intensity is also shown.

| | M1-IC, 50ºC, pH 8 | | | |
|---|---|---|---|---|
| | 1.70 ± 0.07 W $L^{-1}$ | 1.73 ± 0.05 W $L^{-1}$ | 2.54 W $L^{-1}$ | 1.71 ± 0.03 W $L^{-1}$ |
| | DSM 635 @ 72h | DSM 636 @ 167h | DSM 637 @ 23h | DSM 638 @ 25h |
| Maximum specific growth rate ($d^{-1}$) | 0.52 | 0.097 | 0.25 | 0.19 |
| Biomass productivity (mg $L^{-1}$ $d^{-1}$) | 131 | 17 | 40 | 24 |
| Doubling time (d) | 1.3 | 7.2 | 2.8 | 3.6 |

DSM 635 showed the highest values of maximum specific growth rate and DSM 636 showed the lowest but grew the most. This means that the strain DSM 636 grew slower but more than the other strains.

Much like in the case of strain DSM 637, the increase in $OD_{610}$ to about 0.2 could be explained by the consumption of YE by the cultures, as well as some IC, according to Figure 3.5. However, it is necessary to look at the IC removal data to draw further conclusions. This data is represented in Figure 3.11D.

Strain DSM 638 showed negative values, meaning the IC concentration increased. This was most likely due to YE consumption and since the culture stopped growing, no IC removal was observed.

In the case of strain DSM 635, it is possible to see a decrease in IC concentration in the first 23h. Although this decrease was not sustained, the 23h coincided with a period of growth (Figure 3.11A). In the case of strain DSM 636, the removal efficiency values were negative at first, meaning the IC concentration increased. While this is true for the first 47h, what followed was a positive removal

efficiency of IC, meaning the IC concentration decreased. However, this removal, which amounts for 10 % of the initial IC present, is not associated with growth since little growth was observed. So, most likely, this happened due to losses while sampling. The increases in IC concentration that were observed happened due to YE consumption. The VFA concentration in the cultivation broth was zero for all strains, meaning all the organic carbon was consumed for growth.

It could be that it is the lack of sulfide that is limiting the growth and IC consumption by these strains. Because the fact is that after 24h, strain DSM 635 did not have sulfide available. Strain DSM 636 did not have sulfide after 96h.

This leads to the necessity of another test with sulfide pulses. Strain DSM 635 was chosen for this since it showed removal of IC, in the first 24h while sulfide was available could be due to IC fixation and is associated with the time of growth. In the case of DSM 636, in this first period, the IC content increased and that must be due to respiration, meaning it was consuming organic carbon, which could explain the period of growth that it exhibited in the next hours. This is likely since after the sulfide finished this strain did not seem affected, while DSM 635 stopped growing when that happened. Nonetheless, this strain showed the highest removal of IC.

## 3.6 Batch tests with *C. aurantiacus* DSM 635

### 3.6.1 Test 8: Influence of sulfide adjustments on the autotrophic growth and $CO_2$ fixation capability of *C. aurantiacus* strain DSM 635

Test series 8 had the goal of understanding if it was the lack of sulfide that was limiting the capability of strain DSM 635 to utilize IC as the carbon source for growth. In that sense, pulses of 10 mg S $L^{-1}$ were given in the second and fourth day of growth. The test was carried out in 2x500 mL flasks containing M1-IC, at 50ºC, pH 8, under 1.7 W $L^{-1}$. Figure 3.12.shows the growth obtained as well as the sulfide concentration, of both replicates.

In both replicates, no growth was observed. There was an experimental problem which led to not being able to maintain high sulfide concentrations in either flask. Maybe it was the case that the rubber was not correctly positioned at the time of inoculation and oxygen consistently got in the flasks, precipitating the sulfide. This was probably the case since a light pink color could be observed in both flasks during this test, which means that the anaerobiosis was not maintained. Nonetheless, some growth was expected at the beginning since some YE was present, similarly to previous tests with M1-IC (Figure 3.11D). However, in this case, that didn't happen, which raises the question if sulfide presence in the beginning of the growth, when there is YE available, helps the culture to grow. It could be that the

culture needs to be actively growing to be able to utilize $CO_2$ and sulfide (due to the electron demand) to sustain growth when there is little amount of organic carbon present.

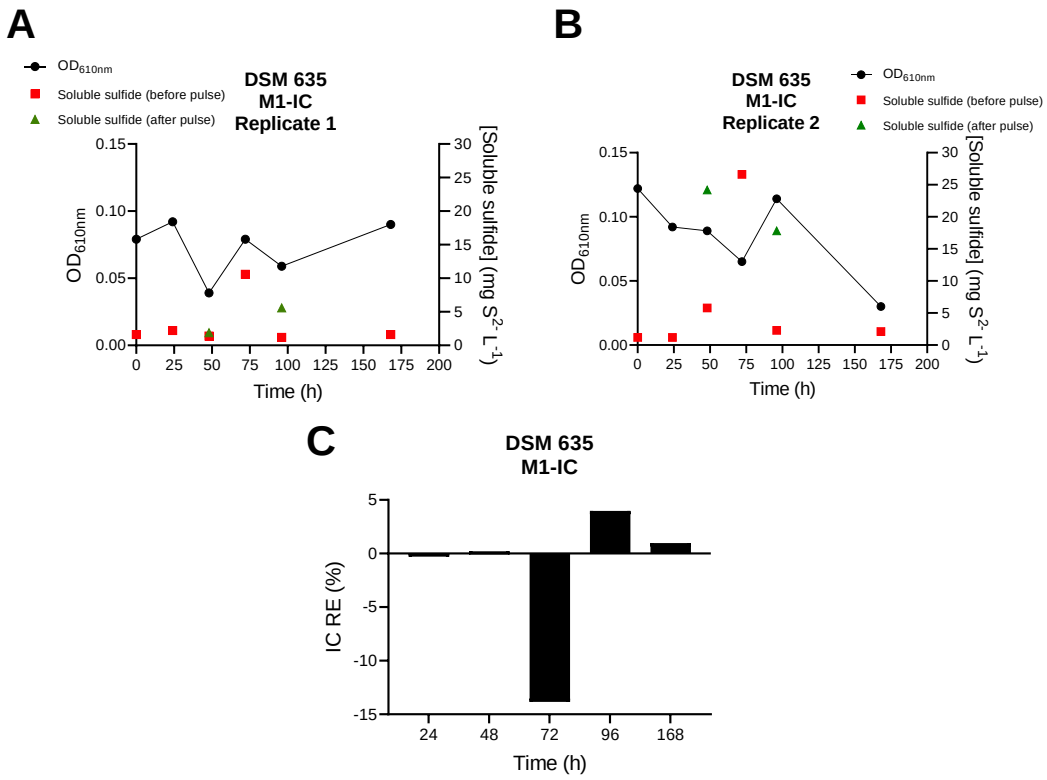


Figure 3.12 - *C. aurantiacus* DSM 635 growth profile, replicate 1 (A) and replicate 2 (B), in M1-IC (50ºC, 1.7 W $L^{-1}$, pH 8), and IC removal efficiency (RE) data (C). (A), (B)– Optical density (left axis, black dots) and Soluble sulfide concentration (right axis, red squares) plotted against time. (C) – IC RE( %) data (average of both replicates).

The IC removal data, in Figure 3.12C, is shown as the average of both replicates since the results obtained for this analysis were similar between them. At 72h there was an increase of about 14 % in the IC content, followed by a small decrease afterwards. This data confirms that there was no IC utilization for growth.

The values of VFA concentration were zero. Ammonium and phosphate data is represented in Table 7.5 in Supplementary materials.

### 3.6.2 Test 9: Influence of pH on the heterotrophic growth and production of value-added products by *C. aurantiacus* strain DSM 635

Test series 9 had the goal of understanding how a culture of *C. aurantiacus* DSM 635 would be affected by different pH values. Thus, the effect of pH 7 and pH 9 on growth was tested and the results compared with the results at pH 8. The two conditions were tested in M1, at 50ºC. The test was carried

out in 4x500 mL flasks (two at pH 7 and two at pH 9) with M1, under 1.7 W $L^{-1}$. The results are shown in Figure 3.13.

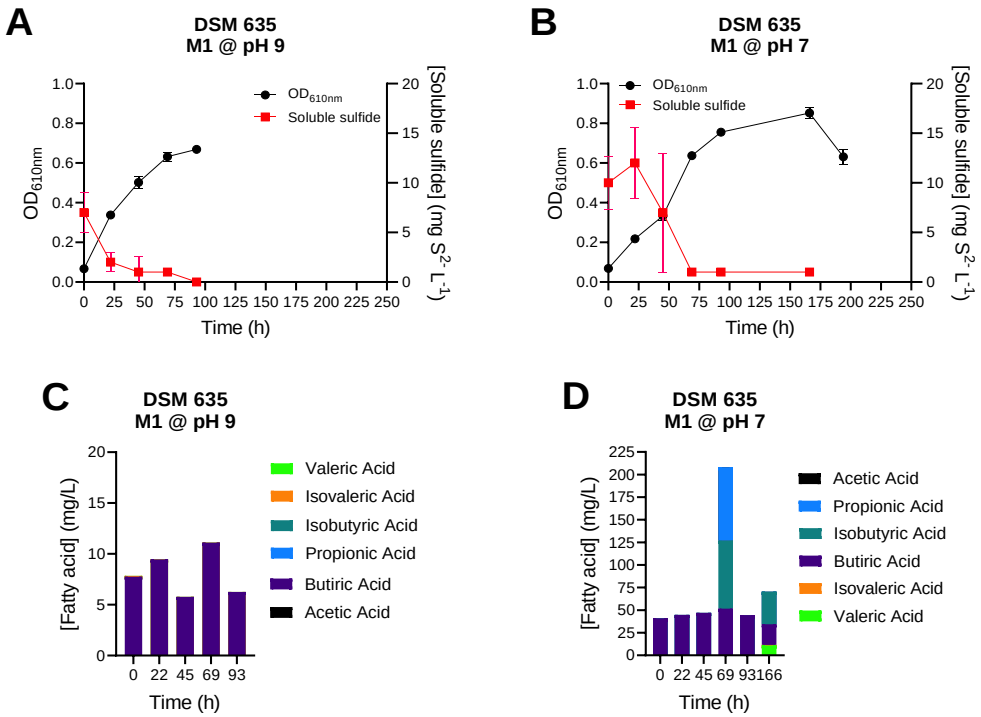


Figure 3.13 - *C. aurantiacus* DSM 635 growth profile at pH 9 (A) and pH 7 (B), in M1-IC. Volatile fatty acids (VFA) content of *C. aurantiacus* DSM 635 culture grown at pH 9 (C) and pH 7 (D) in M1-IC (50ºC, 1.7 W $L^{-1}$). (A), (B)– Optical density (left axis, black dots) and Soluble sulfide concentration (right axis, red squares) plotted against time.

Growth was observed in both cases, with $OD_{610}$ values reaching 0.67 at pH 9, after 93h, and 0.85 at pH 7, after 166h. The VFA content was also analyzed and, similarly to this strain at pH 8, butyric acid was present. However, no acetic acid was present. Additionally, at pH 7, both propionic acid, isobutyric acid and valeric acid were present.

Sulfide was depleted between 24h and 45h at pH 9 and around 69h at pH 7.

Phosphate and ammonium were present during the test in all conditions (see Table 7.6 in Supplementary materials).

The TOC removal data was also analyzed. The results are represented in Figure 3.14. It is possible to observe that while in the beginning the values were negative, by the end of the test both cultures showed a positive removal of the TOC. This was expected since both cultures showed good growth, so the organic carbon must have been consumed. The removal efficiency values are not higher probably because, by the end of the test, cell degradation must have released organic compounds back into the

medium, which influence the value measured by the TOC analysis. Thus, it was not expected to measure 100 % removal efficiency of TOC.

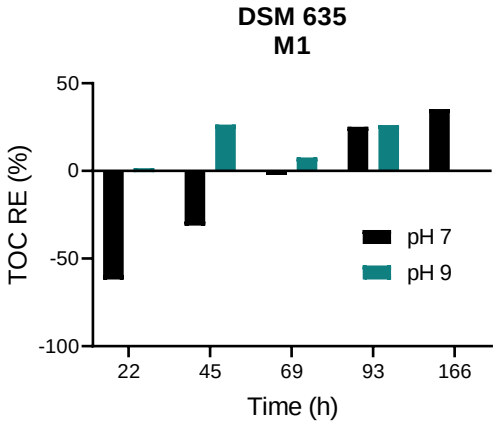


Figure 3.14 - TOC removal efficiency of C. aurantiacus DSM 635 cultures growing with different pH values, pH 7 and pH 9, in M1, plotted against time.

The highest values obtained in these conditions, for all strains, for maximum specific growth rate, biomass productivity and doubling time are represented in Table 3.5, as well as the time of the test they were achieved.

Table 3.5 - Representation of the highest values achieved for maximum specific growth rate, biomass productivity and doubling time for all four *C. aurantiacus* strains, DSM 635, DSM 363, DSM 637 and DSM 638, as well as the time they were achieved. Conditions were growth in M1, 50ºC with pH 7, 8 and 9. The volumetric light intensity is also shown.

| | M1, 50ºC | | |
|---|---|---|---|
| | 1.72 ± 0.08 W $L^{-1}$ | 1.86 ± 0.10 W $L^{-1}$ | 1.66 ± 0.15 W $L^{-1}$ |
| | DSM 635, pH 7 @ 22h | DSM 635, pH 8 @ 48h | DSM 635, pH 9 @ 22h |
| Maximum specific growth rate ($d^{-1}$) | 0.54 | 0.47 | 0.85 |
| Biomass productivity (mg $L^{-1}$ $d^{-1}$) | 152 | 99 | 240 |
| Doubling time (d) | 1.3 | 1.5 | 0.81 |

The culture growing at pH 9 showed the best value for the maximum specific growth rate. Additionally, this value was better than strain DSM 637 growing at pH 8 (0.66 $d^{-1}$), which is a very interesting result. This shows not only the resilience of this strain 637 to different pH but also highlights that from one strain to the other, ideal conditions can also change.

### 3.6.3 Test 10: Influence of temperature on the heterotrophic growth of *C. aurantiacus* strain DSM 635

Test series 10 had the goal of understanding how a culture of *C. aurantiacus* DSM 635 would be affected by lower temperatures. Thus, the effect of 30ºC instead of the usual 50ºC on growth was tested. This was necessary since future work will involve the operation of photobioreactors which may be difficult to heat up and maintain at 50ºC. Furthermore, it was interesting to understand if, at pH 9, this culture would grow well. This was because at pH 9 both sulfide and IC are more soluble and would not be lost as much during the photobioreactor operation. Thus, two conditions were tested at 30ºC, pH 8 and pH 9. The test was carried out in x500 mL flasks with M1, under 1.52 W $L^{-1}$. The results are shown in Figure 3.15.

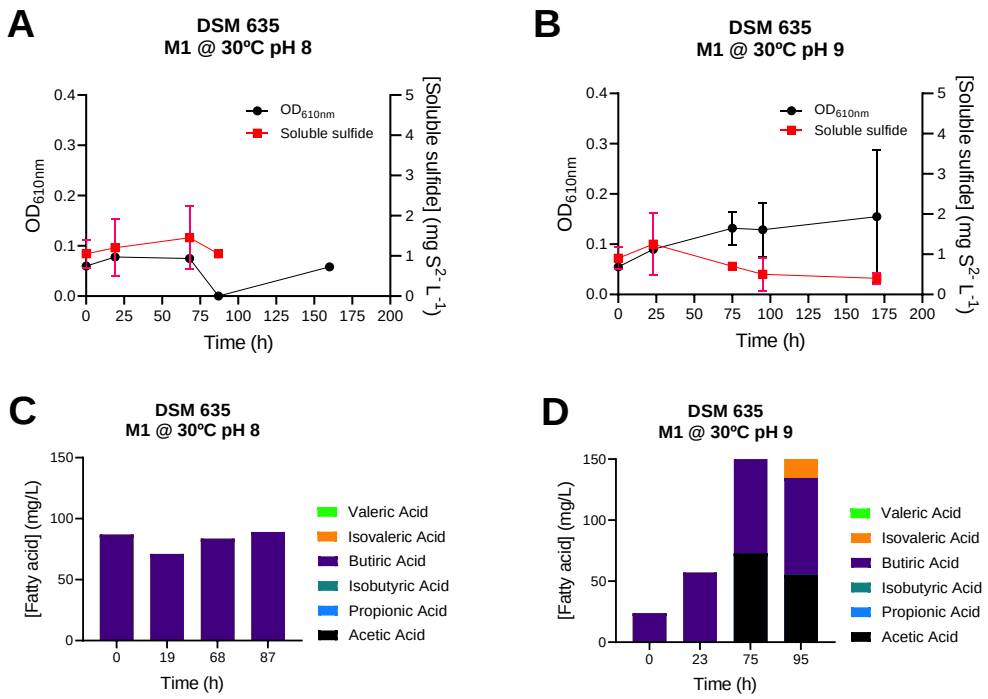


Figure 3.15 - *C. aurantiacus* DSM 635 growth profile at 30ºC, at pH 8 (A) and pH 9 (B), in M1-IC(1.5 W $L^{-1}$). Volatile fatty acids (VFA) content of *C. aurantiacus* DSM 635 culture grown at 30ºC, at pH 8 (C) and pH 9 (D) in M1-IC. (A), (B)– Optical density (left axis, black dots) and Soluble sulfide concentration (right axis, red squares) plotted against time

In both cases, almost no growth was possible at this temperature, with $OD_{610}$ values reaching 0.1 and 0.2, respectively. In the case of the test at pH 9, the big error bar at the end exists because one of the flasks showed a value of 0.06 $OD_{610}$ while the other showed a value of 0.24 $OD_{610}$.

Phosphate and ammonium were present during the test in all conditions (see Table 7.7 in Supplementary materials).

The VFA concentration was also analyzed and, similarly to this strain 635 growth at 50ºC, butyric acid was present since it could not be consumed for growth (lack of $CO_2$). At pH 9, acetic acid and isovaleric acid were still present at the end of the test which means they were not fully consumed by the culture.

These results show the importance of high temperatures during the growth of *C. aurantiacus* cultures. This species is a thermophile and so, the use of high temperatures is of paramount importance for growth.

## 3.7 Carotenoids, bacteriochlorophyll *a* and bacteriochlorophyll *c* production

Throughout some of the tests carried out, the bacteriochlorophyll and total carotenoid content were analyzed. The highest values obtained, for all strains, in all the test series for these pigments are represented in Table 3.6 as well as the time of the test they were achieved.

Looking at this data, it is possible to observe that the best production of Bchl *c* was achieved in test 9, with strain DSM 635, under the conditions: M1, 50ºC at pH 7, with a volumetric light intensity of $1.72 \pm 0.08$ W $L^{-1}$. This volumetric light intensity was one of the lowest among all the tests, which might have contributed to a higher production of Bchl *c*[46]. The highest production of total carotenoids was also achieved in this test. However, a correlation between the low light intensity and this fact cannot be established, based on the literature alone. Maybe this was a result of the lower pH of this test since both pigments showed high concentrations. Nonetheless, it is possible to conclude that pH 7, for strain DSM 635, was beneficial for the total carotenoid and Bchl *c* production. It would be interesting to test if, for the other strains, a different pH would also have a positive impact on pigment production.

The highest production of Bchl *a* was achieved in test 5, with strain DSM 637, under the conditions: M1-IC, 50ºC, at pH 8, a test with sulfide adjustments. This test had the highest volumetric light intensity, at $2.40 \pm 0.20$ W $L^{-1}$, so once again, an obvious link cannot be made between these two values, based on the literature alone. In this case, maybe the higher sulfide availability, together with the presence of IC were a factor in the culture producing more Bchl *a*. Bchl *a* production could be associated with cellular growth, but this was not the case since the TSS was low (275 mg $L^{-1}$). Finally, the quantity of pigments produced was low when compared with other pigment producing microorganisms such as cyanobacteria[60].

Table 3.6 – Representation of the highest values achieved for total carotenoid, bacteriochlorophyll *a* (Bchl *a*) and bacteriochlorophyll *c* (Bchl *c*) content (in % of the cdw) in all tests carried out as well as the conditions of these tests. The volumetric light intensity of the flask and the time the samples were taken are also shown. "Exp" means the samples were taken in the exponential phase, "Sta" means the samples were taken in the stationary phase.

| Test series | Strain | Conditions | Volumetric light intensity (W $L^{-1}$) | Time (h) | Total Carotenoids (% cdw) | Bchl *a* (% cdw) | Bchl *c* (% cdw) |
|---|---|---|---|---|---|---|---|
| 4 | 637 | M1-IC (no $NH_4Cl$), 50ºC, pH 8 | 2.26 | $46^{Exp}$ | 0.15 | 0.041 | 0.13 |
| 5 | 637 | M1-IC, 50ºC, pH 8, sulfide adjustments | 2.40 ± 0.20 | $70^{Sta}$ | 0.46 ± 0.052 | 0.32 ± 0.033 | 0.31 ± 0.056 |
| 6 | 635 | M1, 50ºC, pH 8 | 1.86 ± 0.10 | $100^{Sta}$ | 0.78 ± 0.035 | 0.16 ± 0.007 | 0.23 ± 0.085 |
| | 636 | | 2.05 ± 0.14 | $95^{Sta}$ | 0.57 ± 0.17 | 0.076 ± 0.048 | 0.38 ± 0.30 |
| | 638 | | 1.70 ± 0.11 | $100^{Exp}$ | 0.64 ± 0.00 | 0.070 ± 0.028 | 0.13 ± 0.035 |
| 7 | 635 | M1-IC, 50ºC, pH 8 | 1.70 ± 0.07 | $217^{Sta}$ | 0.35 ± 0.021 | 0.040 ± 0.00 | 0.065 ± 0.007 |
| | 636 | | 1.73 ± 0.05 | $263^{Sta}$ | 0.081 ± 0.013 | 0.039 ± 0.030 | 0.068 ± 0.011 |
| | 638 | | 1.71 ± 0.03 | - | - | - | - |
| 8 | 635 | M1-IC, 50ºC, pH 8, sulfide adjustments | 1.71 ± 0.03 | $168^{Sta}$ | 0.038 ± 0.019 | 0.015 ± 0.012 | 0.020 ± 0.004 |
| 9 | 635 | M1, 50ºC, pH 7 | 1.72 ± 0.08 | $166^{Sta}$ | 0.94 ± 0.063 | 0.15 ± 0.048 | 0.91 ± 0.12 |
| | | M1, 50ºC, pH 9 | 1.66 ± 0.15 | $93^{Sta}$ | 0.56 ± 0.028 | 0.16 ± 0.000 | 0.41 ± 0.11 |

## 3.8 PHA production

Throughout the tests carried out in this thesis, the PHA content was analyzed. The highest values obtained, for all strains, in all the test series are represented in Table 3.7 as well as the time of the test they were achieved. The results are shown as PHB, PHV and PHA (which is the sum of PHB and PHV) as a percentage of the VSS.

Table 3.7 - Representation of the highest values achieved for PHB, PHV and PHA content (in % of the VSS) in all tests carried out as well as the conditions of these tests. The volumetric light intensity of the flask and the time the samples were taken are also shown. "Exp" means the samples were taken in the exponential phase, "Sta" means the samples were taken in the stationary phase.

| Test series | Strain | Conditions | Volumetric light intensity (W $L^{-1}$) | Time (h) | PHB (% VSS) | PHV (% VSS) | PHA (% VSS) |
|---|---|---|---|---|---|---|---|
| 4 | 637 | M1-IC (no $NH_4Cl$), 50ºC, pH 8 | 2.26 | - | 0.00 | 0.00 | 0.00 |
| 5 | 637 | M1-IC, 50ºC, pH 8, sulfide adjustments | 2.40 ± 0.20 | - | 0.00 | 0.00 | 0.00 |
| 6 | 635 | M1, 50ºC, pH 8 | 1.86 ± 0.10 | $168^{Sta}$ | 1.95 | 0.85 | 2.8 |
| | 636 | | 2.05 ± 0.14 | $72^{Exp}$ | 0.43 | 0.95 | 1.4 |
| | 638 | | 1.70 ± 0.11 | $192^{Sta}$ | 1.8 | 2.5 | 4.3 |
| 7 | 635 | M1-IC, 50ºC, pH 8 | 1.70 ± 0.07 | $172^{Sta}$ | 0.00 | 1.6 | 1.6 |
| | 636 | | 1.73 ± 0.05 | - | 0.00 | 0.00 | 0.00 |
| | 638 | | 1.71 ± 0.03 | - | 0.00 | 0.00 | 0.00 |
| 8 | 635 | M1-IC, 50ºC, pH 8, sulfide adjustments | 1.71 ± 0.03 | - | 0.00 | 0.00 | 0.00 |
| 9 | 635 | M1, 50ºC, pH 7 | 1.72 ± 0.08 | $166^{Sta}$ | 0.58 | 1.2 | 1.8 |
| | | M1, 50ºC, pH 9 | 1.66 ± 0.15 | $69^{Exp}$ | 0.00 | 0.18 | 0.18 |

Looking at this data, it is possible to observe that the highest production of PHB was achieved in test 6, with both strains DSM 635 and DSM 638 under the conditions: M1, 50ºC at pH 8. This test was carried out with a volumetric light intensity of 1.86 ± 0.010 and 1.70 ± 0.11 W $L^{-1}$, respectively. The highest production of PHV was achieved also in this test, by strain DSM 638. Thus, this strain, in these conditions achieved the best PHA production overall.

Another important result of this analysis is the fact that in M1-IC no PHA production was observed. This probably happened since the culture did not have any carbon to grow, which is corroborated by the VFA data in these respective tests, not allowing it to store PHA. Furthermore, in this thesis, no strategy of PHA accumulation, like cycles of feast and famine, were used. Thus, further accumulation tests would be necessary to understand if PHA production could be viable under M1-IC.

Overall, samples taken in the stationary phase showed more PHA content than those on the exponential phase. However, these samples were taken at the beginning of the stationary phase. This makes sense since after the exponential phase, the cells accumulate PHA if possible, while carbon is available. After the stationary phase has begun, the PHA content would start to decrease as the cells would access it for growth.

These values of PHA production are low, since previously, a production of 15 % has been achieved, in M1[49]. However, previous attempts were not successful at producing PHA under autotrophic conditions[49]. Finally, it would be interesting to evaluate the PHA production under M1 conditions, with supplementation of $CO_2$ (to utilize butyric acid) and pulses of YE and sulphide, to make sure carbon was available for PHA accumulation.

## 3.9 Results overview

As a final note, Table 3.8 shows the highest values achieved for the maximum specific growth rate, biomass productivity and doubling time for all the tests carried out.

Table 3.8 - Representation of the highest values achieved for the maximum specific growth rate, biomass productivity and doubling time in all tests carried out as well as the conditions of these tests. The volumetric light intensity of the flask and the time the samples were taken are also shown.

| Test series | Strain | Conditions | Volumetric light intensity ($W\ L^{-1}$) | Time (h) | Maximum specific growth rate ($d^{-1}$) | Biomass productivity ($mg\ L^{-1}\ d^{-1}$) | Doubling time (d) |
|---|---|---|---|---|---|---|---|
| 1 | 637 | M1, 50ºC, pH 8 | 4.77 | 24 | 0.66 | 166 | 1.1 |
| 4 | 637 | M1-IC (no $NH_4Cl$), 50ºC, pH 8 | 2.26 | 23 | 0.25 | 40 | 2.8 |
| 5 | 637 | M1-IC, 50ºC, pH 8, sulfide adjustments | 2.40 ± 0.20 | 45 | 0.16 | 29 | 4.2 |
| 6 | 635 | M1, 50ºC, pH 8 | 1.86 ± 0.10 | 48 | 0.47 | 99 | 1.5 |
| | 636 | | 2.05 ± 0.14 | 24 | 0.60 | 107 | 1.2 |
| | 638 | | 1.70 ± 0.11 | 24 | 0.37 | 52 | 1.9 |
| 7 | 635 | M1-IC, 50ºC, pH 8 | 1.70 ± 0.07 | 72 | 0.52 | 131 | 1.3 |
| | 636 | | 1.73 ± 0.05 | 167 | 0.10 | 17 | 7.2 |
| | 638 | | 1.71 ± 0.03 | 25 | 0.19 | 24 | 3.6 |
| 8 | 635 | M1-IC, 50ºC, pH 8, sulfide adjustments | 1.71 ± 0.03 | - | - | - | - |
| 9 | 635 | M1, 50ºC, pH 7 | 1.72 ± 0.08 | 22 | 0.54 | 152 | 1.3 |
| | | M1, 50ºC, pH 9 | 1.66 ± 0.15 | 22 | 0.85 | 240 | 0.81 |

Strains DSM 635 and DSM 636 showed good growth in M1, pH 8 conditions. The maximum specific growth rate was 0.47 $d^{-1}$ for strain DSM 635, 0.6 $d^{-1}$ for strain DSM 636 and 0.66 $d^{-1}$ for strain DSM 637. The maximum specific growth rate for strain DSM 637 was slightly faster but this could be explained by the higher volumetric light intensity, which was more than twice as much. Strain 638 was the slowest. The same could be said for the maximum OD610 reached by these strains.

Additionally, the fastest growth was achieved at pH 9 for strain DMS 635 in M1, with a maximum specific growth rate of 0.85 $d^{-1}$, biomass productivity of 240 $mg\ L^{-1}\ d^{-1,}$ and a doubling time of 0.81 d. This raises the interesting question of whether a different pH would increase the growth of the other strains as well.

Growth in M1-IC was slow for every strain. As mentioned previously, this could be overcome by YE and sulfide supplementation. Furthermore, the vitamins supplementation did not seem to help growth.

## 3.10Experimental challenges

Throughout the laboratory work, several challenges of working with phototrophic organisms in anaerobic conditions had to be overcome. This section highlights these challenges, what steps were taken to overcome them, and what impact they can have on the results.

Challenge 1: The illumination. The experimental setup with the light source pointing towards the incubator was not able to provide the same amount of light to every Erlenmeyer flask. This means that not only replicates could have slightly different values, but also there was some difference between tests. This happened due to light bulb degradation over time, since constant adjustments to the lamp position had to be made, but also to light bulb failure, since many times, over the weekend or on week-days, the light bulbs would stop working. Nonetheless, constant adjustments were made at the beginning and end of each test, so to maintain the same (or around the same) light intensity in all flasks, in all tests.

Challenge 2: Sampling. Sometimes, during sampling, oxygen would get into the Erlenmeyer and serum flasks. This could be due simply to the various needle injections along the test, to the clogging of the gas sampling bag filter, which would stop providing nitrogen to the flasks (clogging that was hard to predict or detect). Since oxygen reacts with sulfide, precipitating it, the cultures would have less access to sulfide with would impact their metabolism.

Challenge 3: Test preparation. The medium preparation and culture revival were also major challenges. The medium could be prepared, bubbled with nitrogen, and autoclaved the same way every time, but sometimes it would contaminate after one, two, or even more days. This was true for M1, which contains almost one gram per liter of YE, making it easier to contaminate. This made the process of preparing for a test much more laborious. Culture revival posed some challenges as well, as sometimes, for unknown reasons, the culture would not grow or grow slowly. This made it so that, to make sure the test would be possible, two cryovials, instead of one, would be revived at a time. This also takes more work and means that more cryovials need to be prepared to maintain a healthy stock of the strain in the -80ºC freezer.

Challenge 3: Scale up. One of the goals of this work was to adapt an airlift bioreactor for operation with *C. aurantiacus*. However, this goal could not be achieved to the complexity of operation in strict anaerobic conditions. The setup for this reactor is shown in Figure 3.16. The anaerobiosis of the system was hard to maintain, and a constant increase in the oxidative reductive potential (ORP) was observed. This was mainly due to gas leaks in the system. The presence of these leaks meant that the nitrogen recirculating would escape the system and the nitrogen gas bags would get empty. After this happened, oxygen would start getting in the system due to negative pressure buildup inside the system. Another setup was proposed, where a rotameter would be inserted before the gas bags, with the goal of supplying the extra nitrogen needed for the bags to be always full. However, this solution did not work as well. Despite the

several attempts to maintain the anaerobic conditions, sulfide was permanently being lost abiotically. Future scale-up tests must consider the challenge of working with sulfide and the need to select highly gas-tight bioreactors

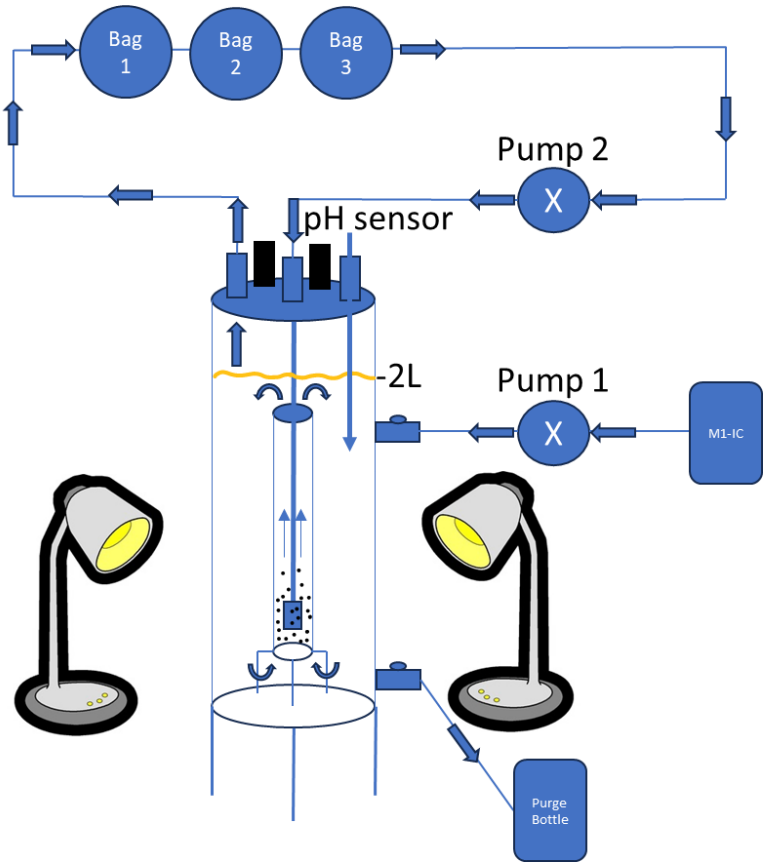


Figure 3.16 - Airlift bioreactor setup

# 4

# CONCLUSIONS

This thesis focused on the development of a photosynthetic sustainable bioprocess aimed at capturing $CO_2$, which is the most important GHG, and the simultaneous removal of sulfide while producing value-added products, such as PHA and natural pigments, in a single-stage process.

Firstly, three tests with strain DSM 637 were conducted, to establish the relationship between biomass concentration as TSS and VSS with $OD_{610}$ and understand its capabilities of $CO_2$ fixation. Changes in parameters like medium composition, vitamin supplementation, and sulfide adjustments were studied. Two abiotic controls were also performed.

The calibration curve obtained for OD plotted against TSS and VSS showed good results, with VSS amounting to 89 % of the TSS, which was expected. It also proved very useful in data analysis.

The abiotic controls showed that there was the possibility for losses of IC and sulfide while sampling. Oxygen could get inside the flasks and react with soluble sulfide, precipitating it. IC could possibly escape when the flasks were punctured. Additionally, it was concluded that light did not play a role in sulfide removal. The TOC content did not change indicating maintenance of microbial sterility.

The tests with strain DSM 637 in M1-IC resulted in slower growth than in M1. However, biomass yield calculations suggest that there was $CO_2$ fixation by this strain. Furthermore, vitamins supplementation did not seem to help growth. This could be because what was limiting the growth was the carbon source (as shown in VFA data) while any necessary vitamins were already present in the medium due to the YE. Sulfide was available but higher concentrations could be tested since this strain proved to be tolerant to concentrations as high as 40 mg S $L^{-1}$. Further tests with YE supplementation could help sustain this growth and $CO_2$ fixation.

Next, strains DSM 635, DMS 636, and DSM 638 were used for kinetic assays either in heterotrophic or autotrophic conditions.

Under heterotrophic conditions, strains DSM 635 and DSM 636 showed good growth in M1, at pH 8. The maximum specific growth rate was 0.47 $d^{-1}$ for strain DSM 635 and 0.6 $d^{-1}$ for strain DSM 636. The maximum specific growth rate for strain DSM 637 (0.66 $d^{-1}$) was slightly higher but

this could be explained by the higher volumetric light intensity, which was more than twice as much. Strain 638 was the slowest and the same could be said for the maximum $OD_{610}$ reached by these strains. Thus, these strains seem to be similar between themselves. Additionally, butyric acid was found at the end of the batch tests and was not consumed likely due to the lack of $CO_2$. Thus, it would be interesting to test $CO_2$ supplementation to M1, along with sulfide supplementation, to utilize this VFA.

Under autotrophic conditions, tests in M1-IC with these strains showed similar results to those with strain DSM 637, with similar biomass yields (based on VSS) and total organic carbon consumption. Notably, strain DSM 638 was the exception, as it did not seem to grow under autotrophic conditions. However, further tests would be necessary to say if it cannot fixate $CO_2$. Thus, it is concluded that strains DSM 635, DSM 636, and DSM 637 behave similarly and could be used for further tests in autotrophic conditions.

Lastly, strain DSM 635 was subject to further tests involving sulfide adjustments, and changes in pH and temperature.

Tests in M1 at pH 7 and pH 9, with strain DSM 635, showed very promising results. Good growth was observed in both conditions, with the fastest growth happening at pH 9. The maximum specific growth rate achieved at 22h was 0.85 $d^{-1}$, the biomass productivity was 240 mg $L^{-1}$ $d^{-1,}$ and the doubling time was 0.81 d. Compared with all the strains and all the conditions tested, this was the best growth achieved, especially since this test was performed in slightly higher volumetric light intensity. However, this raises the interesting question of whether a different pH would increase the growth of the other strains as well. Growth at pH 9 is interesting since it allows for lower sulfide and IC losses while operating these cultures. This is especially relevant for bioreactor operation.

Finally, tests under 30ºC with strain DSM 635 did not result in culture growth. This was to be expected as this species is a thermophile. However, it would be interesting to test different temperatures, like 40ºC, since it is more expensive and difficult to maintain high temperatures, be it in a batch test or a reactor. Different strains could also be tested.

The highest production of PHB was achieved with both strains DSM 635 and DSM 638 under the conditions: M1, 50ºC at pH 8. This test was carried out with a volumetric light intensity of 1.86 ± 0.010 and 1.70 ± 0.11 W $L^{-1}$, respectively. The highest production of PHV was achieved also in this test, by strain DSM 638. Thus, this strain, in these conditions achieved the best PHA production overall. Additionally, samples taken at the beginning of the stationary phase showed more PHA content than those on the exponential phase.

Importantly, in M1-IC no PHA production was observed. The cultures were not taking up any substantial amount of inorganic carbon and did not have any organic carbon available (which is corroborated by the VFA data in these respective tests), and this absence of carbon in excess did not allow

PHA storage. Furthermore, in this thesis, no strategy of PHA accumulation, like cycles of feast and famine or nutrient limitation were used. Thus, further accumulation tests would be necessary to understand if PHA production could be viable under M1-IC.

Additionally, it would be interesting to evaluate the PHA production under M1 conditions, with supplementation of $CO_2$ (to utilize butyric acid) and pulses of YE and sulphide, to make sure carbon was available for PHA accumulation.

The best production of Bchl *c* was achieved with strain DSM 635, under the conditions: M1, 50ºC at pH 7, with a volumetric light intensity of $1.72 \pm 0.08$ W $L^{-1}$. The highest production of Bchl *a* was achieved with strain DSM 637, under the conditions: M1-IC, 50ºC, at pH 8, a test with sulfide adjustments. This test had the highest volumetric light intensity, at $2.40 \pm 0.20$ W $L^{-1}$. Despite what was expected, there was no clear trend between the volumetric light intensity and the type of pigment produced in higher quantity. Furthermore, pigment production was similar between tests and strains. This was mostly because the values obtained were low, especially when compared to other phototrophic microorganisms. Nonetheless, further tests with higher light intensity could improve this production.

# 5

# FUTURE WORK

This work highlighted how sensible a process of this nature can be and the difficulties that exist in optimizing it. Nonetheless, some ideas for further tests have come up while analyzing all the data.

The first suggestion is that further tests could explore higher sulfide concentrations. According to the sulfide consumption equations 13 and 14, sulfide could be oxidized to its elemental form (equation 13) or to sulfate (equation 14)[61].

$$Equation\ (13):$$

$$2H_2S + CO_2 \xrightarrow{light} 2S^0 + (CH_2O) + H_2O$$

$$Equation\ (14):$$

$$H_2S + 2CO_2 + H_2O \xrightarrow{light} 2(CH_2O) + H_2SO_4$$

This means that, for $CO_2$ fixation to happen, a lot of sulfide is required. More precisely, assuming equation 14, which shows the lowest ratio of sulfide needed per IC fixation, there is still a need of 1.3 mg of S to consume 1 mg of IC. Most tests carried out in this thesis had around 10 mg of S $L^{-1}$. This would be enough to consume only 7.7 mg of IC, which is hard to detect in growth. Which leads to the next suggestion, complementation of M1 with IC and sulfide.

For ideal growth, once the organic carbon source finishes, *C. aurantiacus* could utilize $CO_2$ to consume the remaining butyric acid. Furthermore, with supplements of YE and sulfide, it could slowly assimilate more and more IC.

Furthermore, according to the pigment analysis results, pH 7 (in M1, 50ºC and under 1.7 ± 0.08 W $L^{-1}$) produced the best results in terms of pigment production, for strain DSM 635. Thus, it would be interesting to test if, for the other strains, a different pH would also have a positive impact on pigment production.

# 6

# BIBLIOGRAPHY


1. *Science of Plastics.* https://sciencehistory.org/education/classroom-activities/role-playing-games/case-of-plastics/science-of-plastics/. Accessed on 16/08/2023.
2. *History and Future of Plastics.* https://sciencehistory.org/education/classroom-activities/role-playing-games/case-of-plastics/history-and-future-of-plastics/. Accessed on 16/08/2023.
3. Bayer, Forrest. *et al. Guidance and criteria for safe recycling of post consumer polyethylene terephthalate (PET) into new food packaging applications.* EU Publications: 2004-09-21 (2015).
4. *Global plastic production 1950-2021*. https://www.statista.com/statistics/282732/global-production-of-plastics-since-1950/. Accessed on 16/08/2023.
5. *The world's plastic pollution crisis explained*. https://education.nationalgeographic.org/resource/worlds-plastic-pollution-crisis-explained/. Accessed on 05/08/2023.
6. *Great Pacific Garbage Patch*. https://education.nationalgeographic.org/resource/great-pacific-garbage-patch/. Accessed on 05/08/2023.
7. *Plastic waste and recycling in the EU: facts and figures*. https://www.europarl.europa.eu/news/en/headlines/society/20181212STO21610/plastic-waste-and-recycling-in-the-eu-facts-and-figures. Accessed on 17/08/2023.
8. Huang, J.-C., Shew, A. S. & Wang, M.-S. *Biodegradable Plastics: A Review.* Advances in Polymer Technology, Vol. 10, No. 1, 23-30 (1990)
9. *European Bioplastics Fact Sheet*. https://www.european-bioplastics.org/bioplastics-facts-figures/. Accessed on 05/08/2023.
10. Hiraga, K., Taniguchi, I., Yoshida, S., Kimura, Y. & Oda, K. *Biodegradation of waste PET. EMBO Rep* **20**, (2019).
11. Meereboer, K. W., Misra, M. & Mohanty, A. K. *Review of recent advances in the biodegradability of polyhydroxyalkanoate (PHA) bioplastics and their composites*. Green Chemistry vol. 22 5519–5558 Preprint at https://doi.org/10.1039/d0gc01647k (2020).

12. Mü, R.-J., Kleeberg, I. & Deckwer, W.-D. *Biodegradation of polyesters containing aromatic constituents*. Journal of Biotechnology vol. 86 www.elsevier.com/locate/jbiotec (2001).
13. *Biodegradable Plastics Market Size - Global Industry, Share, Analysis, Trends and Forecast 2022 - 2030*. https://www.acumenresearchandconsulting.com/biodegradable-plastics-market. Accessed on 17/08/2023.
14. *Certifications for bioplastics*. https://www.european-bioplastics.org/bioplastics/standards/certification/. Accessed on 27/09/2023.
15. McChalicher, C. W. J. & Srienc, F. *Investigating the structure-property relationship of bacterial PHA block copolymers*. J Biotechnol **132**, 296–302 (2007).
16. McAdam, B., Fournet, M. B., McDonald, P. & Mojicevic, M. *Production of polyhydroxybutyrate (PHB) and factors impacting its chemical and mechanical characteristics*. Polymers vol. 12 1–20 Preprint at https://doi.org/10.3390/polym12122908 (2020).
17. Chen, G. Q., Jiang, X. R. & Guo, Y. *Synthetic biology of microbes synthesizing polyhydroxyalkanoates (PHA)*. Synthetic and Systems Biotechnology vol. 1 236–242 Preprint at https://doi.org/10.1016/j.synbio.2016.09.006 (2016).
18. Crutchik, D. *et al. Polyhydroxyalkanoates (PHAs) production: A feasible economic option for the treatment of sewage sludge in municipalwastewater treatment plants?* Water (Switzerland) **12**, (2020).
19. *Consequences of Climate Change*. https://climate.ec.europa.eu/climate-change/consequences-climate-change_en. Accessed on 05/08/2023.
20. *EU measures against climate change*. https://www.europarl.europa.eu/news/en/headlines/society/20180703STO07129/eu-measures-against-climate-change. Accessed on 20/08/2023.
21. *Climate Change: Atmospheric Carbon Dioxide*. https://www.climate.gov/news-features/understanding-climate/climate-change-atmospheric-carbon-dioxide. Accessed on 20/08/2023.
22. Kroeker, K. J. *et al. Impacts of ocean acidification on marine organisms: Quantifying sensitivities and interaction with warming*. Glob Chang Biol **19**, 1884–1896 (2013).
23. Santos Correa, S., Schultz, J., Lauersen, K. J. & Soares Rosado, *A. Natural carbon fixation and advances in synthetic engineering for redesigning and creating new fixation pathways*. Journal of Advanced Research vol. 47 75–92 Preprint at https://doi.org/10.1016/j.jare.2022.07.011 (2023).
24. McKinlay, J. B. & Harwood, C. S. *Carbon dioxide fixation as a central redox cofactor recycling mechanism in bacteria*. Proc Natl Acad Sci U S A **107**, 11669–11675 (2010).
25. Ángeles, R., Arnaiz, E., Gutiérrez, J., Muñoz, R. & Lebrero, R. *Biogas-based production of glycogen by Nostoc muscorum: Assessing the potential of transforming CO2 into value added products*. Chemosphere **275**, (2021).

26. Berg, I. A. *Ecological aspects of the distribution of different autotrophic CO2 fixation pathways*. Applied and Environmental Microbiology vol. 77 1925–1936 Preprint at https://doi.org/10.1128/AEM.02473-10 (2011).
27. Hügler, M., Huber, H., Stetter, K. O. & Fuchs, G. *Autotrophic CO2 fixation pathways in archaea (Crenarchaeota)*. Arch Microbiol **179**, 160–173 (2003).
28. Hügler, M. & Fuchs, G. *Assaying for the 3-hydroxypropionate cycle of carbon fixation*. Methods in Enzymology vol. 397 212–221 Preprint at https://doi.org/10.1016/S0076-6879(05)97012-2 (2005).
29. Zarzycki, J. & Fuchs, G. *Coassimilation of organic substrates via the autotrophic 3-hydroxypropionate bi-cycle in Chloroflexus aurantiacus*. Appl Environ Microbiol **77**, 6181–6188 (2011).
30. Ardila-Leal, L. D., Poutou-Piñales, R. A., Pedroza-Rodríguez, A. M. & Quevedo-Hidalgo, B. E. *A brief history of colour, the environmental impact of synthetic dyes and removal by using laccases*. Molecules vol. 26 Preprint at https://doi.org/10.3390/molecules26133813 (2021).
31. Micó-Vicent, B. *et al. Stabilized Dye–Pigment Formulations with Platy and Tubular Nanoclays*. Adv Funct Mater **28**, (2018).
32. Olas, B., Białecki, J., Urbańska, K. & Bryś, M. *The Effects of Natural and Synthetic Blue Dyes on Human Health: A Review of Current Knowledge and Therapeutic Perspectives*. Advances in Nutrition vol. 12 2301–2311 Preprint at https://doi.org/10.1093/advances/nmab081 (2021).
33. Golka, K., Kopps, S. & Myslak, Z. W. *Carcinogenicity of azo colorants: Influence of solubility and bioavailability*. Toxicology Letters vol. 151 203–210 Preprint at https://doi.org/10.1016/j.toxlet.2003.11.016 (2004).
34. Natarajan, S., Bajaj, H. C. & Tayade, R. J. *Recent advances based on the synergetic effect of adsorption for removal of dyes from wastewater using photocatalytic process*. Journal of Environmental Sciences (China) vol. 65 201–222 Preprint at https://doi.org/10.1016/j.jes.2017.03.011 (2018).
35. *How to Shop for Natural and Non-Toxic Pigments*. https://www.naturalpigments.com/natural-non-toxic-pigments.html. Accessed on 21/08/2023.
36. Pailliè-Jiménez, M. E., Stincone, P. & Brandelli, A. *Natural Pigments of Microbial Origin*. Frontiers in Sustainable Food Systems vol. 4 Preprint at https://doi.org/10.3389/fsufs.2020.590439 (2020).
37. Ranaweera, S., Arachchige, U., Ranaweera, S. J., Ampemohotti, A. A. L. T. & Arachchige, U. S. P. R. *Advantages and considerations for the applications of natural food pigments in the food industry*. Journal of research technology and engineering **1**, (2020).
38. Barreiro, C., Martinez, S. & Luis Barredo, J. *Main Carotenoids Produced by Microorganisms* Subjects: Microbiology. www.mordorintelligence.com.

39. Kim, N. Y., Yim, T. Bin & Lee, H. Y. *Skin anti-aging activities of bacteriochlorophyll a from photosynthetic bacteria, rhodobacter sphaeroides.* J Microbiol Biotechnol **25**, 1589–1598 (2015).
40. Orlandi, V. T., Martegani, E., Giaroni, C., Baj, A. & Bolognese, F. *Bacterial pigments: A colorful palette reservoir for biotechnological applications*. Biotechnology and Applied Biochemistry vol. 69 981–1001 Preprint at https://doi.org/10.1002/bab.2170 (2022).
41. Pierson, B. K. & Castenholz, R. W. *A Phototrophic Gliding Filamentous Bacterium of Hot Springs, Chloroflexus aurantiacus, gen. and sp. nov*. *Arch*. Microbiol vol. 100 (1974).
42. Madigan, M. T. *Anoxygenic phototrophic bacteria from extreme environments*. *Photosynthesis* Research vol. 76 (2003).
43. Herter, S. *et al. Autotrophic CO2 fixation by Chloroflexus aurantiacus: Study of glyoxylate formation and assimilation via the 3-hydroxypropionate cycle*. J Bacteriol **183**, 4305–4316 (2001).
44. Herter, S., Fuchs, G., Bacher, A. & Eisenreich, W. *A bicyclic autotrophic CO2 fixation pathway in Chloroflexus aurantiacus.* Journal of Biological Chemistry **277**, 20277–20283 (2002).
45. Holo, H. & Sirevhg, R. *Autotrophic growth and C02 fixation of Chloroflexus aurantiacus*. Arch Microbiol vol. 145 (1986).
46. Ma, Y.-Z., Cox, R. P., Gillbro, T. & Miller, M. *Bacteriochlorophyll organization and energy transfer kinetics in chlorosomes from Chloroflexus aurantiacus depend on the light regime during growth*. Photosynthesis Research vol. 47 (1996).
47. Pšenčík, J. *et al. Structural and functional roles of carotenoids in chlorosomes.* J Bacteriol **195**, 1727–1734 (2013).
48. Hassanien, M. F. R. Physalis peruviana: *A rich source of bioactive phytochemicals for functional foods and pharmaceuticals.* Food Reviews International vol. 27 259–273 Preprint at https://doi.org/10.1080/87559129.2011.563391 (2011).
49. Diamantino, R., Fradinho, J. & Torres, C. *Exploring CO2 as feedstock for production of biopolymers by the bacteria Chloroflexus aurantiacus*. (2023).
50. Farnocchia, G., Zanaroli, G., Fradinho, J., Reis, M. *Evaluating the PHA storage capacity and the impacts of growth conditions on Chloroflexus aurantiacus, a green non-sulphur phototrophic bacterium*. (2021).
51. Schmidt, K. *A Comparative Study on the Composition of Chlorosomes (Chlorobium Vesicles) and Cytoplasmic Membranes from Chloroflexus aurantiacus Strain Ok-70-fl and Chlorobium limicola f. thiosulfatophilum* Strain 6230. vol. 124 (1980).
52. Spanoghe, J., Vermeir, P. & Vlaeminck, S. E. *Microbial food from light, carbon dioxide and hydrogen gas: Kinetic, stoichiometric and nutritional potential of three purple bacteria*. Bioresour Technol **337**, (2021).

53. Synnove liaaen-jensen & arne jensen. *Quantitative Determination of Carotenoids in Photosynthetic Tissues*. Methods in Enzymologym, Academic press, (1971).
54. American Public Health Association, American Water Works Association & Water Environment Federation. *Standard Methods for the Examination of Water and Wastewater*. APHA (2005).
55. Sugahara, S., Suzuki, M., Kamiya, H. *Colorimetric Determination of Sulfide in Microsamples*. Analytical sciences october (2016).
56. Fagerbakke, K. M., Heldal, M. & Norland, S. *Content of carbon, nitrogen, oxygen, sulfur and phosphorus in native aquatic and cultured bacteria*. Aquatic microbial ecology (1996).
57. Carroll, J. J. & Mather, A. E. *The solubility of hydrogen sulphide in water from 0 to 90°C and pressures to 1 MPa*. Geochimica d Cosmochimica Acta vol. 53 (1989).
58. Kenneth Y. Chen; J. Carrel1 Morris. *Kinetics of Oxidation of Aqueous Sulfide by O2*. Environmental Science & Technology (1972).
59. Braga, B., Fradinho, J. & Angeles Torres, R. *Report of Project in Biochemistry Photosynthetic Bacterial Pigments Production During Biological Sulphide Removal in a Stirred Tank: Influence of the Light Intensity*. (2023).
60. Pagels, F., Vasconcelos, V. & Guedes, A. C. *Carotenoids from cyanobacteria: Biotechnological potential and optimization strategies.* Biomolecules vol. 11 Preprint at https://doi.org/10.3390/biom11050735 (2021).
61. Cork,', D. J., Garunas,' And, R. & Sajjad2, A. *Chlorobium limicola forma thiosulfatophilum: Biocatalyst in the Production of Sulfur and Organic Carbon from a Gas Stream Containing H2S and CO2.* Applied and environmental microbiology (1983).

# 7

# ANNEX

## 7.1 Supplementary materials

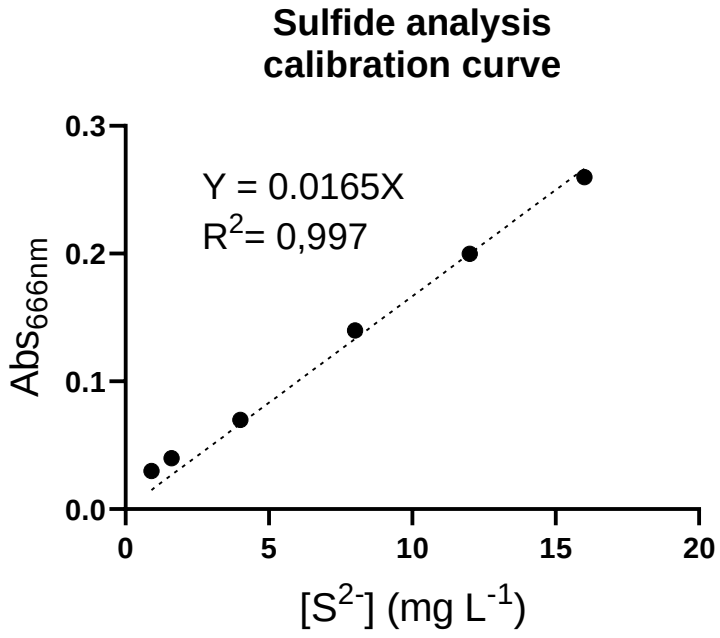


Figure 7.1 - Example of a calibration curve for sulfide analysis.

Table 7.1 - Ammonium and phosphate content during “Test 4: Influence of the sulfide concentration on the autotrophic growth and CO2 fixation capability of *C. aurantiacus* strain DSM 637”.

| Time (h) | Bioreactor | | | | | | | | | |
|---|---|---|---|---|---|---|---|---|---|---|
| | Inoculum | | 20.6 mg S $L^{-1}$ | | 10.7 mg S $L^{-1}$ | | 5.8 mg S $L^{-1}$ | | 3.3 mg S $L^{-1}$ | |
| | $[PO_4^-]$ (mg P $L^{-1}$) | $[NH_3^-]$ (mg N $L^{-1}$) | $[PO_4^-]$ (mg P $L^{-1}$) | $[NH_3^-]$ (mg N $L^{-1}$) | $[PO_4^-]$ (mg P $L^{-1}$) | $[NH_3^-]$ (mg N $L^{-1}$) | $[PO_4^-]$ (mg P $L^{-1}$) | $[NH_3^-]$ (mg N $L^{-1}$) | $[PO_4^-]$ (mg P $L^{-1}$) | $[NH_3^-]$ (mg N $L^{-1}$) |
| 0 | 9.8 | 83.5 | 4.8 | 79.2 | 4.6 | 65.9 | 2.4 | 66.7 | 3.7 | 75.9 |
| 23 | - | - | 5.4 | 70.6 | 4.9 | 73.8 | 3.0 | 66.1 | 5.5 | 76.4 |
| 46 | - | - | 6.7 | 34.1 | 5.4 | 33.4 | 7.3 | 43.6 | 4.7 | 47.9 |
| 71 | - | - | 5.0 | 38.4 | 4.2 | 39.5 | 4.4 | 38.1 | 8.0 | 35.0 |
| 93 | - | - | 7.7 | 75.5 | 4.5 | 75.3 | 5.2 | 80.2 | 7.0 | 76.8 |

Table 7.2 - Ammonium and phosphate content during "Test 5: Exploring the capability of *C. aurantiacus* strain DSM 637 to grow autotrophically and utilize CO2 with the support of vitamins”.

| Time (h) | Bioreactor | | | | | |
|---|---|---|---|---|---|---|
| | Inoculum | | 10.7 mg S $L^{-1}$ + Pulses | | 20.6 mg S $L^{-1}$ | |
| | $[PO_4^-]$ (mg P $L^{-1}$) | $[NH_3^-]$ (mg N $L^{-1}$) | $[PO_4^-]$ (mg P $L^{-1}$) | $[NH_3^-]$ (mg N $L^{-1}$) | $[PO_4^-]$ (mg P $L^{-1}$) | $[NH_3^-]$ (mg N $L^{-1}$) |
| 0 | 27.2 | 197.8 | 17.4 | 189.3 | 17.6 | 186.2 |
| 21 | - | - | 17.4 | 187.2 | 17.2 | 181.6 |
| 45 | - | - | 4.2 | 90.9 | 4.5 | 89.2 |
| 70 | - | - | 16.6 | 187.6 | 18.6 | 189.0 |
| 95 | - | - | 16.2 | 183.8 | 16.1 | 183.0 |

Table 7.3 - Ammonium and phosphate content during “Test 6: Exploring the capability of *C. aurantiacus* strains DSM 635, DSM 636, and DSM 638 to grow under heterotrophic conditions and synthesize value-added products”.

| Time (h) | Bioreactor | | | | | | | | | |
|---|---|---|---|---|---|---|---|---|---|---|
| | Inoculum (DSM 635) | | Inoculum (DSM 636) | | DSM 635 | | DSM 636 | | DSM 638 | |
| | $[PO_4^-]$ (mg P $L^{-1}$) | $[NH_3^-]$ (mg N $L^{-1}$) | $[PO_4^-]$ (mg P $L^{-1}$) | $[NH_3^-]$ (mg N $L^{-1}$) | $[PO_4^-]$ (mg P $L^{-1}$) | $[NH_3^-]$ (mg N $L^{-1}$) | $[PO_4^-]$ (mg P $L^{-1}$) | $[NH_3^-]$ (mg N $L^{-1}$) | $[PO_4^-]$ (mg P $L^{-1}$) | $[NH_3^-]$ (mg N $L^{-1}$) |
| 0 | 25.3 | 25.3 | 22.1 | 65.8 | 33.2 | 58.7 | 9.6 | 75.4 | 33.2 | 57.6 |
| 24 | - | - | - | - | 51.2 | 59.0 | 11.1 | 47.0 | 42.5 | 59.0 |
| 48 | - | - | - | - | 30.6 | 65.5 | 3.8 | 59.4 | 32.6 | 59.4 |
| 72 | - | - | - | - | 7.9 | 66.4 | 8.7 | 80.0 | 10.4 | 61.1 |
| 100 | - | - | - | - | 23.2 | 112.1 | 7.1 | 80.8 | 27.0 | 94.2 |
| 168 | - | - | - | - | 4.1 | 76.1 | 2.4 | 21.3 | 5.6 | 69.4 |
| 192 | - | - | - | - | 4.2 | 73.4 | - | - | 4.2 | 70.3 |
| 216 | - | - | - | - | 21.0 | 149.1 | - | - | 21.9 | 126.1 |

Table 7.4 - Ammonium and phosphate content during "Test 7: Exploring the ability of *C. aurantiacus* strains DSM 635, DSM 636, and DSM 638 to grow autotrophically and utilize CO2".

| Time (h) | Bioreactor | | | | | | | | | |
|---|---|---|---|---|---|---|---|---|---|---|
| | Inoculum (DSM 635) | | Inoculum (DSM 636) | | DSM 635 | | DSM 636 | | DSM 638 | |
| | $[PO_4^-]$ (mg P $L^{-1}$) | $[NH_3^-]$ (mg N $L^{-1}$) | $[PO_4^-]$ (mg P $L^{-1}$) | $[NH_3^-]$ (mg N $L^{-1}$) | $[PO_4^-]$ (mg P $L^{-1}$) | $[NH_3^-]$ (mg N $L^{-1}$) | $[PO_4^-]$ (mg P $L^{-1}$) | $[NH_3^-]$ (mg N $L^{-1}$) | $[PO_4^-]$ (mg P $L^{-1}$) | $[NH_3^-]$ (mg N $L^{-1}$) |
| 0 | 9.3 | 122.6 | 10.0 | 87.8 | 2.2 | 90.4 | 2.6 | 69.1 | 3.0 | 57.3 |
| 23 | - | - | - | - | 1.0 | 81.7 | 3.2 | 75.5 | 3.5 | 72.3 |
| 47 | - | - | - | - | -0.2 | 78.5 | 3.8 | 72.4 | 3.1 | 56.1 |
| 74 | - | - | - | - | 2.4 | 69.1 | 3.0 | 75.4 | - | - |
| 95 | - | - | - | - | -0.4 | 70.5 | 2.8 | 63.2 | - | - |
| 167 | - | - | - | - | -1.6 | 52.0 | 2.2 | 69.3 | - | - |
| 215 | - | - | - | - | - | - | 2.9 | 72.0 | - | - |
| 263 | - | - | - | - | - | - | 3.5 | 71.0 | - | - |

Table 7.5 - Ammonium and phosphate content during "Test 8: Influence of sulfide adjustments on the autotrophic growth and CO2 fixation capability of *C. aurantiacus* strain DSM 635".

| Time (h) | Bioreactor | | | |
|---|---|---|---|---|
| | Inoculum | | DSM 635 | |
| | $[PO_4^-]$ (mg P $L^{-1}$) | $[NH_3^-]$ (mg N $L^{-1}$) | $[PO_4^-]$ (mg P $L^{-1}$) | $[NH_3^-]$ (mg N $L^{-1}$) |
| 0 | 4.7 | 86.1 | 1.4 | 75.0 |
| 24 | - | - | 4.5 | 88.2 |
| 48 | - | - | 0.7 | 77.7 |
| 72 | - | - | -0.4 | 67.8 |
| 96 | - | - | -1.9 | 55.1 |
| 168 | - | - | 3.4 | 74.5 |

Table 7.6 - Ammonium and phosphate content during "Test 9: Influence of pH on the heterotrophic growth and production of value-added products by *C. aurantiacus* strain DSM 635".

| Time (h) | Bioreactor | | | | | | | |
|---|---|---|---|---|---|---|---|---|
| | Inoculum (pH 9) | | Inoculum (pH 7) | | DSM 635 pH 9 | | DSM 635 pH 7 | |
| | $[PO_4^-]$ (mg P $L^{-1}$) | $[NH_3^-]$ (mg N $L^{-1}$) | $[PO_4^-]$ (mg P $L^{-1}$) | $[NH_3^-]$ (mg N $L^{-1}$) | $[PO_4^-]$ (mg P $L^{-1}$) | $[NH_3^-]$ (mg N $L^{-1}$) | $[PO_4^-]$ (mg P $L^{-1}$) | $[NH_3^-]$ (mg N $L^{-1}$) |
| 0 | 3.6 | 60.1 | 5.4 | 56.0 | 3.8 | 46.7 | 9.9 | 46.2 |
| 22 | - | - | - | - | 2.9 | 47.3 | 9.8 | 49.0 |
| 45 | - | - | - | - | 2.1 | 46.8 | 7.6 | 53.6 |
| 69 | - | - | - | - | 3.0 | 51.4 | 4.6 | 62.7 |
| 93 | - | - | - | - | 3.1 | 51.6 | 3.1 | 72.2 |
| 166 | - | - | - | - | - | - | 0.5 | 84.1 |

Table 7.7 - Ammonium and phosphate content during "Test 10: Influence of temperature on the heterotrophic growth of *C. aurantiacus* strain DSM 635".

| Time (h) | Bioreactor | | | | | | | |
|---|---|---|---|---|---|---|---|---|
| | Inoculum (pH 8) | | Inoculum (pH 9) | | 30ºC (pH 8) | | 30ºC (pH 9) | |
| | $[PO_4^-]$ (mg P $L^{-1}$) | $[NH_3^-]$ (mg N $L^{-1}$) | $[PO_4^-]$ (mg P $L^{-1}$) | $[NH_3^-]$ (mg N $L^{-1}$) | $[PO_4^-]$ (mg P $L^{-1}$) | $[NH_3^-]$ (mg N $L^{-1}$) | $[PO_4^-]$ (mg P $L^{-1}$) | $[NH_3^-]$ (mg N $L^{-1}$) |
| 0 | 3.6 | 31.4 | 12.8 | 63.7 | 12.2 | 37.9 | 9.9 | 50.1 |
| 19 | - | - | - | - | 8.2 | 27.9 | 10.2 | 48.5 |
| 68 | - | - | - | - | 13.4 | 29.0 | 12.6 | 81.9 |
| 87 | - | - | - | - | 11.8 | 28.7 | 14.5 | 86.2 |
| 160 | - | - | - | - | - | - | 14.3 | 80.8 |